



VCU

Virginia Commonwealth University
VCU Scholars Compass

Theses and Dissertations

Graduate School

2019

A HYBRID MOLECULE OF MELATONIN AND CURCUMIN FOR THERPEUTIC USE IN PULMONARY FIBROSIS

Varsha V. Nair

Follow this and additional works at: <https://scholarscompass.vcu.edu/etd>



Part of the [Pharmaceutics and Drug Design Commons](#)

© The Author

Downloaded from

<https://scholarscompass.vcu.edu/etd/5982>

This Thesis is brought to you for free and open access by the Graduate School at VCU Scholars Compass. It has been accepted for inclusion in Theses and Dissertations by an authorized administrator of VCU Scholars Compass. For more information, please contact libcompass@vcu.edu.

**A HYBRID MOLECULE OF MELATONIN AND CURCUMIN FOR THERAPEUTIC
USE IN PULMONARY FIBROSIS**

A thesis submitted in partial fulfillment of the requirements for the degree of Master of Science
at Virginia Commonwealth University

by

VARSHA V. NAIR, B. Pharm
Mumbai University, India, 2017

Advisor: MASAHIRO SAKAGAMI, Ph.D.
Professor
Department of Pharmaceutics, School of Pharmacy

Virginia Commonwealth University
Richmond, Virginia
July 2019

ACKNOWLEDGEMENTS

First and foremost, I would like to express my sincere gratitude to my advisor, Dr. Masahiro Sakagami, for giving me this opportunity to pursue my dreams. I believe everything I have learnt in these 2 years are due to his patience and mentorship. Thank you for the stimulating discussions, for being my strongest critic and for the words of encouragement. Thank you for guiding me where necessary and for pushing me to be independent. I will always treasure your teachings and life lessons. I would like to thank my graduate advisory committee members: Drs. Sweet, Zhang, and Kummarapurugu for their support and guidance over the last 2 years to make my work better. I am also very grateful to Abhinav Mohan for his friendship and his help in many research skills, such as western blot, immunofluorescence and animal handling. I am also grateful to Hua Li for her friendship and guidance through the initial course of my graduate studies.

I would like to thank Drs. Gerk, McRae, Hindle, and Sweet for my unrestricted entry to their labs for use of a number of resources for my research. I would also like to thank the Aerosol Research Group members: Drs. Sakagami, Hindle, Byron, Wei, Boc, Dhapare, Hassan, Momin, Kelkar, as well as Serena Bonasera, Abhinav Mohan and Yuan Xiao, for giving me one of the most fulfilling experiences of my graduate life.

I would also like to express my gratitude to the administrative staff of the VCU School of Pharmacy and Department of Pharmaceutics: Shakim Craft, Keyetta Tate and Laura Georgiadis. Throughout these 2 years, I was fortunate to learn a number of courses taught by the extraordinary faculty of the Department of Pharmaceutics: Drs. Sweet, Gerk, Venitz, Halquist, Hawkrigde, Xu, and da Rocha. I am grateful for your expertise, guidance and support.

My graduate studies would not have been as smooth sailing without my friends in Richmond. Purva, Vineet, Serena, Palak, Rushabh, Shwetha, Yash, Nikhila, Shalu, Piyusha and Sayantan, I feel truly lucky to have found a family in you. My friends back in India and across the world – Aleesha, Hirika, Aayushi, Payal, Divya and Arjun, thank you for supporting me through this journey. I would also like to thank my extended family at Northern Virginia for hosting me every holiday and making me feel at home.

Lastly, there is no way I could thank my family back in India enough for their trust in me and for the unconditional love they have showered me in all my life. Acha, Amma and Etta, I dedicate this work to you. Everything I am today; I owe it to you. Thank you.

TABLE OF CONTENTS

| | |
|--|------|
| ACKNOWLEDGEMENTS | ii |
| LIST OF TABLES | viii |
| LIST OF FIGURES | ix |
| ABBREVIATIONS AND SYMBOLS | xvi |
| ABSTRACT | xx |

CHAPTERS

1. BACKGROUND AND SIGNIFICANCE

| | |
|--|----|
| 1.1 Pulmonary fibrosis..... | 1 |
| 1.2 PF pathogenesis..... | 4 |
| 1.2.1 Induced oxidative stress in PF pathogenesis..... | 5 |
| 1.2.2 Induced TGF- β in PF pathogenesis..... | 6 |
| 1.2.3 Induced TGF- β 1 promoting fibroblast proliferation, differentiation and collagen synthesis..... | 8 |
| 1.2.4 Induced epithelial-to-mesenchymal transition (EMT) in PF pathogenesis... | 9 |
| 1.2.5 Role of Tyrosine kinases in pathogenesis of PF..... | 12 |
| 1.3 Treatment options of PF..... | 13 |
| 1.4 Melatonin and curcumin for therapeutic use in PF..... | 16 |
| 1.5 Melatonin-curcumin (MEL-CUR) hybrid molecules..... | 18 |

2. SPECIFIC AIMS AND HYPOTHESES.....24

| | |
|---|----|
| 3. <i>IN VITRO</i> ANTI-OXIDATIVE ACTIVITY OF MEL-CUR HYBRID AM24 | |
| 3.1 Introduction..... | 26 |
| 3.2 Materials and Methods | |
| 3.2.1 Materials..... | 27 |
| 3.2.2 <i>In vitro</i> ABTS-based free radical scavenging assay..... | 27 |
| 3.3 Results and Discussion..... | 29 |
| | |
| 4. <i>IN VITRO</i> ANTI-FIBROTIC ACTIVITIES OF MEL-CUR HYBRID AM24 | |
| 4.1 Introduction..... | 35 |
| 4.2 Material and Methods | |
| 4.2.1 Materials..... | 37 |
| 4.2.2 Human lung fibroblasts: MRC-5 and NHLF cells..... | 37 |
| 4.2.3 <i>In vitro</i> assessment of TGF- β 1 induced lung fibroblast collagen..... | 38 |
| 4.2.4 <i>In vitro</i> assessment of TGF- β 1 induced lung fibroblast proliferation..... | 39 |
| 4.2.5 <i>In vitro</i> assessment of TGF- β 1 induced lung fibroblast differentiation to myofibroblast..... | 39 |
| 4.2.6 Data description and statistical analyses..... | 41 |
| 4.3 Results | |
| 4.3.1 Inhibition against TGF- β 1 induced lung fibroblast collagen increase..... | 42 |
| 4.3.2 Inhibition against TGF- β 1 induced lung fibroblast proliferation..... | 47 |
| 4.3.3 Inhibition against TGF- β 1 induced lung fibroblast differentiation to myofibroblasts..... | 51 |
| 4.4 Discussion..... | 53 |

| | |
|--|----|
| 5. <i>IN VITRO</i> INHIBITORY ACTIVITY OF MEL-CUR HYBRID AM24 AGAINST TGF-β1 INDUCED EPITHELIAL-MESENCHYMAL TRANSITION (EMT) | |
| 5.1 Introduction..... | 59 |
| 5.2 Materials and Methods | |
| 5.2.1 <i>In vitro</i> TGF- β 1 induced EMT assessment in the A549 cells..... | 60 |
| 5.2.2 Data description and statistical analyses..... | 61 |
| 5.3 Results and Discussion | |
| 5.3.1 Effect of AM24 and comparator molecules on TGF- β 1 induced EMT..... | 62 |
| | |
| 6. <i>IN VIVO</i> INTERVENTION OF AM24 IN BLEOMYCIN-INDUCED PULMONARY FIBROSIS IN RATS | |
| 6.1 Introduction..... | 69 |
| 6.2 Materials and Methods | |
| 6.2.1 Animals..... | 70 |
| 6.2.2 A rat model of BLM-induced PF and AM24 treatment..... | 70 |
| 6.2.3 Treadmill exercise endurance test..... | 72 |
| 6.2.4 Histological and morphological airspace examination..... | 73 |
| 6.2.5 Determination of lung tissue collagen..... | 73 |
| 6.2.6 Lung tissue biomarker assessments by Western blot..... | 74 |
| 6.2.7 Data description and statistical analyses..... | 75 |
| 6.3 Results | |
| 6.3.1 Changes of body weight and treadmill exercise endurance..... | 76 |

| | |
|---|------------|
| 6.3.2 Fibrotic tissues and alveolar structure destruction/loss..... | 79 |
| 6.3.3 Lung tissue collagen deposition..... | 83 |
| 6.3.4 Lung expressions of TGF- β 1, PCNA, α -SMA, E-cadherin and vimentin..... | 84 |
| 6.3.5 Lung expressions of cathepsin K..... | 89 |
| 6.4 Discussion..... | 91 |
| 7. CONCLUSIONS..... | 102 |
| | |
| APPENDICES..... | 105 |
| REFERENCES..... | 113 |
| DATA SHEETS..... | 128 |

LIST OF TABLES

| | | |
|-----------|---|----|
| Table 1.1 | Key recommendation on pharmacological treatment of PF according to the 2015 and 2011 guidelines..... | 14 |
| Table 3.1 | The IC ₅₀ and HS values for the ABTS-based free radical scavenging activities of AM24, MEL and CUR, derived from curve-fitting of the profiles shown in Figure 3.1, alongside the COD and MSC values of the curve-fitting..... | 31 |
| Table 6.1 | Experimental groups in the establishment of the dose for PF induction and treatment..... | 92 |

LIST OF FIGURES

| | | |
|------------|--|----|
| Figure 1.1 | Disease progression over time in PF patients. Despite differences in the rate of disease progression among patients, the majority are ‘slow progressors’, i.e., slow but steady progression. Some patients remain ‘stable’, while a few show ‘rapid progression’ i.e., accelerated decline in lung function, leading to death. Few patients show ‘acute worsening’ of disease due to unknown causes as indicated by lightning bolt (Raghu et al., 2010)..... | 3 |
| Figure 1.2 | A reciprocal regulation of TGF- β 1 and redox imbalance in PF lung (Liu et al., 2015) | 5 |
| Figure 1.3 | TGF- β 1 centered pathogenesis of PF. Upon activation due to epithelial injury, TGF- β 1 induces epithelial cell death and EMT as well as fibroblast proliferation and differentiation, thereby resulting in increased ECM (collagen) deposition. Due to the initial injury, there is an increase in the oxidative stress as well as inflammatory markers..... | 7 |
| Figure 1.4 | Differentiation of fibroblasts to myofibroblasts under the influence of TGF- β (Darby et al., 2014)..... | 8 |
| Figure 1.5 | Occurrence of EMT and the transition of stationary epithelial cells to motile mesenchymal cells. (Kalluri et al. , 2009)..... | 10 |
| Figure 1.6 | Injury triggered EMT in physiologic and pathologic conditions. (Stone et al., 2016)..... | 11 |
| Figure 1.7 | Structure of MEL..... | 16 |

| | | |
|-------------|--|----|
| Figure 1.8 | Structure of CUR..... | 17 |
| Figure 1.9 | A series of MEL-CUR hybrid molecules. (Chojnacki et al., 2014)..... | 21 |
| Figure 1.10 | Inhibitory activities of AM24 and AM42 at 10 μ M against TGF- β 1 induced collagen synthesis in the human lung fibroblast MRC-5 cells | 22 |
| Figure 1.11 | Structure of AM24..... | 22 |
| Figure 3.1 | The profiles of fraction of ABTS \bullet + formed vs. logarithmic concentration to demonstrate and assess the radical scavenging activity of AM24, MEL and CUR..... | 30 |
| Figure 3.2 | Single electron transfer in MEL leading to the formation of MEL radical cation that acts as a radical scavenger and gives rise to the cascade radical scavenging activity. (John and Platts et al., 2014)..... | 32 |
| Figure 3.3 | Possible sites of attack of free radical oxidants with CUR and stabilization of phenoxyl intermediate (Priyadarshini KI, 2014)..... | 33 |
| Figure 3.4 | Structure of AM24. The red box indicates the absence of the β -diketone..... | 34 |
| Figure 4.1 | <i>In vitro</i> MRC-5 cellular collagen masses measured with the 540 nm absorbance by the validated picosirius red method following incubation of AM24 at 0-10 μ M for 48 hours in the absence or presence of TGF- β 1 induction (10 ng/ml)..... | 43 |
| Figure 4.2 | Effects of AM24, MEL, CUR, MEL+CUR and PIR at 10 μ M and PIR at 500 μ M on the <i>in vitro</i> MRC-5 cellular collagen mass measured with the 540 nm absorbance by the validated picosirius red method following 48-hour incubation with/without TGF- β 1 induction..... | 44 |

| | | |
|------------|--|----|
| Figure 4.3 | Effects of AM24 at 10 μ M on the <i>in vitro</i> NHLF cellular collagen mass measured with the 540 nm absorbance by the validated picosirius red method at 48 hours following incubation with TGF- β 1 induction..... | 45 |
| Figure 4.4 | Effect of LUZ (0.1 μ M; a pan-melatonin receptor antagonist) on the inhibitory activity of AM24 (10 μ M) against the <i>in vitro</i> TGF- β 1 induced MRC-5 cellular collagen increase measured with the 540 nm absorbance by the validated picosirius red method. | 46 |
| Figure 4.5 | <i>In vitro</i> MRC-5 cell proliferative activities measured with the Δ absorbance at 590 nm by the MTT assay following incubation with AM24, MEL, CUR and PIR at 10 μ M for 48 hours in the absence or presence of TGF- β 1 induction (10 ng/ml) | 48 |
| Figure 4.6 | <i>In vitro</i> MRC-5 cell proliferative activities measured with the Δ absorbance at 590 nm by the MTT assay following incubation with AM24 at 0-10 μ M for 72 hours in the absence or presence of TGF- β 1 induction (10 ng/ml) | 49 |
| Figure 4.7 | Effects of AM24, MEL, CUR, MEL+CUR and PIR at 10 μ M and PIR at 500 μ M on the <i>in vitro</i> MRC-5 cell proliferative activities measured with the Δ absorbance at 590 nm by the MTT assay following 72-hour incubation with/without TGF- β 1 induction. | 50 |
| Figure 4.8 | Representative images of MRC-5 cellular expressions of α -SMA following 72-hour incubation with AM24 (1 or 10 μ M) and CUR, MEL, MEL-CUR and PIR (10 μ M) with TGF- β 1 induction, measured by Western blot. The GAPDH expression of the corresponding samples was used as loading control for quantitative comparison shown in Figure 4.11. | 51 |

| | |
|-------------|---|
| Figure 4.9 | MRC-5 cellular expressions of α -SMA following 72-hour incubation with AM24 (1 or 10 μ M) and CUR, MEL, MEL-CUR and PIR (10 μ M) with TGF- β 1 induction, measured by Western blot. The band signal for α -SMA in each sample was quantified and normalized with that for GAPDH in the corresponding sample, which was then compared among the groups with or without treatment and induction with a value relative to that for the vehicle-treated and uninduced control.52 |
| Figure 4.10 | <i>In vitro</i> induction in collagen synthesis by TGF- β 1 at 10 ng/mL at 48 hours normalized to the proliferation at 48 hours.54 |
| Figure 4.11 | TGF- β 1 induced differentiation of fibroblasts to myofibroblasts A) At 48 hours and B) At 72 hours.55 |
| Figure 5.1 | Representative western blot image of A549 cell expression of E-cadherin and Vimentin at 72 hours with or without TGF- β 1 and/or test molecules.....63 |
| Figure 5.2 | In vitro effect of test molecules AM24 (1, 10 μ M), CUR, MEL, CUR+MEL and PIR at 10 μ M on TGF- β 1 induced EMT and thus the levels of epithelial marker E-cadherin at 72 hours.....64 |
| Figure 5.3 | In vitro effect of test molecules AM24 (1, 10 μ M), CUR, MEL, CUR+MEL and PIR at 10 μ M on TGF- β 1 induced EMT and thus the levels of mesenchymal marker vimentin at 72 hours.....65 |
| Figure 5.4 | In vitro effect of test molecules AM24 (1, 10 μ M), CUR, MEL, CUR+MEL and PIR at 10 μ M on TGF- β 1 induced EMT and thus the levels of mesenchymal marker vimentin at 72 hours. A) Data are n=2 B) Data is n=1 indicating that the |

trend of vimentin increase/decrease remains the same despite high SD.....66

Figure 6.1 An experimental protocol for PF induction with BLM and subsequent AM24 treatment in rats, alongside several tests for assessments. While BLM was dosed to the lungs on day 1, AM24 was dosed to the lungs at 0.1 mg/kg on day 1, 3, 5, 8, 10, 12 and 15 (i.e., ~every other day).....72

Figure 6.2 Body weight changes during 16 days in 3 groups of rats with or without BLM induction and/or AM24 treatment. Healthy: healthy rats without BLM induction and AM24 treatment; BLM + Untreated: BLM-induced rats without AM24 treatment; and BLM + Treated: BLM-induced rats treated with AM24. BLM: 0.6 mg/kg on day 1; and AM24: 0.1 mg/kg every other day over the two week period.77

Figure 6.3 Pre- and post-dose treadmill exercise endurance in three groups of rats with or without BLM induction and/or AM24 treatment. Healthy : healthy rats without BLM induction and AM24 treatment; BLM + Untreated : BLM-induced rats without AM24 treatment; and BLM + Treated : BLM-induced rats treated with AM24. BLM: 0.6 mg/kg on day 1; and AM24: 0.1 mg/kg every78

Figure 6.4 9 hematoxylin-eosin stained airspace images taken from one rat as a representation of each of the 3 different induction/treatment groups. (A) “Healthy” rat; (B) “BLM + Untreated” rat; and (C) “BLM + Treated” rat.....80

Figure 6.5 Lung tissue collagen deposition in the three different induction/treatment groups, measured as the absorbance at 540 nm by the picosirius red assay. Healthy (n=2): healthy rats without BLM induction and AM24 treatment; BLM

| | | |
|-------------|---|----|
| | + Untreated (n=4): BLM-induced rats without AM24 treatment; and BLM + Treated (n=5): BLM-induced rats treated with AM24. BLM: 0.6 mg/kg on day 1; and AM24: 0.1 mg/kg every other day over the two week period..... | 83 |
| Figure 6.6 | Lung tissue expressions of TGF- β 1 in the three different induction/treatment groups of rats, measured by Western blot analysis: Upper panel: representative Western blot band images; and Lower panel: densitometric band signals relative to the “Healthy” rats..... | 85 |
| Figure 6.7 | Lung tissue expressions of PCNA in the three different induction/treatment groups of rats, measured by Western blot analysis: Upper panel: representative Western blot band images; and Lower panel: densitometric band signals relative to the “Healthy” rats..... | 86 |
| Figure 6.8 | Lung tissue expressions of α -SMA in the three different induction/treatment groups of rats, measured by Western blot analysis: Upper panel: representative Western blot band images; and lower panel: Densitometric band signals relative to the “Healthy” rats. | 87 |
| Figure 6.9 | Lung tissue expressions of (A) E-cadherin and (B) vimentin in the three different induction/treatment groups of rats, measured by Western blot analysis: Upper panel: representative Western blot band images; and Lower panel: densitometric band signals relative to the “Healthy” rats. | 88 |
| Figure 6.10 | Lung tissue expressions of cathepsin K in the three different induction/treatment groups of rats, measured by Western blot analysis: Upper panel: representative Western blot band images; and lower panel: Densitometric band signals relative to the “Healthy” rats..... | 90 |

Figure 6.11 Comparison of exercise endurance time (min) across 3 doses of BLM which led to the selection of 0.6 mg/kg BLM.....93

Figure 6.12 Representative images of 4 rats dosed with different doses of BLM for visual observation of variation in the development of fibrotic mass. (A) BLM – 4 mg/kg (B) BLM- 0.8 mg/kg (C) BLM – 0.6 mg/kg (D) BLM – 0.4 mg/kg.....94

Figure 6.13 Comparison of exercise endurance time (min) across 2 doses of AM24 which led to the selection of 0.1 mg/kg of AM24.97

Figure 6.14 Representative images of histological sections of two concentrations of AM24, (A) 0.05 mg/kg (B) 0.1 mg/kg.98

ABBREVIATIONS AND SYMBOLS

| | |
|--------|--|
| % | percentage |
| = | equal to |
| ~ | approximately |
| < | less than |
| > | greater than |
| ± | plus or minus |
| °C | temperature in celsius scale |
| α-SMA | alpha smooth muscle actin |
| A549 | Adenocarcinomic human alveolar basal epithelial cells |
| AAALAC | Association for Assessment and Accreditation of Laboratory Animal Care |
| ABTS | 2,2'-azino-di-[3-ethylbenthalzoline sulphonate] |
| ABTS•+ | 2,2-azinobis(3-ethyl-benzothiazoline-6-sulphonic acid) |
| ΔAbs | Change in absorbance |
| ALAT | American Lung Association of Texas |
| ANOVA | analysis of variance |
| ATCC | American Type Culture Collection |
| ATS | American Thoracic Society |
| BLM | Bleomycin |
| BSA | Bovine serum albumin |
| C | Concentration |
| CHAPS | 3-[(3-cholamidopropyl)dimethylammonio]-1-propanesulfonate |

| | |
|-------|---|
| CI | Confidence interval |
| COD | Coefficient of determination |
| CUR | Curcumin |
| Da | Dalton |
| DCI | Dichloro-isocoumarin |
| DDW | Distilled deionized water |
| DMEM | Dulbecco's Modified Eagle media |
| DMSO | Dimethyl sulfoxide |
| E64 | trans-epoxysuccinyl-leucylamido-[4-guanido]butane |
| EBV | Epstein-barr virus |
| ECM | Extracellular matrix |
| EDTA | Ethylenediaminetetraacetic acid |
| ELISA | Enzyme linked immunosorbent assay |
| EMT | Epithelial to mesenchymal transition |
| EtOH | Ethanol |
| ERS | European Respiratory Society |
| FBS | Fetal bovine serum |
| FDA | Food and Drug Administration |
| FGF | Fibroblast growth factor |
| FGM | Fibroblast growth media |
| FVC | Forced vital capacity |
| GAPDH | Glyceraldehyde 3-phosphate dehydrogenase |
| GPCR | G-protein coupled receptor |

| | |
|------------------|---|
| GRADE | Grading of recommendation, assessment, development and evaluation |
| GSH | Glutathione |
| H&E | hematoxylin-eosin |
| HIPPO | protein kinase hippo |
| HRP | Horseradish peroxidase |
| HS | Hill slope |
| IACUC | Institutional Animal Care and Use Committee |
| IC ₅₀ | Half-maximal inhibitory concentration |
| IgG | Immunoglobulin G |
| JRS | Japanese Respiratory Society |
| kDa | kilo dalton |
| LogP | partition coefficient |
| LUZ | Luzindole |
| mAB | monoclonal Antibody |
| MEL | Melatonin |
| MEL-CUR | Melatonin and curcumin physical ad-mixture |
| min | minutes |
| MMP | Matric metalloproteinase |
| MRC-5 | Medical Research Council cell strain 5 |
| MSC | Model selection criterion |
| MT1 | Melatonin receptor-1 |
| MT2 | Melatonin receptor-2 |
| MTT | 3-[4,5-dimethylthiazol-2-yl]-2,5-diphenyltetrazolium bromide |

| | |
|----------------|---|
| NAC | N-acetylcystein |
| NADPH | Nicotinamide adenine dinucleotide phosphate |
| NHLF | Normal human lung fibroblasts |
| NP-40 | Nonidet P-40 lysis buffer |
| NS | Not significant |
| PBS | Phosphate buffered saline |
| PCNA | Proliferating cell nuclear antigen |
| PDGF | Platelet derived growth factor |
| PF | Pulmonary Fibrosis |
| PIR | Pirfenidone |
| ROS | Reactive oxygen species |
| SD | Standard deviation |
| SE | Standard error |
| T | temperature |
| TBS | tris buffered saline |
| TGF- β 1 | Transforming growth factor beta-1 |
| US | United States |
| VEGF | Vascular endothelial growth factor |
| VCU | Virginia Commonwealth University |
| WHO | World Health Organization |
| YAP1 | Yes associated protein-1 |

ABSTRACT

A HYBRID MOLECULE OF MELATONIN AND CURCUMIN FOR THERAPEUTIC USE IN PULMONARY FIBROSIS

by Varsha V. Nair, B.Pharm.

A thesis submitted in partial fulfillment of the requirements for the degree of Master of Science at Virginia Commonwealth University

Advisor : Masahiro Sakagami, Ph.D.
Professor
Department of Pharmaceutics, School of Pharmacy

Pulmonary fibrosis (PF) is a serious lung disease, as its life expectancy is only 3-5 years upon occurrence and more than 50 % of the cases are idiopathic, i.e., unknown cause. Two drugs, pirfenidone (PIR) and nintedanib, have recently been approved; however, their efficacies are moderate without evidence of prolonged survival. While this is primarily due to our insufficient knowledge about key PF pathogenesis, inductions of oxidative stress and transforming growth factor- β 1 (TGF- β 1) have been suggested in PF lungs. Hence, anti-oxidative melatonin (MEL) and curcumin (CUR) have been studied yet their efficacies remain moderate without clear understanding about the mechanisms of action. Accordingly, this project hypothesized that a novel hybrid molecule of MEL and CUR, AM24, was a more potent inhibitor against oxidative stress and TGF- β 1 induced PF pathobiologic events than MEL or CUR, so that its pulmonary delivery enabled therapeutic intervention in an animal model of PF. Free radical scavenging activity and various *in vitro* lung cell-based anti-fibrotic activities of AM24 were determined and compared with those of MEL and CUR as well as their admixture (MEL+CUR) and PIR. Pulmonary

administration of AM24 was then examined for therapeutic intervention in a rat model of bleomycin (BLM)-induced experimental PF.

AM24 was equipotent to MEL, but less potent than CUR in the hydrogen peroxide-induced free radical (ABTS) scavenging assay, ranked with the half-maximal inhibitory concentration (IC₅₀) of 25.7, 32.0 and 11.4 μ M, respectively. However, in the *in vitro* human lung fibroblast systems, AM24 was shown to be more potent than MEL or CUR and notably than MEL+CUR or PIR in the TGF- β 1 induced 1) collagen synthesis by the picosirius red assay, 2) proliferation by the MTT assay; and 3) differentiation to myofibroblast by western blot analysis of a myofibroblast marker, α -smooth muscle actin (α -SMA). In detail, at 10 μ M, AM24 inhibited TGF- β 1 induced 1) collagen synthesis by 90 %; 2) proliferation by ~72 %; and 3) differentiation to myofibroblast completely, while MEL, CUR, MEL+CUR and PIR resulted in 30-55 % or insignificant inhibition. In addition, in the *in vitro* human lung alveolar epithelial cell system, AM24 at 10 μ M almost completely inhibited TGF- β 1 induced epithelial-mesenchymal transition (EMT), as measured with western blot expressions of an epithelial marker, E-cadherin, and a mesenchymal marker, vimentin. Again, MEL, CUR, MEL+CUR and PIR exerted much less inhibitory activities. Hence, all these results consistently suggested that AM24 was a unique hybrid molecule of MEL and CUR and possessed highly potent anti-fibrotic activities in addition to the free radical scavenging activity.

AM24 was then examined for therapeutic intervention in an *in vivo* rat model of BLM-induced PF. BLM was orotracheally spray-dosed to the lungs at 0.6 mg/kg on day 1 to develop experimental PF in 14 days. Lung administrations of AM24 at 0.1 mg/kg commenced at 6 hours of BLM induction on day 1 and continued thrice weekly over two weeks. Functional treadmill exercise endurance was measured on day 12 and 15; and lungs were harvested upon sacrifice on

day 16. Overall, AM24 showed significant intervention activities as follows: 1) exercise endurance was reduced only ~20%, much lower than 78% of the untreated PF rats; 2) reduced fibrotic tissue area and alveolar structural destruction were seen by histological examinations; and 3) lung's induced collagen deposition was inhibited by ~78 %. However, unlike the literature, the lung's TGF- β 1, PCNA (a cell proliferation marker), and α -SMA (a differentiation marker), were not largely induced in the BLM-induced PF model, so that the intervention activities of AM24 to these markers were not clearly shown. In contrast, induced EMT was seen in the BLM-induced model, represented by increased mesenchymal marker, vimentin, and by decreased epithelial marker, E-cadherin; and AM24 appeared to counter this induced EMT. Accordingly, while the BLM-induced PF model may need further optimizations for clearer pathogenic changes, AM24 exerted certain degree of *in vivo* efficacies with a lung dose of 0.1 mg/kg, which was much lower than the effective doses of MEL, CUR, PIR and nintedanib seen in the literature with BLM induced PF model.

In conclusion, this thesis study has provided an early proof-of-concept for AM24, a novel MEL-CUR hybrid molecule, being potently anti-oxidative and anti-fibrotic in the *in vitro* lung cell-based assessments. As a result, AM24 enabled therapeutic intervention just with a lung dose of 0.1 mg/kg in the BLM-induced rat model of experimental PF.

CHAPTER 1

BACKGROUND AND SIGNIFICANCE

1.1 Pulmonary fibrosis

Pulmonary fibrosis (PF) is a life-threatening lung disease that progressively causes formation of scarred, thickened and stiff alveoli (Zisman et al, 2005). More than 50 % of the cases are idiopathic i.e. causes are unknown. Such idiopathic PF is defined as a specific form of chronic, progressive fibrosing interstitial pneumonia of unknown origin (Raghu et al, 2011). This fibrosis replaces healthy tissues with altered extracellular matrix (ECM) and destroys alveolar architecture, leading to restricted ventilation, disrupted gas exchange, exercise limitation, poor quality of life, and ultimately, death (Ley and Collard, 2005). The life expectancy of PF patients is only 3-5 years upon disease occurrence. PF is more common in men than in women and is seen mostly in elderly (>50 years old) populations. The median age of diagnosis is 65 years old. PF prevalence is estimated to range from 2.8 to 18 cases per 100,000 people in Europe and North America and 0.5 to 4.2 cases per 100,000 people in Asia and South America (Richeldi et al, 2017). It has also been shown that whites are more predisposed to develop PF than blacks, while the mortality rate is higher in blacks (Swigris et al, 2012).

No symptom may be seen in the early stage of PF, i.e., asymptomatic; yet progression of the disease is relatively fast and highly variable (Raghu et al, 2011). The initial characteristic symptom is breathlessness, while the other symptoms include unexplained chronic exertional dyspnea, cough (without sputum for over 30 days), bibasilar inspiratory crackles, finger clubbing and unintended weight loss (Raghu et al, 2011; American Lung Association, 2018; National

Organization of Rare Disorders, 2017). In idiopathic PF, a number of potential risk factors have been identified, as follows (Baumgartner et al, 1997; King, 2011; Raghu et al, 2011):

- a) Cigarette smoking
- b) Environmental exposure, e.g., metal (lead, brass, asbestos) and wood dusts
- c) Microbial agents, e.g., Epstein-Barr virus (EBV) and hepatitis C
- d) Genetic factors, e.g., genes encoding for profibrotic molecules (transforming growth factor- β 1), surfactant protein A and B, and matrix metalloproteinase (MMP); and polymorphism of genes encoding for certain cytokines (IL-4, IL-6, IL-8 and IL-10)
- e) Comorbidities, e.g., gastroesophageal reflux, obstructive sleep apnea, coronary artery disease, emphysema, pulmonary hypertension

Even so, PF is difficult for diagnosis in terms of its causes, symptoms and pathogenesis due to its poor disease characterization. Despite a lack of specific test for PF diagnosis, a diagnostic criterion has been published as the ATS/ERS/JRS/ALAT consensus statement, recommending a use of high resolution computerized tomography to identify the presence of usual interstitial pneumonia as its diagnosis (Raghu et al, 2011). The PF diagnosis also includes other criteria, such as exclusion of other known interstitial lung diseases, abnormally-restricted lung function (reduced vital capacity), impaired gas exchange and transbronchial lung biopsy or bronchoalveolar lavage negating the presence of any other interstitial lung disease. Minor criteria for diagnosis include age > 50 years old, illness lasting for > 3 months, dyspnea on exertion and presence of inspiratory crackles (Lynch et al, 2018; Raghu et al, 2011; Wells et al, 2013).

PF shows a progressive decline in lung functions, eventually leading to death due to respiratory failure or other comorbidity. Such PF progression differs among patients and has been classified as shown in Figure 1.1 (Raghu et al, 2010). Most patients are slow progressors, while

some remain stable and others show a rapid progression. Few patients experience acute respiratory worsening. The causes of such different disease progression among patients may be geographic, ethnic, racial or presence of comorbid diseases like emphysema and pulmonary hypertension (Gross et al, 2001; Ley et al, 2010; Meltzer and Noble, 2007; Raghu et al, 2010).

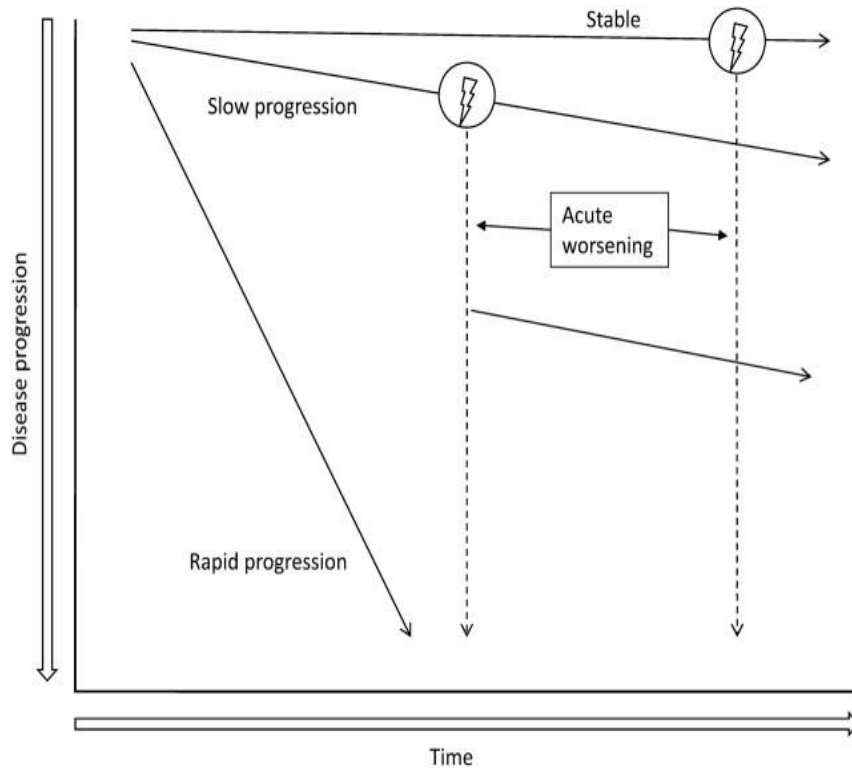


Figure 1.1: Disease progression over time in PF patients. Despite differences in the rate of disease progression among patients, the majority are ‘slow progressors’, i.e., slow but steady progression. Some patients remain ‘stable’, while a few show ‘rapid progression’ i.e., accelerated decline in lung function, leading to death. Few patients show ‘acute worsening’ of disease due to unknown causes as indicated by lightning bolt (Raghu et al, 2010).

1.2 PF pathogenesis

As the causes of PF are not completely known, the pathogenesis of PF remains still unclear, yet several hypotheses have been proposed in this complex interstitial disease. In early times, PF was thought to be a chronic inflammatory disorder that gradually progressed to fibrosis. However, since anti-inflammatory therapy failed to improve the condition of PF patients, this hypothesis was discredited. Currently, PF is considered to be a consequence of genetic predisposition and age-related factors along with recurrent micro injuries to the aged alveolar epithelia. This injury leads to increased oxidative stress and abnormal epithelial-fibroblast communication to induce myofibroblasts for ECM production, which leads to ECM deposition and an imbalance between profibrotic and fibrotic mediators, and thus, chronic fibroproliferation. Increased oxidative stress could also be associated with aging (Meyer, 2017; Richeldi et al, 2017; Sgalla et al, 2018).

1.2.1 Induced oxidative stress in PF pathogenesis

Oxidative stress is an important mechanism that encompasses molecular, cellular and tissue abnormalities underlying fibrosis, as the lungs are exposed to the highest level of oxygen. These abnormalities occur as a result of excess reactive oxygen species (ROS) production and depletion of antioxidant enzymes (Cheresh et al, 2013). In fact, oxidant-antioxidant imbalance has been seen in the lungs of patients with idiopathic PF due to increased ROS production a) with environmental toxins (e.g., tobacco, asbestos, and radiation) and b) from lung cells like epithelial, endothelial and mesenchymal cells. The bronchoalveolar lavage fluid of idiopathic PF patients show elevated levels of eosinophils and myeloperoxidase, which suggested the pathogenic role of neutrophils, oxidation and inflammation in PF. The decreased levels of antioxidant enzymes (e.g., glutathione

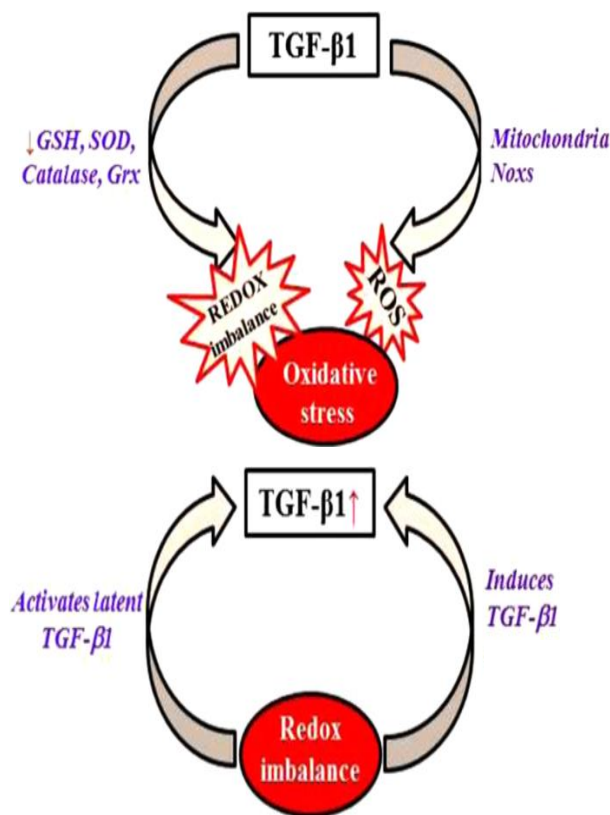


Figure 1.2: A reciprocal regulation of TGF-β1 and redox imbalance in PF lung (Liu et al., 2015)

(GSH), glutathione peroxidase, catalase, and superoxide dismutase) also adds to this imbalance. In fact, the lower levels of GSH has been shown in the lung epithelial lining fluid of IPF patients, compared to healthy subjects (Fois et al, 2018; Kinnula, 2005). TGF-β1 aggravates this redox imbalance by inducing mitochondrial ROS production and nicotinamide adenine dinucleotide phosphate (NADPH) oxidases, and by downregulating the expression/activity of GSH, catalase, superoxide dismutase and glutaredoxin, as seen in Figure 1.2 (Liu et al., 2015).

1.2.2 Induced TGF- β in PF pathogenesis

One of the most extensively studied profibrotic cytokines is transforming growth factor- β (TGF- β). TGF- β exists in 3 isoforms (TGF- β 1/2/3) that are normally bound to latency-associated protein in their inactive form. Each isoform is expressed in a distinct tissue specific manner. TGF- β 1 is however said to be the most prevalent form while the other isoforms are expressed in a lesser number of cells and tissues. However, despite the presence of all 3 isoforms in fibrotic tissue, the development of fibrosis is attributed to TGF- β 1 (Biernacka et al, 2011). During PF development, recurrent injury to the alveolar epithelial cells lead to TGF- β activation (Wolters et al, 2013). Thus, the levels of active TGF- β have been shown to be increased in patients with PF which promotes epithelial cell apoptosis, epithelial to mesenchymal transition (EMT), fibroblast proliferation and differentiation to myofibroblast, and therefore ECM deposition (Figure 1.2). As a response to repeated injury to the epithelia, oxidative stress is also increased. This increase of oxidative stress is indeed promoted by aging. Increased inflammatory factors are also seen in PF patients as a response to the recurrent injury (Meyer, 2017; Sgalla et al, 2018; Wilson and Wynn, 2008; Wolters et al, 2013).

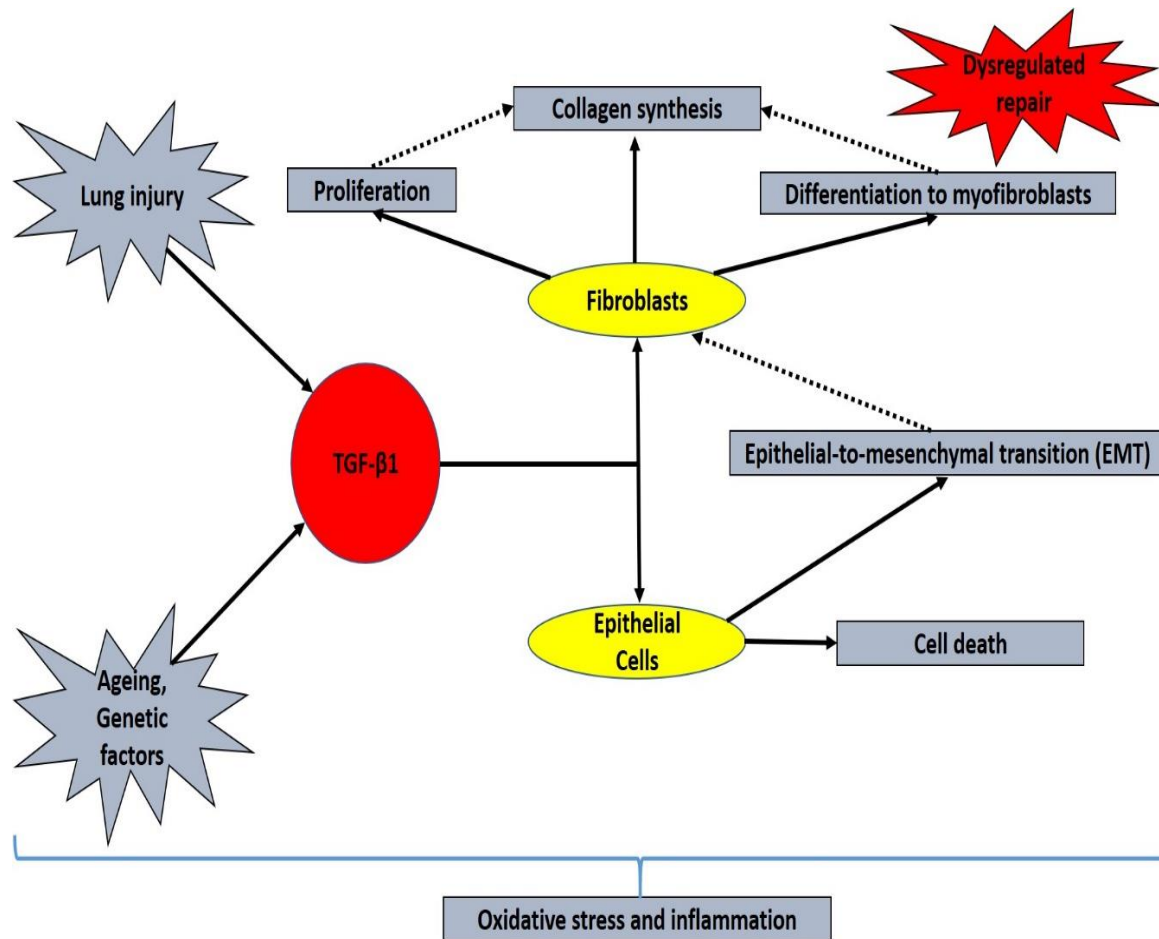


Figure 1.3: TGF-β1 centered pathogenesis of PF. Upon activation due to epithelial injury, TGF-β1 induces epithelial cell death and EMT as well as fibroblast proliferation and differentiation, thereby resulting in increased ECM (collagen) deposition. Due to the initial injury, there is an increase in the oxidative stress as well as inflammatory markers.

1.2.3 Induced fibroblast proliferation, differentiation and collagen synthesis

TGF- β 1 is an important mediator of fibroblast phenotype and function. TGF- β 1 has been suggested to induce fibroblast proliferation by inducing fibroblast growth factor-2; (Yue et al, 2010), however, its exact mechanism is still unclear. TGF- β 1 also activates fibroblasts to undergo phenotypic changes to myofibroblasts (Figure 1.4). Myofibroblasts are the cellular orchestrators of ECM synthesis and thus fibrosis. Myofibroblasts are phenotypically intermediate between fibroblasts and smooth muscles, while differing from fibroblasts due to the presence of α -smooth muscle actin (α -SMA). Under normal conditions, myofibroblasts are involved in wound healing. However, under disease conditions, they induce excessive ECM synthesis. Myofibroblasts may be derived from two cellular sources: 1) proliferation and differentiation of fibroblasts; 2) epithelial-mesenchymal transition (EMT). Notably, both events are induced as a result of TGF- β 1 induction (Darby and Hewitson, 2007; Darby et al, 2014; Phan, 2008; and Yue et al, 2010).

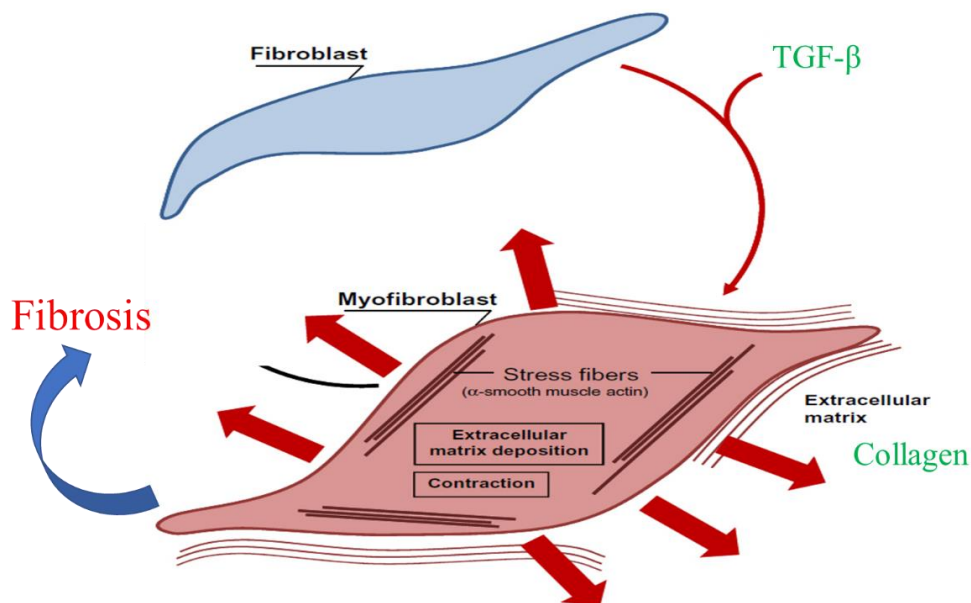


Figure 1.4: Differentiation of fibroblasts to myofibroblasts under the influence of TGF- β (Darby et al., 2014)

TGF- β 1 is also a potent inducer of ECM production and promotes matrix preservation and deposition by enhancing matrix protein synthesis and changing the balance between matrix-preserving and matrix-degrading signals (Biernacka, 2011; Verrecchia et al., 2007). Increased ECM production of collagen, fibronectin, and tenascin C cause formation of fibrotic tissues. Animal models of PF have suggested that elevation of TGF- β 1 expression causes increased collagen synthesis and deposition. Collagen I is the major collagen produced by both fibroblasts and myofibroblasts; and consists of two α 1 (COL1 α 1) and one α 2 (COL1 α 2) chains. TGF- β 1 potently stimulates the transcription of both COL1 α 1 and COL1 α 2 (Leask and Abraham, 2004; Yue et al, 2010).

Taken all together, therefore, TGF- β 1 induction has deleterious effects on fibroblasts, as causing abnormally induced proliferation, differentiation and thereby deposition of excess ECM to form fibrotic scars in the lung tissues.

1.2.4 Induced epithelial-to-mesenchymal transition (EMT) in PF pathogenesis

EMT is a central mechanism by which epithelial cells undergo phenotypic changes and convert to mesenchymal cells, as depicted in Figure 1.5 (Kalluri et al., 2009). Epithelial cells are stationary, yet undergo phenotypic changes like losses of cell-cell adhesion and apical-basal polarity to form migratory mesenchymal cells. EMT is identified by a change in the epithelial proteome. Epithelial proteins such as E-cadherin are lost, while mesenchymal proteins such as vimentin, N-cadherin, and fibronectin, emerge. E-cadherin is responsible for the maintenance of cell-cell contact via adherent junctions and thus contribute to the immobility of the cells (Huang et al., 2012). E-cadherin is also downregulated as a result of increased vimentin which increases

the cell surface trafficking (Mendez et al., 2010). Loss of E-cadherin is a hallmark event of EMT that leads to a series of signaling events and major cytoskeletal reorganization (Xu et al, 2009).

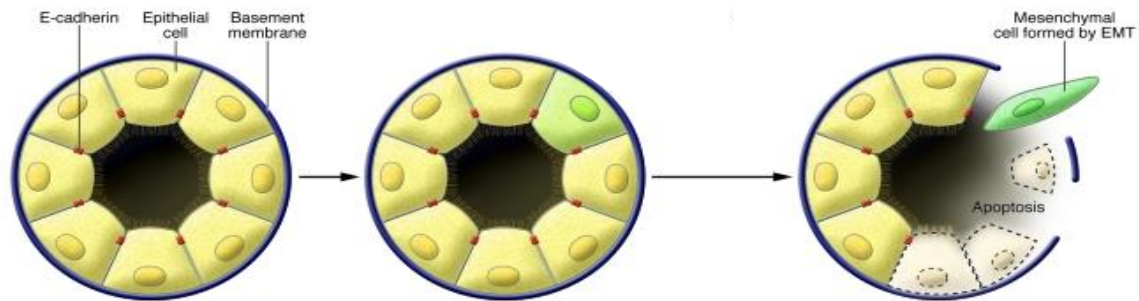


Figure 1.5: EMT: transition of stationary epithelial cells to motile mesenchymal cells (Kalluri et al., 2009).

However, EMT is not a process exclusive for PF and can be classified into three subtypes:

Type I – EMT during embryogenesis, implantation and organ development

Type II – EMT associated with tissue regeneration and organ fibrosis

Type III – EMT associated with cancer progression and metastasis

Unlike Type I and III, Type II EMT is the only one that is caused by damage and inflammation and thus is involved in fibrosis (Volk et al., 2013). EMT is also required for proper re-epithelialization (wound healing) and ECM deposition. Continued transition of epithelial cells to mesenchymal cells leads to excessive myofibroblasts formation, and thus PF. Figure 1.6 differentiates the normal wound healing process from the genesis of fibrosis. TGF- β 1 has been identified as the main inducer of EMT due to its ability to continually sustain myofibroblast activation, however the exact mechanism of this action remains unknown (Stone et al., 2016).

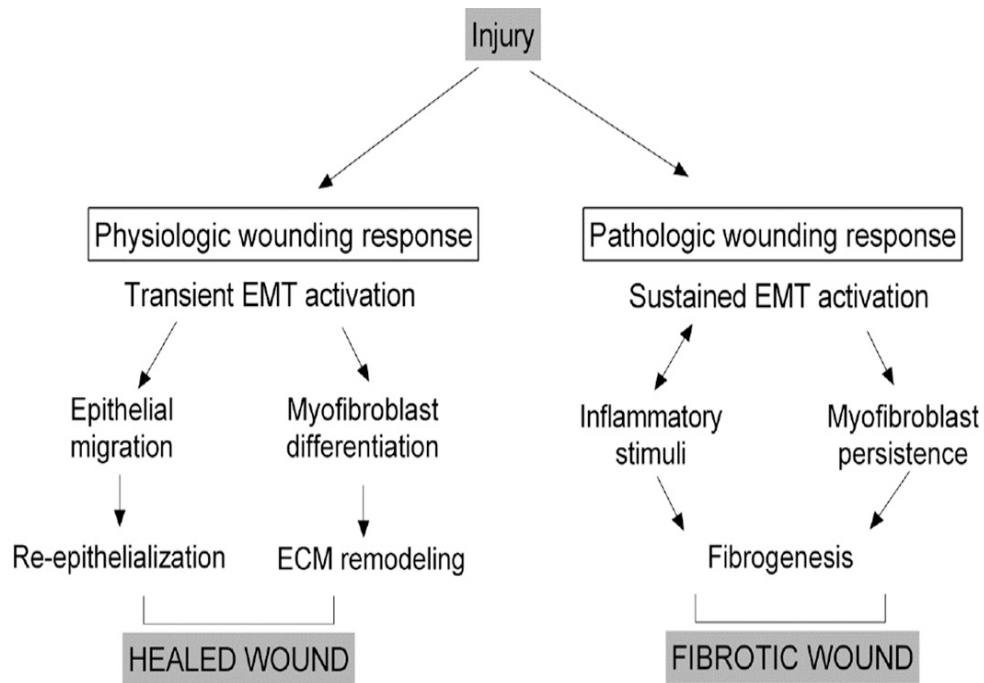


Figure 1.6: Injury triggered EMT in physiologic and pathologic conditions (Stone et al., 2016).

The most commonly accepted mechanism of these TGF- β 1 induced effects is the activation of the Smad pathway. However, evidence suggests that TGF- β 1 also exerts these effects in a non-Smad dependent pathway (Feranandez and Eickelberg, 2012; Tatler and Jenkins, 2012).

1.2.5 Role of tyrosine kinases in the pathogenesis of PF

Apart from oxidative stress and TGF- β 1, tyrosine kinases are also hypothesized to be involved in the pathogenesis of PF (Beyer and Distler, 2013). Tyrosine kinases are involved in several signaling pathways that are essential for cellular homeostasis such as metabolism, growth, differentiation and apoptosis. Abnormal tyrosine kinase activity disturbs the cellular homeostasis and can lead to cancer, vascular disease, and fibrosis. Recently, it has been suggested that receptor tyrosine kinases, such as platelet-derived growth factor receptor (PDGF), vascular endothelial growth factor receptor (VEGF) and fibroblast growth factor receptor (FGF) as well as non-receptor tyrosine kinases play a critical role in the pathogenesis of PF. The mechanism of action of tyrosine kinases is phosphorylation of target proteins at tyrosine residues. This allows formation of multiprotein complexes critical in signal transduction (Beyer and Distler, 2013; Grimminger et al., 2015). PDGF is a potent mitogen for fibroblasts and plays an essential role in inducing myofibroblasts by stimulating proliferation, migration and survival. These induced myofibroblasts would cause increased ECM deposition. Studies conducted on alveolar macrophages of IPF patients suggest that the level of PDGF released is 4 times higher than that in healthy subjects (Bonner, 2004; Clark et al., 1993). FGFs and their receptors (FGFRs) regulate cell proliferation, differentiation, migration and survival. FGF-2 is also said to be a potent mitogen for fibroblasts and type II alveolar epithelial cells. FGF-2 has also been shown to induce collagen synthesis in lung fibroblasts and myofibroblasts. Higher FGF-2 and FGFR-1 levels on epithelial, endothelial and myofibroblast were detected in the lungs of patients with IPF. Another factor contributing to induction of FGF is TGF- β which increases FGFR-1 and FGF-2 in human lung fibroblasts. Meanwhile, rodent experiments suggest that inhibition of VEGF receptor reduced fibrosis

however, their exact role in PF is still unclear (Chen et al., 2003; Inoue et al., 1996; Melloni et al., 1996; Wollin et al., 2015).

1.3 Treatment options of PF

PF treatment has evolved significantly over the last decade. Due to an initial belief of inflammation as a cause of fibrosis, immunosuppression was adopted in PF treatment. Prednisone, azathioprine and N-acetylcysteine (NAC) were evaluated, yet this trial was discontinued due to adverse events and deaths (Fujimoto, 2015; Lota et al, 2013). The treatment protocol was then modified and the trial arm with NAC alone is now under Phase III trial (Lota et al, 2013). With the failure of this trial, there was a shift from immunosuppression treatment to targeting profibrotic signaling pathways. Since then, two consensus statements have been issued in 2011 and 2015 as recommendations for PF treatment. As per the 2015 guidelines, PF treatment options are classified into two types: 1) pharmacologic; and 2) non-pharmacologic options (Raghu et al, 2015). For the pharmacologic treatments, the GRADE (Grading of Recommendations Assessment, Development and Evaluation) methodology was used to grade the certainty of effect as high, medium, low or very low, and thereby make a strong or conditional recommendation for or against use of each drug (Spagnolo et al, 2018, Lota et al, 2013). These recommendations are summarized in Table 1.1. The recommendations were based on the strength of evidence based upon clinical trials, outcomes studies, desirable and undesirable consequences of the treatment, costs and feasibility of treatment. Note that, in most of the clinical trials, forced vital capacity (FVC) and exercise tolerance tests have been adopted as end points.

Table 1.1: Key recommendations on pharmacologic treatment of PF according to the 2015 and 2011 guidelines (Raghu et al, 2015)

| AGENT | 2015 GUIDELINE | 2011 GUIDELINE |
|---|--|--|
| Anti-coagulation (warfarin) | Strong recommendation against use | Conditional recommendation against use |
| Combination prednisone + azathioprine + N-acetylcysteine | Strong recommendation against use | Conditional recommendation against use |
| Selective endothelial receptor antagonist (ambrisentan) | Strong recommendation against use | Not addressed |
| Imatinib, a tyrosine kinase inhibitor with one target | Strong recommendation against use | Not addressed |
| Nintedanib, a tyrosine kinase inhibitor with multiple targets | Conditional recommendation for use | Not addressed |
| Pirfenidone | Conditional recommendation for use | Conditional recommendation against use |
| Dual endothelin receptor antagonists (macitentan, bosentan) | Conditional recommendation against use | Strong recommendation against use |
| Phosphodiesterase-5-inhibitor (sildenafil) | Conditional recommendation against use | Not addressed |

Despite of the recommendation of many drugs as shown above, the United States Food and Drug Administration (FDA) has approved only 2 drugs to date for PF treatment: pirfenidone (PIR) and nintedanib. PIR is an orally active, synthetic, low molecular weight (185 g/mole) compound that exerts anti-fibrotic, anti-inflammatory and anti-oxidative activities. Its anti-fibrotic activity is attributed to inhibitions of fibroblast proliferation, differentiation, collagen synthesis and production of TGF- β 1 and tumor necrosis factor- α (Shaney et al, 2018; Fujimoto et al, 2015). Nintedanib is also a low molecular weight compound (540 g/mole), and its anti-fibrotic activity is by virtue of triple kinase inhibition of VEGF, PDGF and FGF (Shaney et al, 2018). Nintedanib prevents fibroblast proliferation, fibroblast to myofibroblast differentiation, induction of TGF- β 1 and deposition of collagen. Clinical trials demonstrated significantly slower declines in FVC in

patients by treatment with PIR or nintedanib, compared with placebo (Shaney et al, 2018). By now, however, no clear evidence has been shown regarding which drug should be the first line treatment option of PF (Shaney et al, 2018; Bonella, 2015; Fujimoto et al, 2015). A recent review (Loveman et al. 2015) reported a slower FVC decline in patients treated with nintedanib than in those treated with PIR. Nintedanib was also shown to be significantly better than placebo in the management of acute exacerbations, while PIR was better than placebo in terms of mortality (Loveman et al, 2015). The adverse effects associated with these drugs also differ. Skin-related and gastrointestinal issues are experienced in patients treated with PIR, while nintedanib causes liver dysfunction (Fujimoto et al, 2015; Lota et al, 2013). Accordingly, the current first line treatment for PF is individualized (Shaney et al, 2018; Fujimoto et al, 2015; Raghu et al, 2015; Schünemann, 2006).

Non-pharmacologic options for PF treatment are oxygen therapy, pulmonary rehabilitation and lung transplant. Since smoking is one of its leading causes, complete smoking cessation is also recommended to prevent the worsening of the disease (American Lung Association, 2018).

Currently, a number of new drugs are in clinical trials as potential treatments of PF, such as TRK-250 as a TGF- β 1 inhibitor and TD139 as a galectin-3 inhibitor (clinicaltrials.gov). However, both PIR and nintedanib only slow the disease progression and show moderate efficacy against the PF pathogenic features at relatively high doses, thus, there is still a need for drugs that can effectively treat PF in a more beneficial manner to patients.

1.4 Melatonin and curcumin for therapeutic use in PF

Melatonin (MEL) (232 g/mole) is an endogenous hormone secreted by the pineal gland. MEL regulates the circadian rhythm and modulates several other molecular pathways associated with inflammation, oxidative stress and injury. The pharmacologic activities of MEL are due to

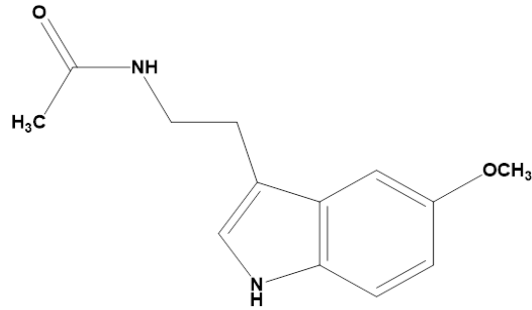


Figure 1.7: Structure of MEL

receptor mediated (since under stress conditions, the level of MEL receptors in the lung are upregulated) and non-receptor mediated effects (Hu et al, 2016; Olegario et al, 2013). As an antioxidant, MEL has been suggested to be therapeutic in PF by reversing the oxidant-antioxidant imbalance (Liu et al, 2010). MEL treatment in a rodent model of bleomycin (BLM)-induced PF enabled increased glutathione (GSH), superoxide dismutase and catalase, and reduced lipid peroxidation (Arslan et al, 2002; Yildirim et al, 2006). This MEL's activity was implied to be mediated through binding to MEL receptors (Hosseinzadeh et al, 2018). MEL has also been shown to reduce collagen synthesis and ECM deposition by correcting the effect of TGF- β (Hosseinzadeh et al, 2018; Hu et al, 2016; Karimfar, 2015; Shin et al, 2017).

Both *in vivo* and *in vitro*, MEL effectively inhibited EMT and thereby prevented formation of excessive myofibroblasts which led to decreased ECM deposition (Yu et al, 2016; Zhao et al, 2014). However, MEL exerted its effects only at very high doses. Arslan et al (2002) reported that MEL inhibited BLM-induced oxidative stress, reduction in antioxidant enzymes and collagen synthesis by ~30 % at a dose of 10 mg/kg. Karmifar et al (2015) later confirmed this result. Yildirim et al (2006) also reported that MEL at 4 mg/kg only moderately decreased the collagen levels and corrected the induced oxidative stress in the BLM-induced PF model. Also, in all the 3 studies,

MEL was assessed for its preventive effect by prophylactic administration of MEL before by BLM. Thus, MEL's anti-fibrotic effects require excessively high doses and its effect has been so far limited to prevention, which now requires a caution to predict the therapeutic success in patients with PF.

Curcumin (CUR) (368 g/mole) is a yellow colored pigment and a component of a spice, turmeric. It is potently anti-oxidative and anti-inflammatory (Hewlings and Kalman, 2017). Again, as an antioxidant, CUR has been used in a preclinical PF model,

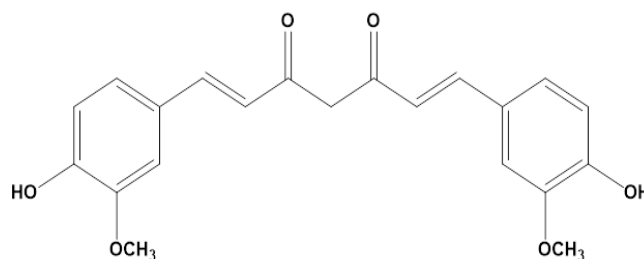


Figure 1.8 : Structure of CUR

demonstrating prevention of excess ROS production induced by injury. Dietary treatment of CUR in a mouse model of induced PF reduced generation of ROS and an oxidative marker, heme-oxygenase 1 by endothelial cells (Lee et al, 2010). Its mechanism of action has been suggested to be inhibition of free radicals and induced injury. CUR has also been shown to inhibit collagen synthesis and deposition both *in vitro* and *in vivo*, thereby exerting the anti-fibrotic effects (Punithavathi et al, 2000; Smith et al, 2010). When dosed at 300 mg/kg in a BLM-induced model, CUR inhibited collagen synthesis by ~60 % and significantly reduced the levels of superoxide anion thereby reducing oxidative stress (Punithavathi et al, 2000). In an *in vitro* TGF- β 1 induced system, CUR significantly inhibited collagen synthesis as well as fibroblast differentiation to myofibroblasts at 20 μ M (Smith et al, 2000). However, this study demonstrated that CUR failed to exert potent inhibitory activity against BLM-induced PF when pretreated with CUR at 300 mg/kg (Smith et al, 2010; Li et al, 2013). *In vivo* studies in rats also suggested that CUR exerted its anti-fibrotic action by TGF- β 1 inhibition which was seen by the reduction in TGF- β 1 levels in

the bronchoalveolar lavage fluid upon treatment with 50 mg/kg of CUR (Zhang et al, 2007). Intriguingly, Zhang et al (2011) attributed the effect of CUR to overexpression of cathepsin K, given that the cathepsin K levels were higher upon treatment with CUR, compared to untreated PF animals. Cathepsin K is a collagenase enzyme which is downregulated under disease conditions. CUR at high concentrations inhibited this downregulation, thereby preventing ECM deposition and fibrosis (Zhang et al, 2011). CUR also showed anti-proliferative effects in normal and PF fibroblasts by causing cell cycle arrest, thereby preventing the formation of excess fibrotic tissue (Smith et al, 2010). However, like MEL, CUR requires high doses as well as pretreatment in order to exert its anti-fibrotic effects. Another issue with the use of CUR is its very poor aqueous solubility which is a limitation as an oral dosage form.

1.5 Melatonin-curcumin (MEL-CUR) hybrid molecules

Recently, Dr. Shijun Zhang of the VCU School of Pharmacy Medicinal Chemistry and his group have synthesized a series of hybrid molecules of MEL and CUR for use as neuroprotective agents in Alzheimer's disease, as shown in Figure 1.9 (Chojnacki et al, 2014). An attempt was made to retain or dismiss potentially critical structural features of MEL and CUR in the hybrid molecules. As for MEL, its 5-methoxy, acetamide and indole moieties are pivotal for anti-oxidative and radical scavenging properties, so that these moieties were maintained in all 5 hybrid molecules. However, the MEL structure was chemically corrected to a symmetrical half of CUR, as the hybrid molecules were anticipated to be more potent than MEL or CUR alone. In CUR, phenolic oxygens and β -diketones have been suggested to be responsible for its anti-oxidative activities (Priyadarshini, 2014). The hybrid molecules were each synthesized by eliminating one or more of these groups to form hybrids 4, 5, 6 and 7. Molecule 3 is the most direct hybrid of MEL

and CUR since it includes the 5-methoxy of MEL and the phenoxy oxygens of CUR while the β -diketone of CUR and acetamide of MEL are combined to form the β -ketone amide moiety. Molecules 4 and 5 were synthesized to assess the effect of the removal of one of the phenolic oxygens. Molecule 6 does not have either of the phenolic oxygens while molecule 7 possess the phenolic oxygen at position 4 and does not contain the double bond between the phenyl ring and the β -ketone. These 5 hybrid molecules were assessed in an *in vitro* cellular Alzheimer's disease model which was associated with oxidative stress induced cellular toxicities under the absence of tetracycline (- TC), in comparison with MEL and CUR. Briefly, human CNS nerve MC-65 cells were incubated in 96-well plates with or without the test molecules and/or tetracycline for 72 hours and the cytoprotective activity of the test molecules was assessed by the MTT assay. MEL, CUR and MEL+CUR showed no neuroprotective activity, hybrid 3 significantly protected cells from - TC induced cell death by 60%. Complete loss of neuroprotective activity was seen on removal of the 4 - OH group (hybrid 4), while removal of 3-methoxy group did not reduce the activity (hybrid 5). Hybrid 6 showed lower neuroprotective activity due to the absence of the phenolic oxygens. Finally, compound 7 evaluated the role of the double bond between the phenyl ring and the β -ketone and suggested that the double bond was not necessary for its neuroprotective action . Thus, compound 7 (AM24) and 5 (AM42) were identified as the two most potent molecules in the Alzheimer's disease model. However, their exact mechanism of action has still yet to be fully clarified (Chojnacki et al, 2014). Given *in vitro* and *in vivo* evidences for use of MEL and CUR in PF described in the above section (1.4), it was therefore rationally hypothesized that these MEL-CUR hybrid molecules are also potently effective in the treatment of PF lungs. Therefore, this thesis project chose AM24 (compound 7) and AM42 (compound 5) for an early proof-of-concept study and first assessed their *in vitro* inhibitory activities against TGF- β 1 induced collagen

synthesis in the fibroblast cells in the system used in Chapter 4. As shown in Figure 1.10, AM24 and AM42 at 10 μM respectively exhibited $\sim 90\%$ and $\sim 70\%$ inhibition against TGF- $\beta 1$ induced collagen synthesis, so that AM 24 had been chosen for further studies in this thesis project.

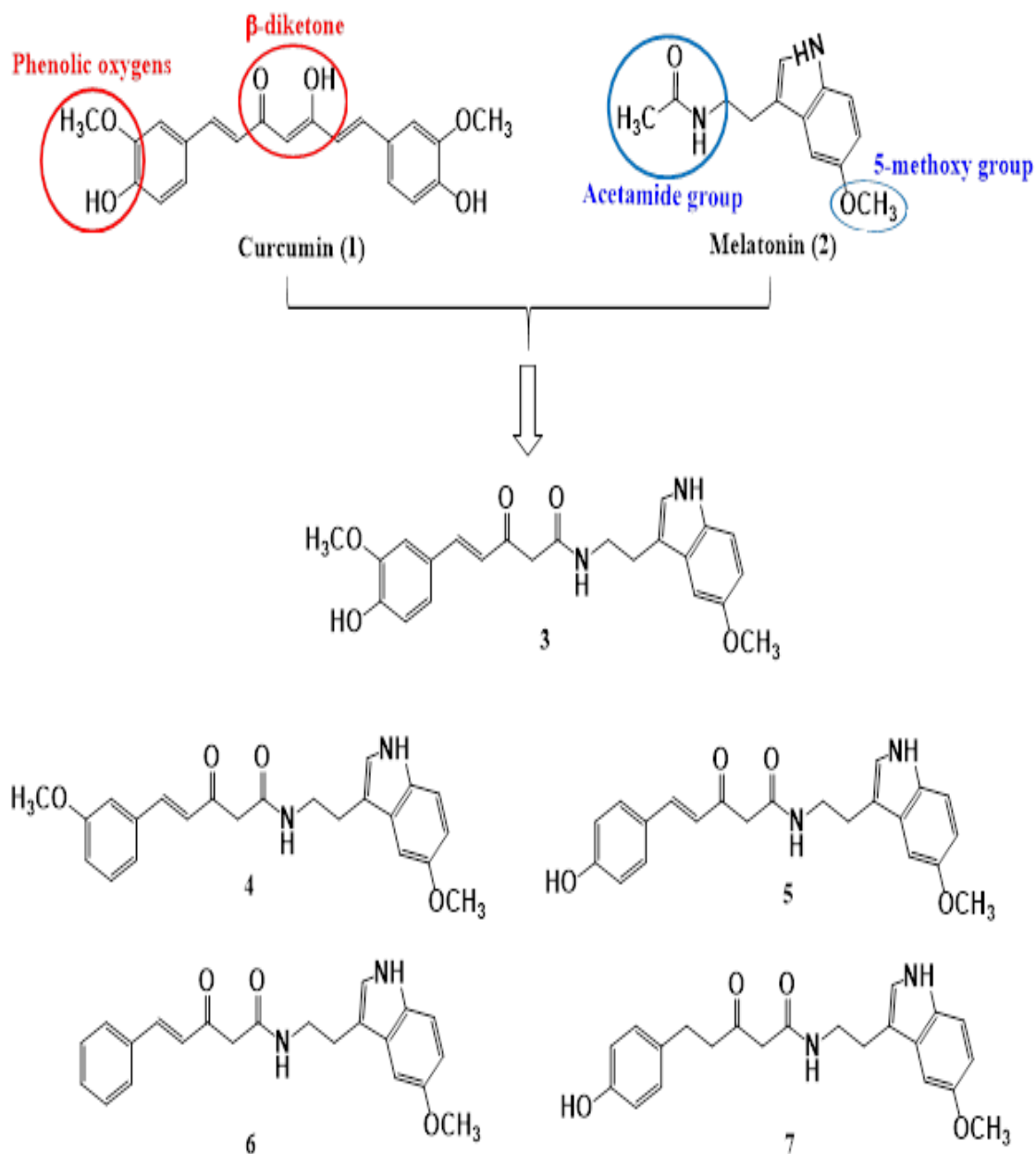


Figure 1.9: A series of MEL-CUR hybrid molecules (Chojnacki et al., 2014)

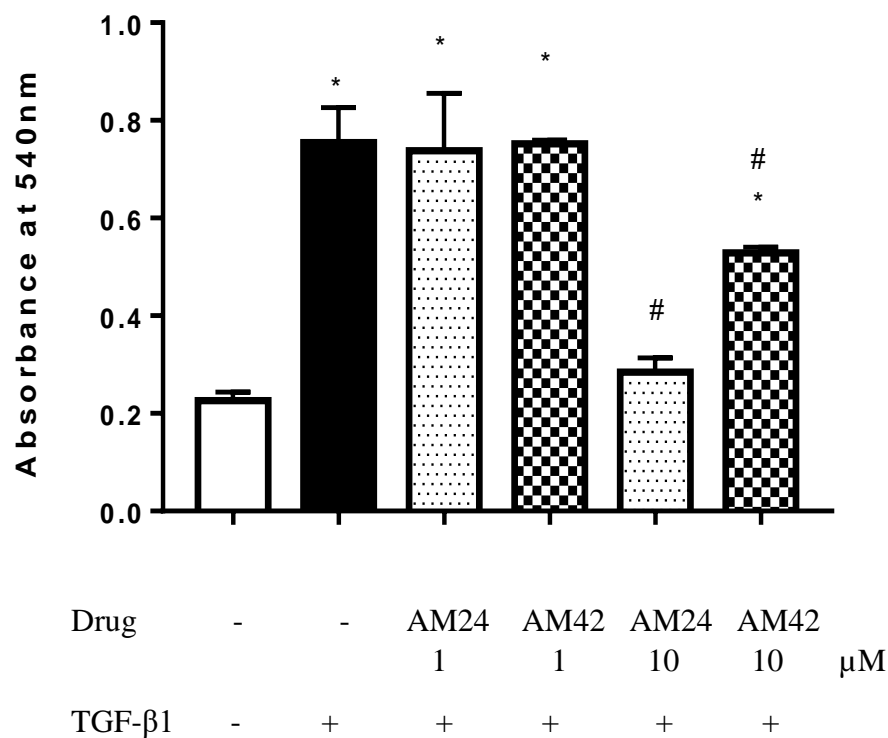


Figure 1.10: Inhibitory activities of AM24 and AM42 at 10 μM against TGF- β 1 induced collagen synthesis in the human lung fibroblast MRC-5 cells. Data: mean \pm SD from n=3-8. *p<0.05 vs. vehicle control; and #p<0.05 vs. TGF- β 1 induced control, by ANOVA and Tukey's HSD post hoc test.

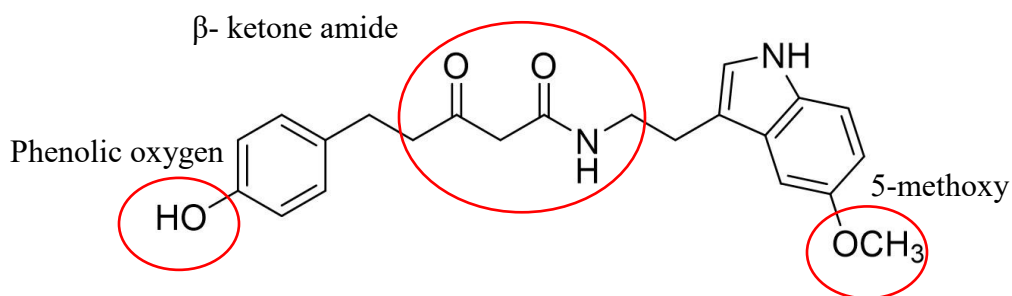


Figure 1.11: Structure of AM24

Structurally, AM24 (Figure 1.11) retains the 5-methoxy and acetamide groups of MEL but dismisses one of the phenolic oxygens and β -diketone of CUR. AM24 can also be recognized as a hybrid of MEL and raspberry ketone. However, these structural alterations improved the cytoprotective activity of AM24 (Chojnacki et al, 2014). AM24 (380 g/mole) is a small lipophilic molecule. Its cLog P (calculated partition co-efficient) is 3.3 and follows the Lipinski's rule of 5 and thus, AM24 is recognized as "membrane permeable". It is a weak acid with an acidic pKa of 9.5, so that at a physiological pH 7, AM24 remains unionized for transcellular diffusion. However, AM24 has a limited aqueous solubility $\sim 62 \mu\text{g/ml}$.

This project focuses on the anti-fibrotic efficacies of AM24 (a MEL-CUR hybrid) in both *in vitro* and *in vivo* systems in comparison to their parent molecules MEL and CUR as well as a FDA approved anti-PF drug PIR. Given the anti-fibrotic activities of MEL and CUR, it is hypothesized that a hybrid of the two would be more potent and exert its effect at a lower concentration/ dose both *in vitro* and *in vivo*. While MEL and CUR have been both given orally, this project focuses on AM24 delivery via the pulmonary route to assess its intervention activities to retard or prevent the progression of the disease. Pulmonary delivery could further reduce the required doses. As both MEL and CUR are antioxidants, the anti-oxidative activity of AM24 was first assessed, followed by the assessment of AM24 in the TGF- β 1 induced fibroblast/epithelial cell systems for its inhibitory activities against induced collagen synthesis, fibroblast proliferation and differentiation as well as EMT. Finally, AM24 was studied in an *in vivo* rat model of PF via pulmonary delivery to assess its therapeutic intervention activities.

CHAPTER 2

SPECIFIC AIMS AND HYPOTHESES

This thesis project aimed to demonstrate the anti-fibrotic activities of AM24, a novel hybrid molecule of MEL and CUR, for pulmonary delivery to treat PF lungs. It was hypothesized that AM24 was more potent than its parent origin, CUR and MEL, in the anti-fibrotic activities for PF intervention both *in vitro* and *in vivo*. Specifically, the project was designed to:

- 1) verify that AM24 retains the free radical scavenging (i.e., anti-oxidative) activity of MEL and CUR
- 2) demonstrate that AM24 possesses more potent anti-fibrotic activities in the *in vitro* lung fibroblast and epithelial cell systems than MEL, CUR, and their physical admixture
- 3) determine the intervention activities of AM24 in an *in vivo* rat model of BLM induced PF

Hence, this project pursued the following 5 hypotheses:

1. AM24 exhibits a more potent or equipotent anti-oxidative activity in the *in vitro* free radical scavenging assay relative to MEL and CUR
2. AM24 inhibits TGF- β 1 induced collagen synthesis, proliferation and differentiation in the *in vitro* PF-like lung fibroblast cell systems in a more potent fashion, compared to MEL, CUR and their physical admixture
3. AM24 inhibits TGF- β 1 induced epithelial-mesenchymal transition (EMT) in the *in vitro* PF-like lung epithelial cell system in a more potent fashion, compared to MEL, CUR and their physical admixture

4. The *in vitro* anti-fibrotic activities of AM24 shown above are also more potent than those of an FDA-approved, orally active PF drug, PIR
5. Pulmonary delivery of AM24 is capable of intervention in the development of experimental PF pathogenesis in a rat model induced with bleomycin (BLM)

Accordingly, AM24 will be examined for its free radical scavenging activity in Chapter 3; for its inhibitory activities against TGF- β 1 induced cellular collagen synthesis, proliferation, and differentiation to myofibroblast in the lung fibroblast systems in Chapter 4; and for its inhibitory activity against TGF- β 1 induced EMT in the lung epithelial cell system in Chapter 5. These anti-fibrotic activities of AM24 will be compared with those of MEL, CUR, their physical admixture and PIR. In Chapter 6, using an *in vivo* rat model of BLM-induced PF, the intervention activities of AM24 in the development of experimental PF pathogenesis (functional exercise capacity, lung histology and morphology, and several key biomarkers) will be assessed following thrice weekly, two-week lung administrations at a low dose of 0.1 mg/kg. Finally, Chapter 7 will summarize all the results and provide overall conclusions and future scope.

CHAPTER 3

IN VITRO ANTI-OXIDATIVE ACTIVITY OF MEL-CUR HYBRID AM24

3.1 Introduction

As described in Chapter 1, oxidant-antioxidant imbalance has been shown in the lungs of patients with PF, attributed to increased endogenous (e.g., epithelial, endothelial and mesenchymal cells) and exogenous (e.g. tobacco, asbestos) production of reactive oxygen species (ROS) and decreased anti-oxidative enzymes (e.g., glutathione peroxidase, GSH, superoxide dismutase and catalase) (Kinnula et al, 2005). TGF- β 1 has been suggested to play a central role of aggravating this redox imbalance by inducing mitochondrial ROS production and NADPH oxidases, and downregulating expression and activity of GSH, catalase, superoxide dismutase, and glutaredoxin (Liu et al, 2010). Both MEL and CUR have been shown to possess potent anti-oxidative activities, which was hypothesized to be the mechanism for their inhibitory activities against several pathogenic features of PF (Karimfar et al, 2015; Lee et al, 2010). Accordingly, the anti-oxidative activity of their hybrid molecule, AM24, was of interest to identify if the chemical combination enabled the synergistic and more potent anti-oxidative activity.

The ABTS (2,2'-azino-di-[3-ethylbenthialzoline sulphonate]) radical scavenging method has commonly been used to assess the antioxidant activities of test molecules in question. ABTS free radicals (ABTS^{•+}) become stable by accepting a hydrogen ion from the antioxidant, if any, thereby losing blue color that can be measured in a spectrophotometric manner. This reaction is quick, so that the assay becomes less time consuming. In addition, the ABTS assay can be used in

a kinetic mode to monitor the reaction over time. By virtue of its simplicity and sensitivity, it has widely been used in comparisons of antioxidant molecules (Amorati et al, 2014).

3.2 Materials and Methods

3.2.1 Materials

AM24 was received as amorphous white powder from the laboratory of Dr. Shijun Zhang (VCU School of Pharmacy Medicinal Chemistry) and stored at -20 °C. MEL was purchased from Bio Basic (>99 % purity; Ontario, Canada) and stored at -20 °C. CUR was obtained from ACROS Organics (98 % purity; Fisher Scientific, Pittsburgh, PA) and stored at room temperature. In each study, MEL was freshly prepared as a 5.25 mM stock solution in distilled deionized water (DDW), while CUR and AM24 were prepared as a 5.25 mM stock solution in a 50:50 admixture of DDW and ethanol (EtOH).

3.2.2 *In vitro* ABTS-based free radical scavenging assay

The anti-oxidative activity was assessed using the *in vitro* antioxidant assay kit as per the manufacturer's protocol (Cayman Chemical Company, Ann Arbor, MI). This assay measures the ability of a molecule in question to inhibit oxidation of ABTS to a chromogenic cationic free radical, ABTS^{•+}, by H₂O₂ (hydrogen peroxide) in the presence of metmyoglobin. H₂O₂ causes metmyoglobin to produce a ferryl myoglobin radical, thereby oxidizing ABTS to generate ABTS^{•+}, which is measured as absorbance at 750 nm using a spectrophotometer. Using the 5.25 mM stock solution prepared above, each test molecule (AM24, MEL and CUR) was prepared at different concentrations in DDW or DDW/EtOH as 21X test solutions. Using 96-well plates, 10 µL of the test solution sample was added, followed by addition of metmyoglobin (10 µl), ABTS solution

(150 μl) and H_2O_2 (40 μl) to examine the inhibitory activities of the test molecules at 0.1-250 μM ; the vehicle alone (10 μl) was used to obtain $\text{ABTS}^{+\cdot}$ formation in the absence of the test molecules. The change in absorbance at 750 nm (ΔAbs) was monitored for the first 5 min using a Synergy™ 2 Multi-mode Microplate Reader (BioTek Instruments, Winooski, VT).

The absorbance was linearly increased over 5 min, so that the ΔAbs in 5 min ($\Delta\text{Abs}_{5\text{min}}$) was used to calculate a fraction of $\text{ABTS}^{+\cdot}$ formation (Y) from:

$$Y = \Delta\text{Abs}_{5\text{min}} \text{ in the presence of test molecule} / \Delta\text{Abs}_{5\text{min}} \text{ for the vehicle control}$$

The data (Y) were expressed as mean \pm standard deviation (SD) from triplicate experiments (n=3). The half-maximal inhibitory concentration (IC_{50}) and Hill slope (HS) values were then derived from the mean concentration-dependent response curves using Scientist® 3.0 (MicroMath, St. Louis, MO) via nonlinear curve-fitting to the following equation below:

$$Y = Y_{\text{min}} + (Y_0 - Y_{\text{min}}) / [1 + (C/\text{IC}_{50})^{\text{HS}}]$$

where Y_0 was $\Delta\text{Abs}_{5\text{min}}$ ratio in the absence of the test molecule; Y_{min} was the lowest asymptotic $\Delta\text{Abs}_{5\text{min}}$ ratio seen at the highest testing concentration (i.e., 250 μM); and C was concentration of the test molecule. For all 3 test molecules, Y_0 was by definition 1, and Y_{min} appeared to approach 0, so that both were respectively fixed during curve-fitting. The “goodness-of-fit” was assessed with visual inspection of residuals in the profiles, 95 % confidence intervals (95% CIs) of the IC_{50} and HS values, and Scientist-calculating coefficient of determination (COD) and model selection criterion (MSC).

3.3 Results and Discussion

Figure 3.1 shows the fraction of ABTS^{•+} formed vs. concentration profiles to demonstrate and assess the free radical scavenging activities of AM24, MEL and CUR. The ABTS^{•+} formation was inhibited in a concentration-dependent manner, indicating the anti-oxidative activities via free radical scavenging action. The curve-fitting was successful for all three molecules, given small residuals in the profiles (Fig. 3.1). As shown in Table 3.1, the Scientist-calculating COD and MSC values were >0.96 and >3.0, respectively, which was also sufficient. As a result, the IC₅₀ and HS values were derived with relatively small 95% CIs, as shown in Table 3.1. The IC₅₀ value of AM24 was 25.7±3.2 μM, which was statistically comparable to that of MEL, 32.0±4.3 μM. However, both AM24 and MEL were less potent than CUR that yielded 11.4±1.1 μM as the IC₅₀ value. Despite these activity differences, the HS values were all close to 1 (Table 3.1), suggesting the absence of either positive (>1) or negative (<1) cooperativity.

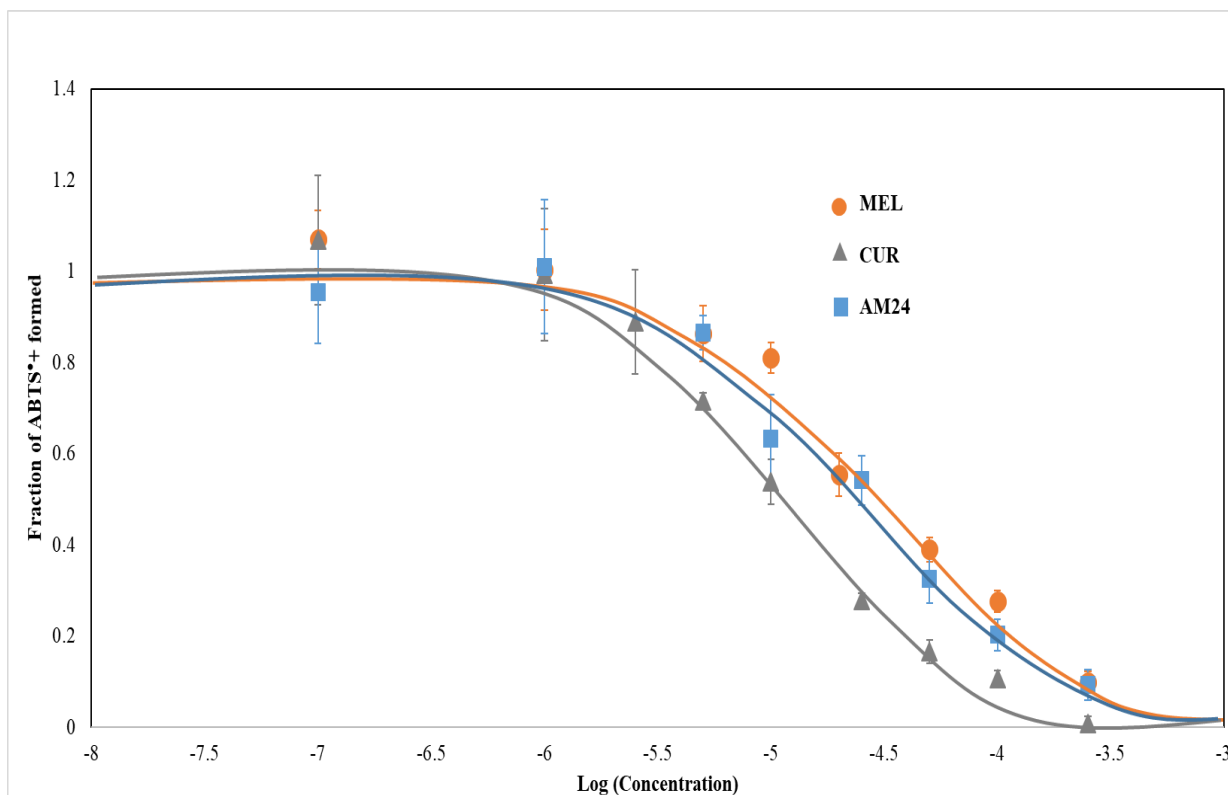


Figure 3.1: The profiles of fraction of ABTS•+ formed vs. logarithmic concentration to demonstrate and assess the radical scavenging activity of AM24, MEL and CUR. Data are mean \pm S.D. (n=3). The curves are the curve-fitted lines drawn using the IC₅₀ and HS estimates (Table 3.1) by simulation.

Table 3.1: The IC₅₀ and HS values for the ABTS-based free radical scavenging activities of AM24, MEL and CUR, derived from curve-fitting of the profiles shown in Figure 3.1, alongside the COD and MSC values of the curve-fitting.

| Drug | IC ₅₀ (μM) | 95% CIs (lower, upper) | HS | 95% CIs (lower, upper) | COD; MSC |
|------|-----------------------|---------------------------|------------|---------------------------|------------|
| AM24 | 25.7 ± 3.2 | 18.1, 33.2 | 0.98 ± 0.1 | 0.6, 1.3 | 0.96; 2.99 |
| MEL | 32.0 ± 4.3 | 21.4, 42.5 | 1.02 ± 0.1 | 0.6, 1.3 | 0.97; 3.20 |
| CUR | 11.4 ± 1.1 | 8.8, 13.9 | 1.14 ± 0.1 | 0.8, 1.4 | 0.98; 4.01 |

As shown in Table 3.1, AM24 was statistically equipotent to MEL, but less potent than CUR in the ABTS-based free radical scavenging activity. Similar ABTS-based studies have ranked the anti-oxidative activities of MEL and CUR relative to Trolox, a water-soluble analog of vitamin E commonly used as a reference antioxidative molecule. Ak and Gülcin (2008) ranked CUR > Trolox, while Kraus et al (2005) reported MEL (IC₅₀ of 8 μM) > Trolox (IC₅₀ of 30 μM). Note that different IC₅₀ values between the present study and the literature are presumably due to differences in the volumes of sample, metmyoglobin, H₂O₂ and ABTS, as well as difference in the time point for the measurement. However, from the literature, both MEL and CUR were ranked greater than Trolox. Meanwhile, Saluja et al (2013) reported 0.29 mM of the IC₅₀ value for Trolox using the same Cayman's ABTS antioxidant assay kit. Thus, given the rank-order in the literature, it can be concluded that both MEL and CUR are more potent antioxidants than Trolox thereby suggesting that AM24 which was shown to be similar in its antioxidative potency to MEL is also a more potent antioxidant in comparison to Trolox, as shown below:

$$\text{CUR} > \text{AM24/MEL} > \text{Trolox.}$$

Structurally, the anti-oxidative activity of MEL was shown to arise from its indole ring (Dx et al, 2002; Hardeland, 2005). This ring can undergo single-electron transfer reactions to exert the

anti-oxidative effect, as described in Figure 3.2 (Johns and Platts et al, 2014). Modification of the pyrrole moiety in this indole ring showed a loss of antioxidant activity, indicating that an intact indole ring is essential for the activity (Herraiz and Galisteo, 2004). A comparison of 29 indole ring containing compounds showed that N-methylation of this ring decreased the activity, while protonation of this nitrogen completely suppressed it (Herraiz and Galisteo, 2004). These further advocates the need for an intact indole ring and hints that the antioxidant activity seems to be mediated through this indole nitrogen . Presence of substituents on the indole ring, such as methoxy in MEL, showed an increased activity (Herraiz and Galisteo, 2004; Dx et al, 2002). The 5-methoxy and acetamide moieties from MEL are also known to contribute to the antioxidant activity (Chojnacki et al, 2014)

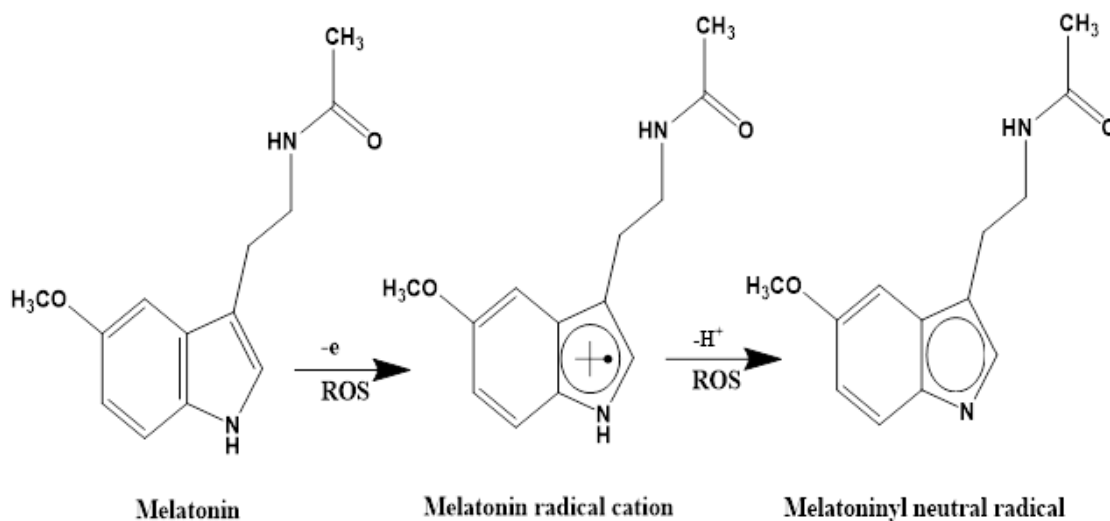


Figure 3.2: Single electron transfer in MEL that leads to the formation of MEL radical cation acting as a radical scavenger (Johns and Platts et al., 2014)

CUR is a symmetric molecule and has 2 chemical groups in its structure which are majorly responsible for its antioxidant and radical scavenging activity (Priyadarshini, 2014). The two aromatic rings with hydroxy and methoxy groups (phenolic oxygens) play an essential role in the antioxidant activity of CUR (Chojnacki et al, 2014). The free radical scavenging action by CUR involves abstraction of a H-atom from the phenolic-OH which gives rise to a phenoxyl radical as seen in Figure 3.3 (Priyadarshini, 2003; Priyadarshini, 2014). This in turn is stabilized by the α,β -unsaturated β -diketone moiety present in the structure as the second important contributor, responsible for its activity. The phenoxyl radical is stabilized by the keto-enol tautomerism of this functional group (Priyadarshini, 2009). Absence of this tautomerism leads to a decrease in the activity as the phenoxyl radicals cannot be stabilized further (Priyadarshini, 2009).

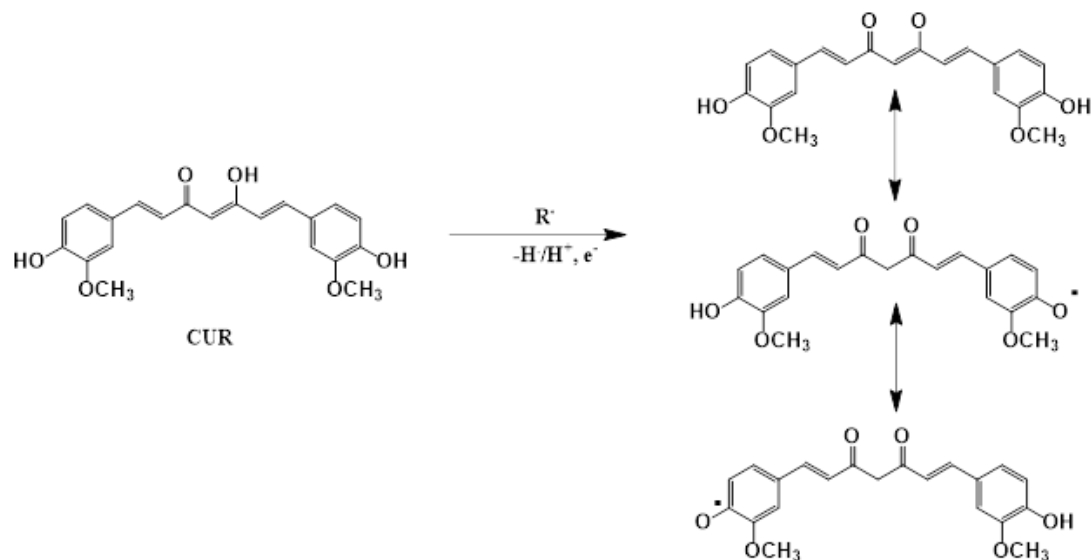


Figure 3.3: Possible sites of attack of free radical oxidants with CUR and stabilization of phenoxyl intermediate (Priyadarshini, 2014).

AM24 is a chemical hybrid of the two antioxidative molecules - MEL and CUR (Figure 3.4). It was thus expected to have a more potent antioxidant activity, compared to both molecules if an additive or synergistic effect exists. However, our results indicate that was not the case. The hybrid molecule retains a half of CUR but loses the α,β -unsaturated β -diketone moiety and thus does not show keto-enol tautomerism. It was highly likely that this prevented the stabilization of the phenoxyl radical as mentioned earlier. As a result, despite the presence of phenolic-OH group, the functional groups needed for the radical stabilization are absent, and this half portion did not contribute to the antioxidant activity. Instead, the activity of AM24 was most likely due to its MEL portion, given that AM24 retains the structure of MEL, including the indole ring with a methoxy substituent. This deduction was further supported by the HS values being 1 for both AM24 and MEL.

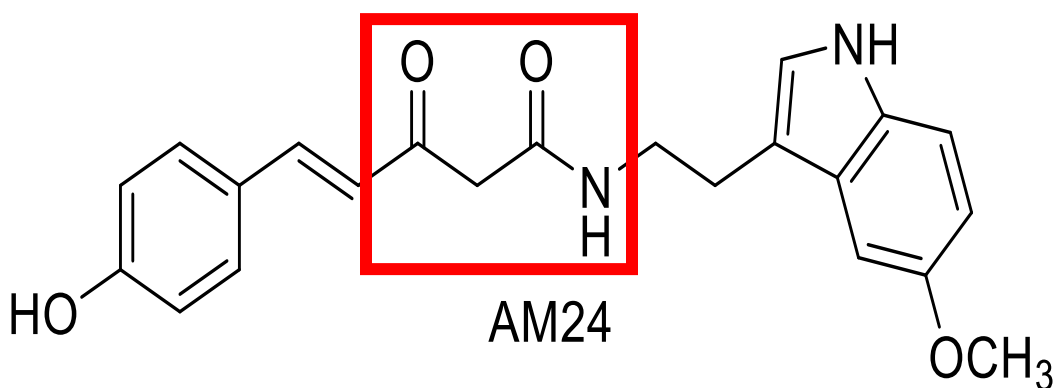


Figure 3.4: Structure of AM24. The red box indicates the absence of the β -diketone

CHAPTER 4

***IN VITRO* ANTI-FIBROTIC ACTIVITIES OF MEL-CUR HYBRID AM24**

4.1 Introduction

Fibroblasts are recognized as the ‘workhorses’ of the connective tissue since they are the main source of ECM and also the mediators of fibrotic deposition of ECM, cellular proliferation and differentiation into myofibroblasts that occurs as a result of epithelial injury or inflammation (Kendall and Feghali-Bostwick, 2014). As introduced in chapter 1, increased collagen synthesis, proliferation and differentiation of fibroblast are the hallmark events in PF. Both MEL and CUR have been shown to moderately inhibit each of these fibrotic events. In PF lungs, these events somehow occur as a result of dysregulated repair of injury which activates a number of profibrotic pathways including upregulation of TGF- β 1 (Wynn, 2011). Hence, TGF- β 1 is recognized as the profibrotic master switch, i.e., the central coordinator, integrator and amplifier of fibrotic responses. Induction of the TGF- β 1 levels upon epithelial injury gives rise to a series of fibrotic events that leads to honeycombing and organ fibrosis. Thus, the TGF- β 1 induced fibroblast models have been used in many *in vitro* studies (Wynn and Wilson, 2009).

Xu et al (2007) suggested that a lack of quantitative *in vitro* fibrosis models is at least in part responsible for slow research progress toward the development of anti-fibrotic drugs. Thus, they developed an *in vitro* direct quantitative method for collagen synthesis using the picosirius red method, as opposed to indirect measurement of hydroxyproline. By contrast, proliferation and differentiation of fibroblasts can be assessed using the MTT (3-(4,5-dimethylthiazol-2-yl)-2,5-

diphenyltetrazolium bromide) assay and western blot, respectively. In order for AM24 to be classified as an anti-PF drug, its inhibitory activities against PF-like induced collagen synthesis, fibroblast proliferation and differentiation would be essential to be shown. Such activities of AM24 in comparison with those for MEL and CUR would enable identification between their free radical scavenging anti-oxidative activities and each of the anti-PF activities. Therefore, in this chapter, the inhibitory activities of AM24 against TGF- β 1 induced cellular collagen synthesis, proliferation and differentiation were assessed in the *in vitro* lung fibroblast cell systems, in comparison with its structural origins, MEL and CUR, and one of the approved PF drugs, PIR.

4.2 Materials and Methods

4.2.1 Materials

AM24, MEL and CUR were obtained, as described in Chapter 3. PIR (> 95% purity) was obtained from Cayman Chemical as a crystalline solid and stored at -20 °C. For each experiment, the test molecule solutions were freshly prepared in the incubation media. MEL, CUR and AM24 were prepared as 100 µM stock solutions, while PIR was as a 5 mM stock solution. TGF-β1 (≥ 95% purity) was obtained from R&D systems (Minneapolis, MN) and stored at -20 °C. Its stock solution was prepared in sterile 4 mM HCl containing 0.1 % bovine serum albumin, as per the manufacturer's instructions. The incubation media were used for dilution to prepare each test samples. Luzindole (≥ 98 % purity) was obtained from Cayman Chemical as a crystalline solid and stored in -20 °C. Its stock solution was prepared at 10 µM in the incubation media.

4.2.2 Human lung fibroblasts: MRC-5 and NHLF cells

Human fetal lung fibroblasts, MRC-5 cells were obtained from American Type Culture Collection (ATCC; Manassas, VA) and maintained in culture, according to the ATCC's protocol. Briefly, they were grown in the DMEM/F-12K, GlutaMAX™ media (Fisher Scientific, Hampton, NH) supplemented with 10 % fetal bovine serum (FBS; Thermo Fischer, Waltham, MA) and 1 % Penicillin-Streptomycin (PS; ATCC). Normal human lung fibroblasts, NHLF cells were obtained from Lonza (Basel, Switzerland) and maintained in culture, according to the Lonza's protocol. Briefly, they were grown in the FGM™-2 Fibroblast Growth Medium-2 BulletKit™ supplemented with 10 % FBS (Lonza) and 1 % PS (Lonza). Both MRC-5 and NHLF cells were cultured in the incubator (Nuair Laboratory Equipment, Plymouth, MN) maintained at 37 °C and 95 % air/5 % CO₂, and used in experiments at passages 1 to 23, respectively.

4.2.3 *In vitro* assessments of TGF- β 1 induced lung fibroblast collagen

The MRC-5 and NHLF cells were plated in 48-well plates at a density of 20,000 cells per well. The cells were grown to confluence and then incubated with or without test molecules and/or TGF- β 1 in 200 μ l of the culture media. For this incubation, each of the test molecules (20 μ l) was first added as a 100X solution, and then, at 2 hours, TGF- β 1 or the vehicle (2 μ l) was added as a 100X solution for collagen induction. AM24 was examined at 0.1, 1, 5 and 10 μ M; MEL was at 10 μ M; CUR was at 10 μ M, a physical mixture of MEL and CUR (MEL+CUR) was at 10 μ M in each; PIR was at 10 and 500 μ M; and TGF- β 1 was applied at 10 ng/ml. At 48 hours after addition of the test molecules, the incubation media were removed. Cellular collagen was quantified by the picosirius red method originally developed by Xu et al (2007) and established/validated with slight modifications, as described in Appendix I. Briefly, the cells were incubated with picosirius red (0.2 ml; sirius red (Sigma-Aldrich, St. Louis, MO), picric acid (Ricca chemicals, Pocomoke city, MD) for 1 hour and washed with 10 mM HCl (0.2 ml; Fisher Scientific) twice to remove the unbound dye. Subsequently, the bound dye was solubilized in 100 mM NaOH (0.15 ml; Fisher Scientific). This solution was then transferred into 96-well plates and the absorbance was measured at 540 nm using the microplate reader (SynergyTM 2, BioTek Instruments).

To explore if the inhibitory activity of AM24 against TGF- β 1 induced collagen increase was associated with MEL receptors, a MEL receptor antagonist, LUZ was used. LUZ was first incubated with the cells at 0.1 μ M for 2 hours. AM24 was then incubated at 10 μ M for 2 hours, followed by addition of TGF- β 1. At 48 hours after AM 24 addition, cellular collagen was quantified by the method described above. The experiment also examined the effects of LUZ alone in the absence and presence of TGF- β 1 (without AM24) as controls.

4.2.4 *In vitro* assessments of TGF- β 1 induced lung fibroblast proliferation

TGF- β 1 induced proliferation of MRC-5 cells and its inhibition with the test molecules were measured using the MTT cell proliferation assay kit (BioVision, San Francisco, CA), as per the manufacturer's protocol. In 96-well plates, 7,000 cells were seeded and allowed to settle overnight. Subsequently, the cells were incubated with AM24 at 1, 5, 10 μ M, MEL at 10 μ M, CUR at 10 μ M, MEL+CUR at 10 μ M, and PIR at 10 and 500 μ M for 2 hours in the culture media, followed by addition of TGF- β 1 at 10 ng/ml or the vehicle. At 48 or 72 hours after addition of the test molecules, the media were removed, and the cells were incubated with an admixture of 50 μ l of MTT reagent (BioVision) and 50 μ l of the FBS-deprived culture media for 3 hours at 37 °C. Following removal of the MTT reagent/culture media, 150 μ l of MTT dissolving solvent (isopropanol; BioVision) was added to the well. The well-plate was wrapped in a foil and kept on an electronic Schüttler mts 4 shaker (IKA, Staufen, Germany) for 15 minutes. The absorbance was then read at 590 nm using the Synergy™ 2 micro plate reader. The absorbance was also measured for the cells at 0 hour (before addition of the test molecule or TGF- β 1). The cellular proliferation is expressed as the difference in the absorbance (Δ Abs) between 0-48 hours or 0-72 hours.

4.2.5 *In vitro* assessments of TGF- β 1 induced lung fibroblast differentiation to myofibroblast

TGF- β 1 induced differentiation of MRC-5 cells to myofibroblast and its inhibition with the test molecules were assessed with a myofibroblast marker, α -SMA, measured by the western blot analysis. In 10 cm dishes (Greiner Bio-One, Monroe, NC), the MRC-5 cells (2×10^6 cells per dish) were grown to confluence, and then incubated with the test molecules and TGF- β 1, added similarly to that for the collagen and proliferation studies described above. However, 500 μ M PIR was not

assessed in this experimental system due to resource and time constraints. At 72 hours after addition of the test molecules, the media were removed, and the cells were washed with phosphate buffered saline (PBS) (Quality Biological, Gaithersburg, MD), scraped off with a scraper (Greiner Bio-One) and lysed in 0.5 ml of the lysis buffer. The lysis buffer was a 1 % Nonidet P-40 (NP-40; Thermo Fischer Scientific, Waltham, MA), 50 mM Tris (pH 8; Sigma-Aldrich) and 150 mM NaCl (Thermo Fischer Scientific), supplemented with enzyme inhibitors added as cOmplete mini™ protease inhibitor cocktail tablet and PhosSTOP™ phosphatase inhibitor tablet (Roche diagnostics, Indianapolis, IN), according to Roche's guidelines for use. The cells were then centrifuged at 10,000 rpm for 10 minutes at 4 °C (Avanti JE Centrifuge; Beckman Coulter). Western blot procedure is fully described in Appendix II. For α -SMA quantification, following electrophoresis and protein transfer, the nitrocellulose membrane was incubated with 1A4-(asm-1) α -SMA antibody (1:250; Invitrogen, Rockford, IL) at 4 °C overnight. The membrane was then incubated with horseradish peroxidase-linked goat anti-mouse IgG antibody (1:3,000; Bio-Rad) for 1 hour at room temperature. The protein was then detected using SuperSignal™ West Pico PLUS chemiluminescent substrate (ThermoFisher) in a film processor (X-Omat 2000A; Eastman Kodak, Rochester, NY). The same membrane was then subjected for detection of GAPDH with its antibody (1:5,000; ThermoFisher) as loading control for normalization. The signal of each band was quantified using ImageJ (NIH, Bethesda, MD). The α -SMA band signal was normalized with the corresponding GAPDH (loading control) signal and are expressed as the value relative to the vehicle control.

4.2.6 Data description and statistical analyses

The data are expressed as mean±SD from n=3-8. Treatment groups were statistically compared with Prism[®] 7 (GraphPad Software, San Diego, CA) by one-way analysis of variance (ANOVA), followed by Tukey's or Dunnett's post hoc test for multiple comparison. p<0.05 was considered as significant.

4.3 Results

4.3.1 Inhibition against TGF- β 1 induced lung fibroblast collagen increase

Figure 4.1 shows collagen masses in the MRC-5 cells measured with the absorbance at 540 nm by the validated picosirius red method following incubation of AM24 at 0-10 μ M for 48 hours in the absence or presence of TGF- β 1 (10 ng/ml) induction. TGF- β 1 induced cellular collagen mass increase by 3.5-fold, and AM24 exhibited inhibition in a concentration-related manner. At 10 μ M, AM24 inhibited TGF- β 1 induced collagen increase significantly by ~91 % ($p < 0.05$; Fig. 4.1), while AM24 alone caused no change. Accordingly, this inhibitory activity of AM24 was then compared with the activities of MEL, CUR, MEL+CUR and PIR at 10 μ M, as well as PIR at 500 μ M, as shown in Figure 4.2. Note that, like AM24, these molecules alone did not affect cellular collagen mass at least at 10 μ M. Both MEL and CUR caused significant inhibition, yet in a lesser extent than AM24, i.e., by 25.5 and 25.8 %, respectively, while the physical MEL+CUR mixture failed to cause inhibition. By contrast, as an FDA-approved PF drug, PIR was shown to be inhibitory to this TGF- β 1 induced collagen increase only at 500 μ M, but not at 10 μ M. Likewise, as shown in Figure 4.3, TGF- β 1 induced collagen increase in the NHLF cells by 1.9-fold, and AM24 at 10 μ M exerted significant 57 % inhibition ($p < 0.05$).

To examine if this inhibitory activity of AM24 against TGF- β 1 induced collagen increase in the MRC-5 cells was mediated through melatonin receptors, LUZ, a pan-melatonin receptor antagonist, was added in the experiment. As shown in Figure 4.4, the inhibitory activity of AM24 was completely opposed by addition of LUZ (0.1 μ M). Note however that LUZ alone did not affect collagen mass in the absence or presence of TGF- β 1 induction.

Taken all these data together, AM24 was shown to inhibit *in vitro* TGF- β 1 induced collagen increase in the lung fibroblasts. Its activity was more potent than MEL, CUR, MEL+CUR, or PIR, and suggested to be mediated, at least in part, through the melatonin receptors.

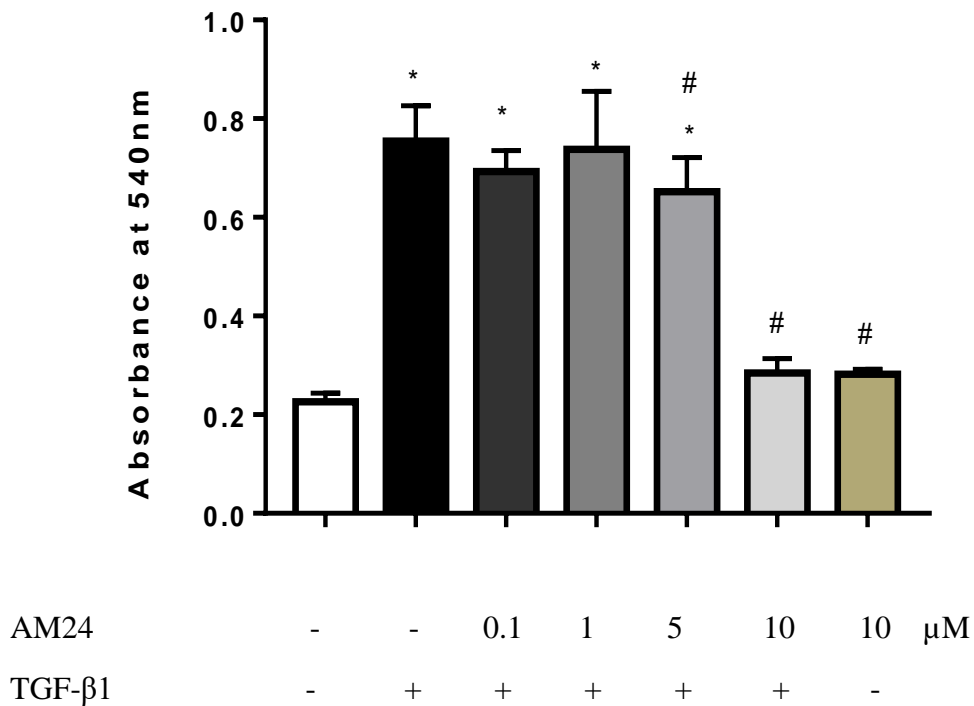


Figure 4.1: *In vitro* MRC-5 cellular collagen masses measured with the 540 nm absorbance by the validated picosirius red method following incubation of AM24 at 0-10 μ M for 48 hours in the absence or presence of TGF- β 1 (10 ng/ml) induction. Data: mean \pm SD from n=3-8. *p<0.05 vs. vehicle control; and # p<0.05 vs. TGF- β 1 induced control, by ANOVA and Tukey's HSD post hoc test.

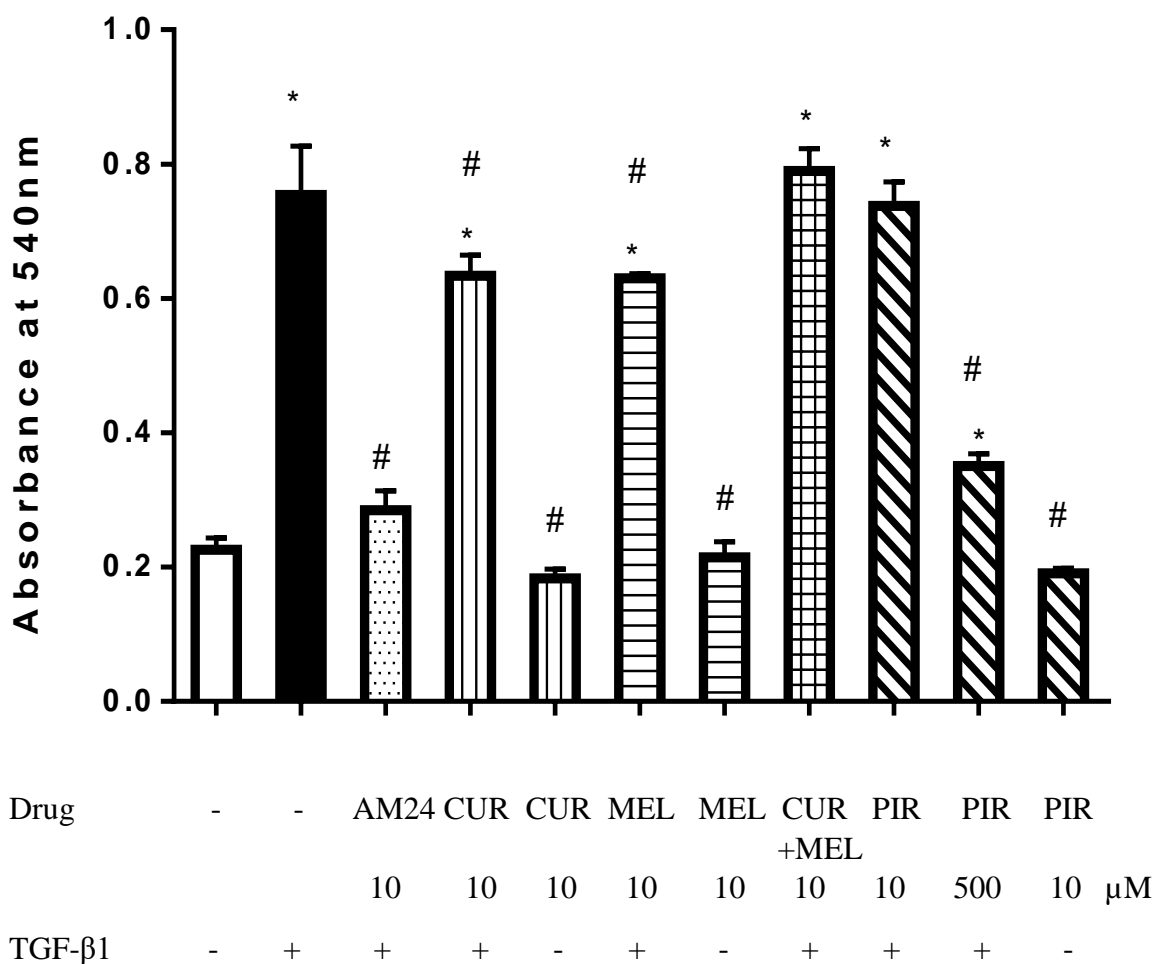


Figure 4.2: Effects of AM24, MEL, CUR, MEL+CUR and PIR at 10 μ M and PIR at 500 μ M on the *in vitro* MRC-5 cellular collagen mass measured with the 540 nm absorbance by the validated picrosirius red method following 48-hour incubation with/without TGF- β 1 induction. Data: mean \pm SD from n=3-8. *p<0.05 vs. vehicle control; and # p<0.05 vs. TGF- β 1 induced control, by ANOVA and Tukey's HSD post hoc test.

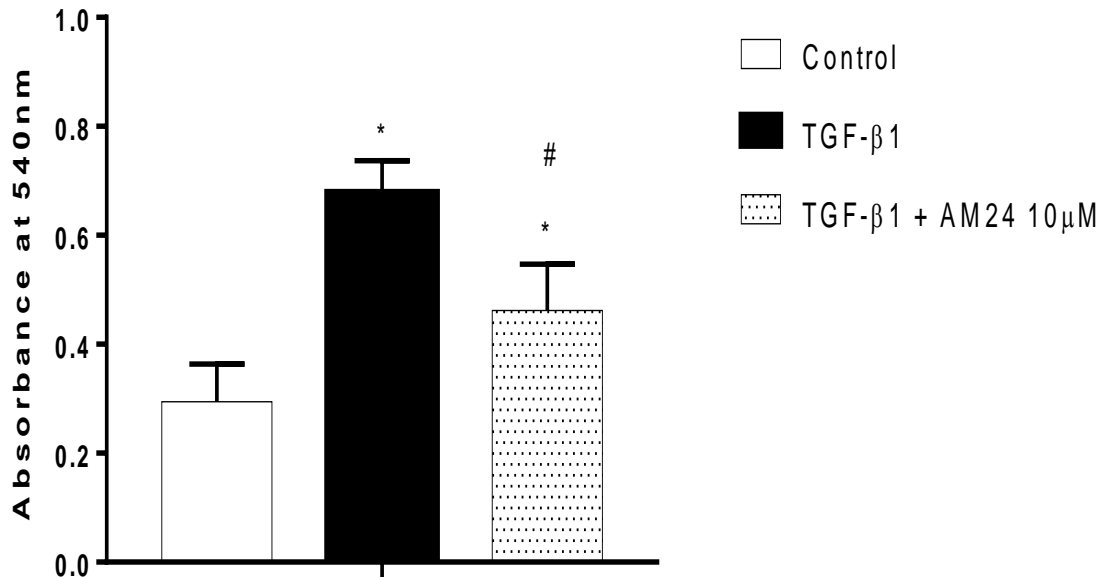


Figure 4.3: Effects of AM24 at 10 μ M on the *in vitro* NHLF cellular collagen mass measured with the 540 nm absorbance by the validated picosirius red method at 48 hours following incubation with TGF- β 1 induction. Data: mean \pm SD from n=3-6. *p<0.05 vs. vehicle control; and # p<0.05 vs. TGF- β 1 induced control, by ANOVA and Tukey's HSD post hoc test.

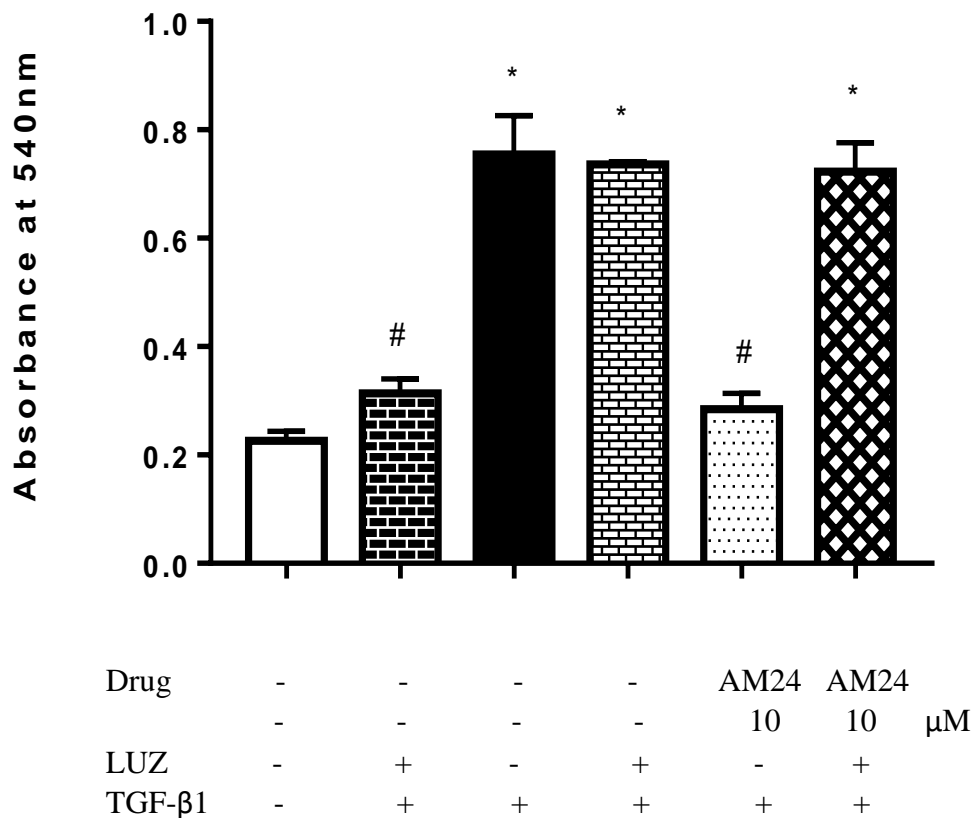


Figure 4.4: Effect of LUZ (0.1 μM; a pan-melatonin receptor antagonist) on the inhibitory activity of AM24 (10 μM) against the *in vitro* TGF-β1 induced MRC-5 cellular collagen increase measured with the 540 nm absorbance by the validated picosirius red method. Data: mean±SD from n=3-8. *p<0.05 vs. vehicle control; and # p<0.05 vs. TGF-β1 induced control, by ANOVA and Tukey's HSD post hoc test.

4.3.2 Inhibition against TGF- β 1 induced lung fibroblast proliferation

The TGF- β 1 induced MRC-5 cellular collagen increases and its inhibition with AM24 (and other test molecules) shown above may have resulted simply from increased and decreased cellular proliferation, respectively, rather than stimulation and suppression of the cell activity. Therefore, the cell proliferative activity was assessed following incubation of AM24, MEL, CUR and PIR at 10 μ M for 48 hours in the absence or presence of TGF- β 1 (10ng/ml) induction. Figure 4.5 shows the results measured with the Δ absorbance at 590 nm by the MTT assay. Neither TGF- β 1 nor any of the test molecules affected cell proliferation. Thus, it was highly likely that the TGF- β 1 induced cellular collagen increase and its inhibition with AM24 (and other test molecules) shown above arose from the activity changes of cellular collagen synthesis.

In contrast, when the experiment was extended to 72-hour incubation, TGF- β 1 (10 ng/ml) did stimulate MRC-5 cell proliferation significantly by 2.6-fold, and AM24 caused inhibition at \geq 1 μ M without clear concentration-dependence, as shown in Figure 4.6. In fact, at 10 μ M, AM24 inhibited TGF- β 1 induced cell proliferation significantly by 72 % ($p < 0.05$; Fig. 4.7), while AM24 alone caused no change. Accordingly, this inhibitory activity of AM24 was compared with the activities of MEL, CUR, MEL+CUR, and PIR at 10 μ M, as well as PIR at 500 μ M, as shown in Figure 4.7. Note that, like AM24, neither MEL nor CUR alone affected cell proliferation at 10 μ M. MEL, CUR, MEL+CUR and PIR at 10 μ M indeed inhibited the TGF- β 1 induced MRC-5 cell proliferation significantly by 51-57 %, but these activities were not as potent as the activity of AM24 (i.e., 72 %). As a FDA-approved PF drug, PIR more potently inhibited the TGF- β 1 induced cell proliferation by 86 % but at 500 μ M (Fig. 4.7).

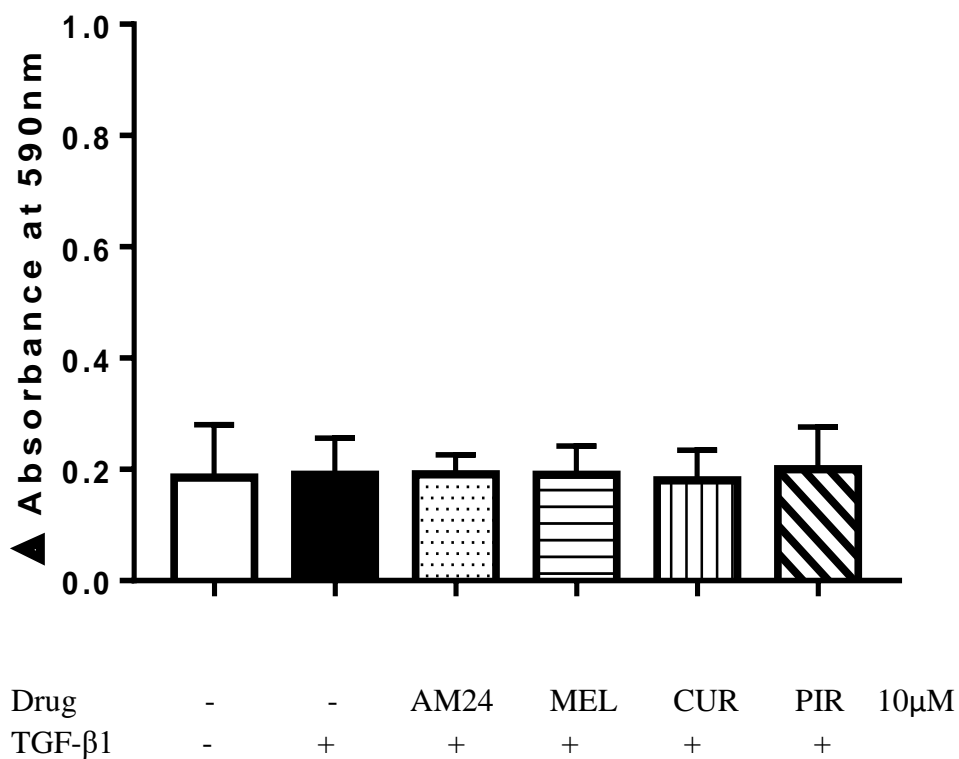


Figure 4.5: *In vitro* MRC-5 cell proliferative activities measured with the Δ absorbance at 590 nm by the MTT assay following incubation with AM24, MEL, CUR and PIR at 10 μ M for 48 hours in the absence or presence of TGF- β 1 (10 ng/ml) induction. Data: mean \pm SD from n=3-9. No statistical difference was seen across groups, analyzed by ANOVA.

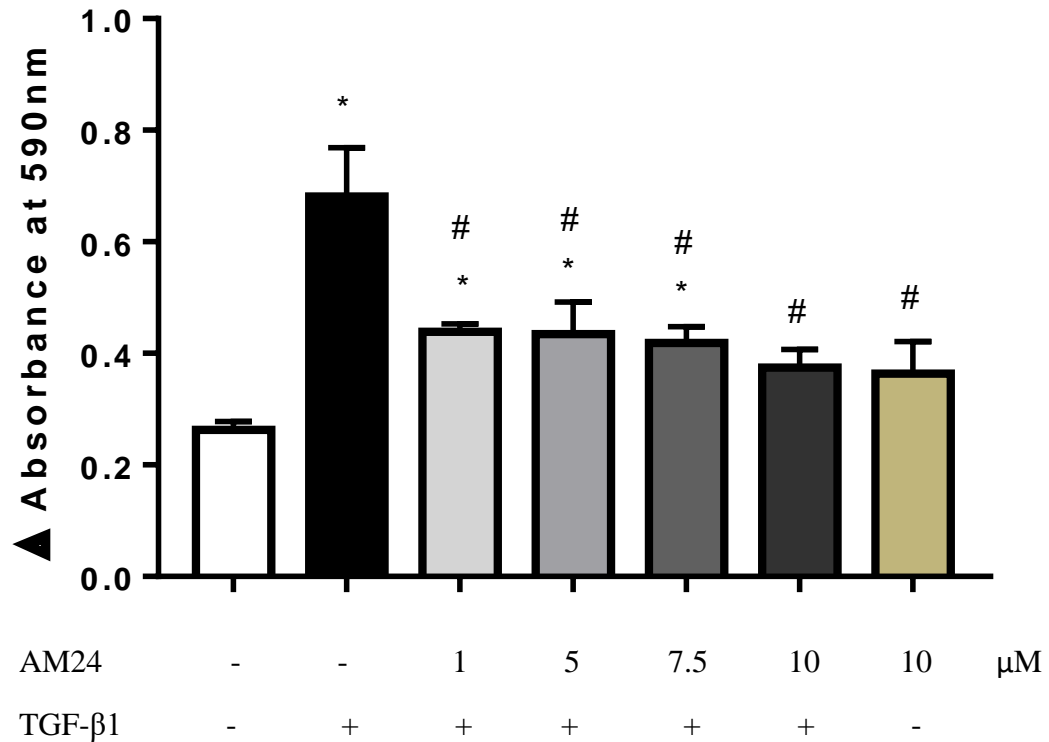


Figure 4.6: *In vitro* MRC-5 cell proliferative activities measured with the Δ absorbance at 590 nm by the MTT assay following incubation with AM24 at 0-10 μ M for 72 hours in the absence or presence of TGF- β 1 (10 ng/ml) induction. Data: mean \pm SD from n=3. *p<0.05 vs. vehicle control; and # p<0.05 vs. TGF- β 1 induced control, by ANOVA and Tukey's HSD post hoc test.

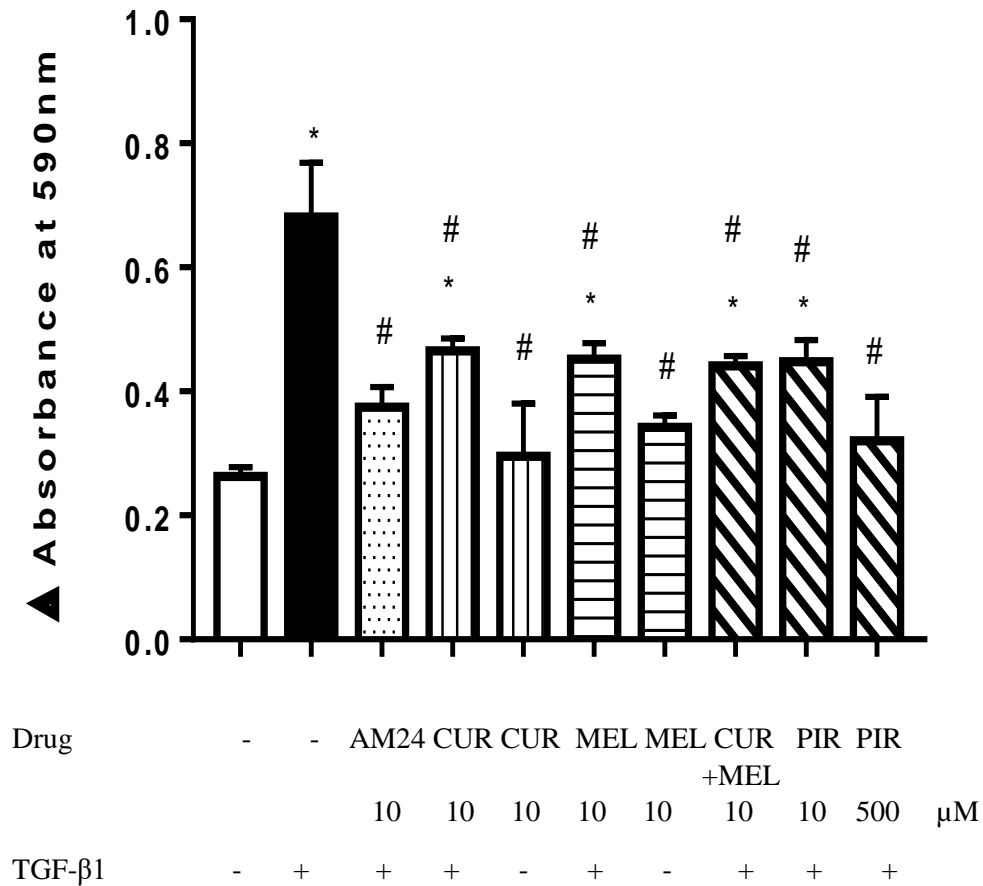


Figure 4.7: Effects of AM24, MEL, CUR, MEL+CUR and PIR at 10 μ M and PIR at 500 μ M on the *in vitro* MRC-5 cell proliferative activities measured with the Δ absorbance at 590 nm by the MTT assay following 72-hour incubation with/without TGF- β 1 induction. Data: mean \pm SD from n=3. *p<0.05 vs. vehicle control; and # p<0.05 vs. TGF- β 1 induced control, by ANOVA and Tukey's HSD post hoc test.

4.3.3 Inhibition against TGF- β 1 induced lung fibroblast differentiation to myofibroblast

In addition to stimulation of cell proliferation, TGF- β 1 has been suggested to induce lung fibroblast differentiation to myofibroblast to promote fibrotic thickening and scarring in PF lungs. Hence, the inhibitory activities of AM24 and other test molecules against TGF- β 1 induced fibroblast (MRC-5) differentiation to myofibroblast over 72 hours were assessed, measured with the cellular expression of α -SMA, a myofibroblast marker, by Western blot. The results are shown in Figures 4.8 and 4.9. TGF- β 1 (10 ng/ml) induced a significant ~2-fold increase of the α -SMA expression ($p < 0.05$), demonstrating induced MRC-5 differentiation to myofibroblast. However, AM24 at 10 μ M, but not at 1 μ M, inhibited such TGF- β 1 induced differentiation by over 100 % (i.e., 189 %), as shown in Figure 4.11. By contrast, MEL, CUR, MEL+CUR and PIR all failed to inhibit the TGF- β 1 induced differentiation at 10 μ M, suggesting their much less potent activities, compared to AM24.

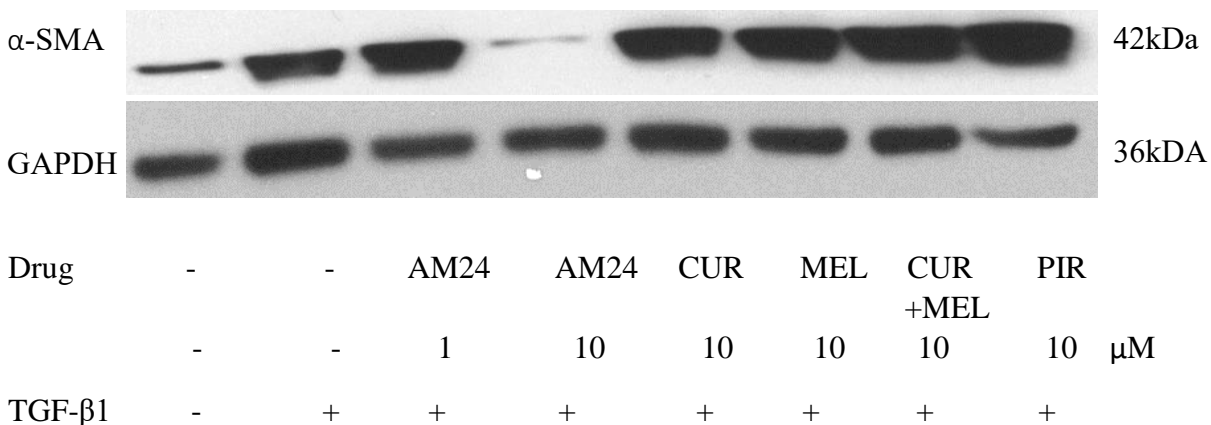


Figure 4.8: Representative images of MRC-5 cellular expressions of α -SMA following 72-hour incubation with AM24 (1 or 10 μ M) and CUR, MEL, MEL-CUR and PIR (10 μ M) with TGF- β 1 induction, measured by Western blot. The GAPDH expression of the corresponding samples was used as loading control for quantitative comparison shown in Figure 4.9.

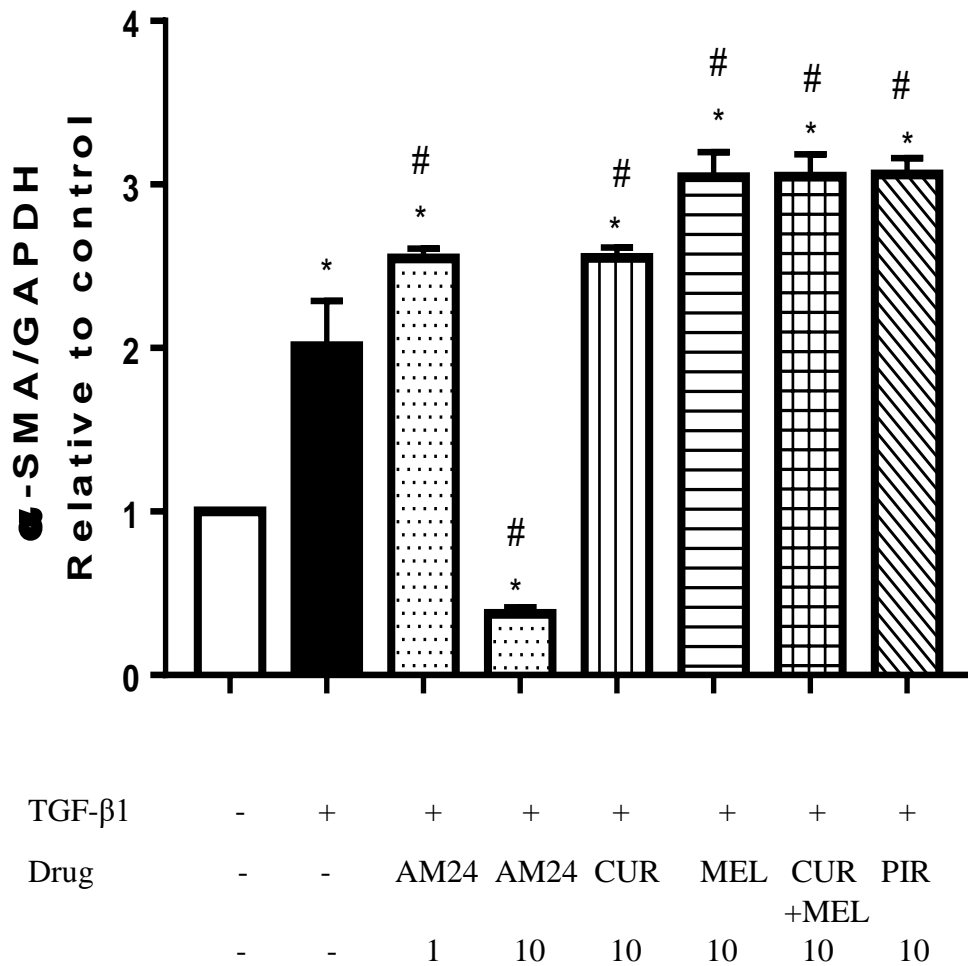


Figure 4.9: MRC-5 cellular expressions of α -SMA following 72-hour incubation with AM24 (1 or 10 μ M) and CUR, MEL, MEL-CUR and PIR (10 μ M) with TGF- β 1 induction, measured by Western blot. The band signal for α -SMA in each sample was quantified and normalized with that for GAPDH in the corresponding sample, which was then compared among the groups with or without treatment and induction with a value relative to that for the vehicle-treated and uninduced control. Data: mean \pm SD from n=3. *p<0.05 vs. vehicle control; and # p<0.05 vs. TGF- β 1 induced control, by ANOVA and Tukey's HSD post hoc test.

4.4 Discussion

TGF- β 1 induced *in vitro* fibroblast models are widely used for the assessment of anti-fibrotic agents. As seen in the literature (Chen et al, 2012; Zhang et al, 2014), in the present study, TGF- β 1 at 10 ng/ml significantly induced collagen synthesis, fibroblast proliferation and differentiation. Given the complexity of the disease pathogenesis, inductions of TGF- β 1, collagen synthesis, fibroblast proliferation and differentiation, it became necessary to separately assess the inhibitory effects on these pathogenic events. At 48 hours, TGF- β 1 failed to induce proliferation in the MRC-5 cells (Fig. 4.5), while increasing collagen synthesis by 3.5-fold (Fig. 4.1). Hence, the induced collagen synthesis was not a result of an increased number of the cells by proliferation. In fact, Figure 4.10 shows the collagen synthesis at 48 hours normalized with the proliferation activity at 48 hours. Induction of collagen synthesis by TGF- β 1 was 3.3-fold which was inhibited with AM24 at 10 μ M by ~80 %, while MEL, CUR and PIR at 10 μ M inhibited collagen synthesis by only ~30 %. This would be more accurate, yet led to the same conclusion that AM24 inhibited the cellular activity of collagen synthesis in the MRC-5 cells without changes in proliferation.

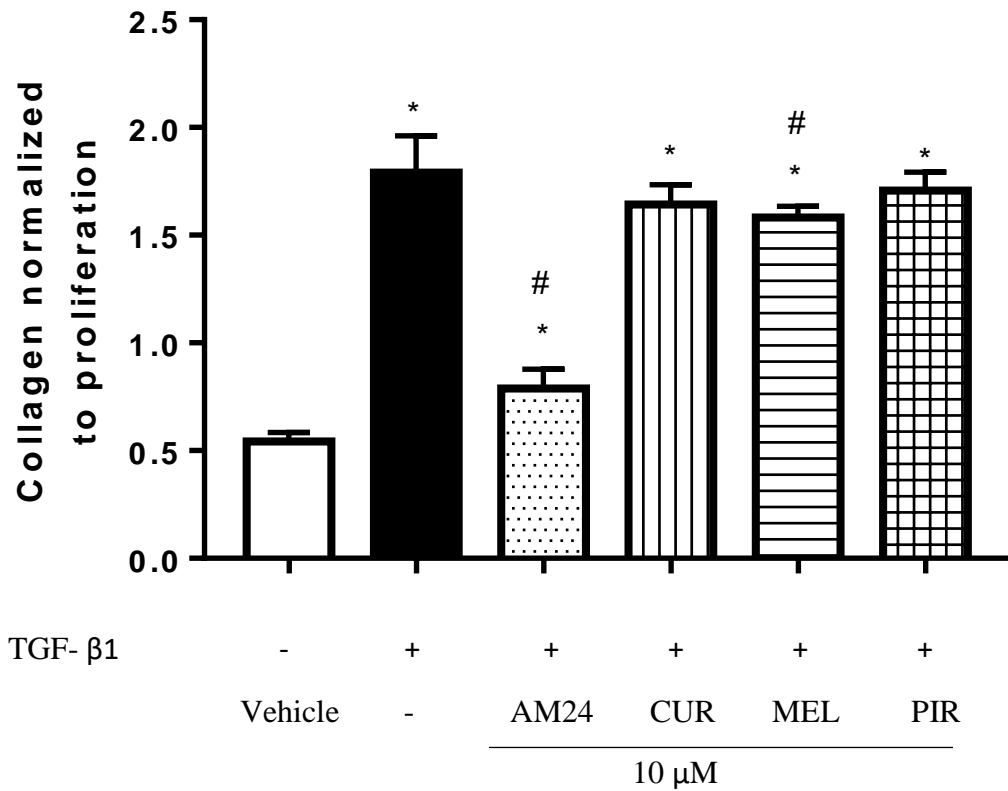


Figure 4.10: *In vitro* induction in collagen synthesis by TGF-β1 at 10 ng/mL at 48 hours normalized to the proliferation at 48 hours. Data are mean ± S.D. (n=3) *p<0.05 vs. vehicle control and # p<0.05 vs. TGF-β1 induced control. Data are analyzed by ANOVA and post hoc Tukey's HSD test.

Myofibroblasts are known to be the cellular orchestrators of ECM production (Zent and Guo, 2018). Thus, we also studied the effect of TGF- β 1 at 10 ng/ml on differentiation of fibroblast to myofibroblasts at 48 hours. This was also to examine if the increased collagen synthesis was associated with increased differentiation of fibroblasts to myofibroblasts. The results are shown in Figure 4.11. At 48 hours, TGF- β 1 did not induce differentiation, given that the cellular α -SMA levels were consistent between the vehicle control and TGF- β 1 groups. However, as shown above, at 72 hours, a marked increase was seen in the α -SMA levels upon TGF- β 1 incubation, indicating increased differentiation. This again proved that the induced collagen synthesis seen at 48 hours was not caused by increased differentiation of fibroblasts to myofibroblasts.

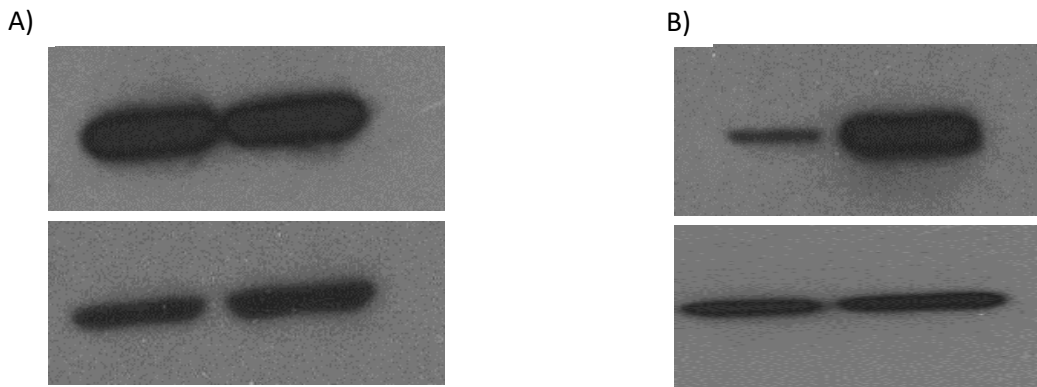


Figure 4.11: TGF- β 1 induced differentiation of fibroblasts to myofibroblasts A) At 48 hours and B) At 72 hours.

Collagen synthesis in given treatments was comparable between the MRC-5 and NHLF cells (Fig. 4.2 and 4.3), so that the majority of the studies were carried out with the MRC-5 cells, despite their fetal origin. In the MRC-5 cells, MEL and CUR at 10 μ M inhibited TGF- β 1 induced collagen synthesis by ~25 % (Fig. 4.2). These activities were reasonably consistent with the

literatures where MEL at 400 μM and CUR at 10 μM exerted ~ 100 and ~ 30 % inhibition against TGF- $\beta 1$ induced collagen synthesis in fibroblasts (Liu et al, 2016; Saidi et al, 2019; Monica et al, 2010; Zhao et al, 2018). However, the physical mixture of MEL and CUR at 10 μM showed no effect on the collagen synthesis. Notably, PIR showed no inhibition of TGF- $\beta 1$ induced collagen synthesis in the MRC-5 cells at 10 μM , but at 500 μM , it showed ~ 76 % inhibition. This activity was again similar to that seen in the literature where PIR at 1-5 mM completely inhibited TGF- $\beta 1$ induced collagen synthesis (Conte et al, 2014; Hisatomi et al, 2012; Stahnke et al, 2017).

TGF- $\beta 1$ significantly induced fibroblast proliferation in the MRC-5 cells which was inhibited by MEL and CUR by ~ 50 % (Fig. 4.7). These results corroborate with those seen in the literature where MEL at 400 μM caused complete inhibition of proliferation induced by TGF- $\beta 1$, while CUR at 10-20 μM exerted rather an anti-proliferative activity in a concentration- and time-dependent manner (Liu et al, 2016; Smith et al, 2010; Zhao et al, 2018). PIR showed ~ 54 % inhibition against TGF- $\beta 1$ induced proliferation at 10 μM ; however, at 500 μM , it showed 86 % inhibition. This was again consistent with the literature for PIR at 1-5 mM causing nearly complete inhibition of TGF- $\beta 1$ induced proliferation in the human intestinal fibroblasts. Nintedanib on the other hand is much more potent since at 1 μM , it inhibited TGF- $\beta 1$ induced proliferation by almost 80 % (Conte et al, 2014; Sun et al, 2018; Lin et al, 2018).

TGF- $\beta 1$ significantly induced differentiation of fibroblasts to myofibroblasts, while MEL and CUR failed to show inhibition (Figs. 4.8 and 4.9). Once again, Zhao et al (2018) suggested MEL at a higher concentration, 400 μM , inhibited differentiation. CUR was also shown to inhibit differentiation at >20 μM , but at 10 μM , it did not show a marked inhibition (Liu et al, 2016; Saidi et al, 2019; Smith et al, 2010; Zhao et al, 2018). Through these data in the literature and the present study, it could be concluded that both MEL and CUR at 10 μM do not possess the inhibitory effects

against TGF- β 1 induced fibroblast differentiation as assessed by α -SMA levels. PIR could also not completely inhibit fibroblast differentiation at a low 10 μ M concentration which was consistent with by Kurita et al (2017) who reported that PIR required 2.7 mM to inhibit differentiation of fibroblasts, while nintedanib could inhibit differentiation at 1 μ M (Lin et al, 2018).

Despite unclear concentration-dependence, AM24 at 10 μ M showed 90 % inhibition against collagen synthesis, ~72 % inhibition of fibroblast proliferation and complete inhibition of differentiation to myofibroblasts. Notably, AM24 exerted these effects at a concentration lower than that for the anti-oxidative activity identified in Chapter 3, i.e., 25 μ M. It has also been evidenced in the literature that MEL (10 mg/kg) and CUR (50mg/kg) in *in vivo* rat model are equipotent to quercetin in their ability to maintain the levels of antioxidative enzymes like GSH, catalase and superoxide dismutase (Ebyl et al., 2008). Quercetin once again has been shown to have IC₅₀ lower than Trolox in the ABTS assay (Lee et al., 2014). Thus, the results from the chemical assay can be used to get some mechanistic clarity of how AM24 exerts its anti-fibrotic effects. Thus, the anti-fibrotic effects of AM24 is unlikely associated with its anti-oxidative activity. In terms of its anti-oxidative activity, AM24 was similar to MEL but less potent than CUR; however, in the anti-fibrotic activities AM24 was significantly more potent than MEL and CUR. Interestingly, the physical mixture of MEL and CUR (MEL+CUR) failed to show the inhibitory activity on the TGF- β 1 induced fibrotic effects. These results suggest that the anti-fibrotic activities of AM24 were not a result of simple additive effect of MEL and CUR, while such an independent mechanism still remains to be identified. In this respect, Zhao et al (2018) suggested the involvement of the Hippo/Yap1 (Yes-associated protein) pathway and MEL receptors in the development of PF. The study demonstrated that MEL acted on the G protein-coupled MEL receptors (MT1 and MT2 receptors), activated the Hippo signaling pathway, and

thereby induced degradation of YAP1 (Xhao et al, 2018). Such YAP1 degradation was thus attributed to the anti-fibrotic effects of MEL i.e. decreased collagen synthesis, proliferation and differentiation. The complete inhibitory activities of AM24 on the TGF- β 1 induced collagen synthesis upon addition of the MEL receptor antagonist LUZ provided a supportive proof that AM24 may act on the MEL receptors (MT1 and MT2). However, Zhao et al (2018) used 400 μ M, while AM24 showed its effect at 10 μ M, making it 40 times more potent. This significantly higher potency of AM24 could be by virtue of additional activity derived from the CUR part of the hybrid; however, no proof about this effect is available to date. Note that, this mechanistic study using LUZ was conducted only for TGF- β 1 induced collagen synthesis. Similar studies using LUZ would be necessary to assess the involvement of the MEL receptors on the AM24 inhibition of fibroblast proliferation and differentiation. In addition, whether AM24 is a TGF- β 1 inhibitor or not is of great interest to be ruled out, as all the studied described here were based on TGF- β 1 induced systems. Further experiments using TGF- β 1 receptor inhibitors like Koh et al (2015) may be worth of consideration to further explore the mechanism of these promising activities of AM24.

CHAPTER 5

***IN VITRO* INHIBITORY ACTIVITY OF MEL-CUR HYBRID AM24 AGAINST TGF- β 1 INDUCED EPITHELIAL-MESENCHYMAL TRANSITION (EMT)**

5.1 Introduction

In addition to the pathologically-abnormal fibroblast activations of induced proliferation and differentiation as examined in Chapter 4, induced epithelial-mesenchymal transition (EMT) has also been implicated with the process of such fibroblast activations in PF lungs (Chapter 1). While generally remaining stationary, epithelial cells undergo phenotypic changes in EMT, such as losses of apical-basal polarity and intercellular contacts, thereby acquiring a mesenchymal and motile phenotype (Huang, 2012). This EMT has been shown to be induced in PF lungs and thus implied, at least in part, as an origin of excessive myofibroblast formation and ECM deposition (Volk et al, 2013) . Like fibroblast activation, TGF- β 1 is believed to be a pathologic inducer for EMT in PF lungs (Stone, 2016). Hence, it is logically desired that drugs effectively treating PF lungs possess the inhibitory activity against TGF- β 1 induced EMT. Therefore, in this chapter, TGF- β 1 induced EMT and its inhibition with our test molecules were studied using the *in vitro* human alveolar epithelial A549 cell system. TGF- β 1 induced loss of an epithelial cell marker, E-cadherin, and gain of a mesenchymal cell marker, vimentin, were measured as EMT in the absence or presence of each test molecule by western blot analyses.

5.2 Materials and Methods

5.2.1 *In vitro* TGF- β 1 induced EMT assessment in the A549 cells

The human adenocarcinoma alveolar epithelial A549 cells (ATCC) were maintained in culture with the Ham's F12-K medium (ATCC) with 10 % FBS (Thermo Fischer) and 1 % PS (ATCC) and used between passage 11 to 17. The A549 cells were grown to confluence in 10 cm culture dishes (Greiner Bio-One) and then, incubated for 72 hours with or without TGF- β 1 at 10 ng/ml in the absence or presence of the test molecules in the culture media. As was used in the studies described in Chapter 4, TGF- β 1 was added as 1,000X solution prepared in the sterile 4 mM HCl containing 0.1 % human or bovine serum albumin. Each test molecule was prepared as a stock solution of 100 μ M in the culture media. Using these stock solution, appropriate volumes were added in the 10 cm dish to get the desired concentrations. 500 μ M PIR was not assessed in this experimental system due to resource and time constraints. At 72 hours, the incubation media was removed, and the cells were washed with PBS twice, scraped with the cell scraper (Greiner Bio-One) and lysed with 500 μ L of the lysis buffer described in Chapter 4 and Appendix II. The cells and the lysis buffer were then centrifuged at 10,000 rpm for 10 minutes at 4 °C (Avanti JE Centrifuge), and the supernatant was collected as cytosolic samples.

The cytosolic samples were analyzed for E-cadherin and vimentin expressions by Western blot, as fully described in Appendix II. Briefly, with the protein contents of the samples determined using the BCA assay (Thermo Fischer Scientific), 40 μ g protein samples of the supernatant were denatured, electrophoresed, and transferred to nitrocellulose membranes. The membranes were blocked and incubated overnight at 4 °C with each of the following primary monoclonal antibodies (mAb): a) E-cadherin 1:500; Molecular weight 135 kDa; rabbit mAb b) Vimentin 1:500; molecular weight 57 kDa ; rabbit mAb. Subsequently, the membranes were incubated in secondary antibody

and the protein was then detected using SuperSignal™ West Pico PLUS chemiluminescent substrate (Thermo, Rockford, IL) in a film processor (X-Omat 2000A; Eastman Kodak, Rochester, NY). The signals of each of the bands was quantified using ImageJ (NIH, Bethesda, MD). Each protein signal was normalized using corresponding β -actin (loading control) signal obtained from the same membrane. The β -actin antibody used was β -Actin; molecular weight 42 kDa Mouse mAb (1: 5000; Cell Signaling Technology, Danavers, Massachusetts).

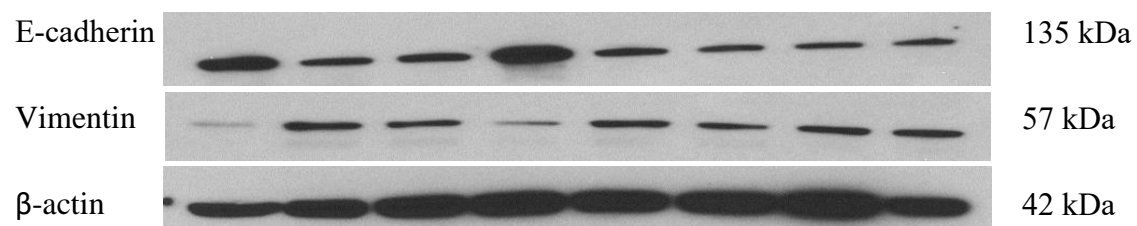
5.2.2 Data description and statistical analyses

The Western blot band images were scanned, and the bands corresponding to E-cadherin, vimentin and β -actin were each analyzed to yield the densitometric values using ImageJ software. The expressions of E-cadherin and vimentin were determined as their densitometric values relative to the β -actin (loading control) signal and are expressed as the values relative to the vehicle-treated control. Experiment were carried out in triplicate. One-way analysis of variance (ANOVA) was used followed by post hoc Tukey's HSD for statistical comparison between groups. $p < 0.05$ was considered as significant.

5.3 Results and Discussion

5.3.1 Effect of AM24 and comparator molecules on TGF- β 1 induced EMT

Representative Western blot band images for E-cadherin, vimentin and β -actin are shown in Figure 5.1. At 72 hours, TGF- β 1 induced transition of epithelial to mesenchymal cells as seen by the higher levels of E-cadherin and the comparatively lower levels of vimentin in Figure 5.2 and Figure 5.3 respectively. AM24 at 10 μ M inhibited TGF- β 1 induced EMT completely as seen in the blots as well as the densitometric quantification. However, at a lower concentration of 1 μ M, AM24 failed to inhibit this induced EMT. MEL, CUR and PIR at 10 μ M showed no significant effects on the TGF- β 1 induced EMT. Figure 5.2 and 5.3 depict the densitometric quantification of the blots of E-cadherin and vimentin, respectively. TGF- β 1 showed a significant 51 % reduction of the E-cadherin level which was inhibited by AM24 at 10 μ M, but was not by MEL, CUR or PIR. For vimentin, a significant induction by TGF- β 1 was not seen, while the intensity of the bands was slightly higher in the TGF- β 1 group than those for the vehicle control or AM24 (10 μ M), which was supportive of EMT induction. High variability of vimentin expressions seen in Figure 5.2 may have been due to one outlier in the triplicate experiments.



| | | | | | | | | |
|----------------|---|---|------|------|-----|-----|-------------|-----|
| TGF- β 1 | - | + | + | + | + | + | + | + |
| Drug | - | - | AM24 | AM24 | CUR | MEL | CUR +MEL | PIR |
| Conc(μ M) | - | - | 1 | 10 | 10 | 10 | 10 | 10 |

Figure 5.1: Representative western blot image of A549 cell expression of E-cadherin and Vimentin at 72 hours with or without TGF- β 1 and/or test molecules.

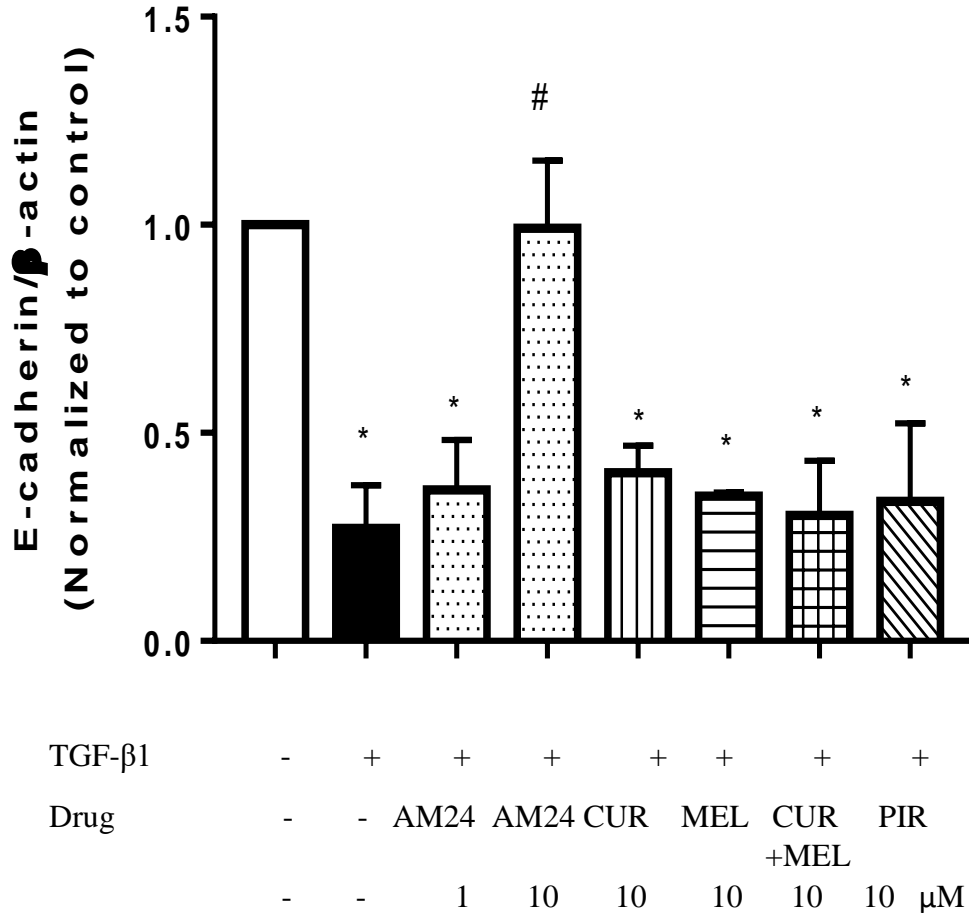


Figure 5.2: In vitro effect of test molecules AM24 (1, 10 μ M), CUR, MEL, CUR+MEL and PIR at 10 μ M on TGF- β 1 induced EMT and thus the levels of epithelial marker E-cadherin at 72 hours. Data are mean \pm SD (n=3) *p<0.05 vs. vehicle control and # p<0.05 vs. TGF- β 1 induced control. Data are analyzed by ANOVA and post hoc Tukey's HSD test.

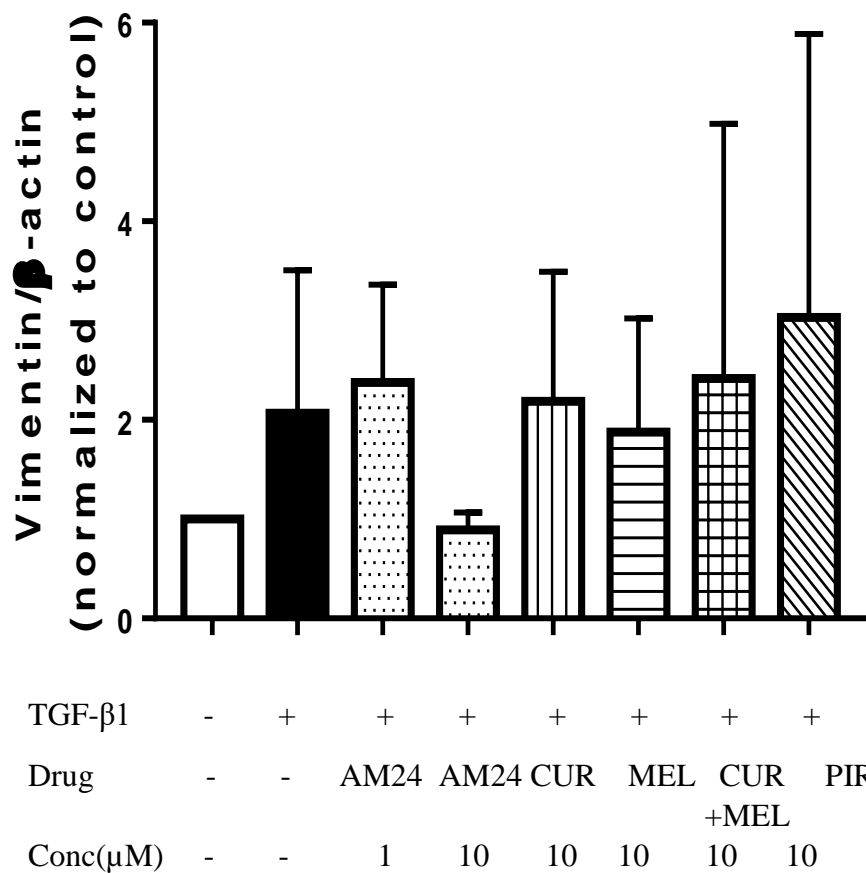


Figure 5.3: In vitro effect of test molecules AM24 (1, 10 μ M), CUR, MEL, CUR+MEL and PIR at 10 μ M on TGF- β 1 induced EMT and thus the levels of mesenchymal marker vimentin at 72 hours. Data are mean \pm SD (n=3). No significant difference was seen.

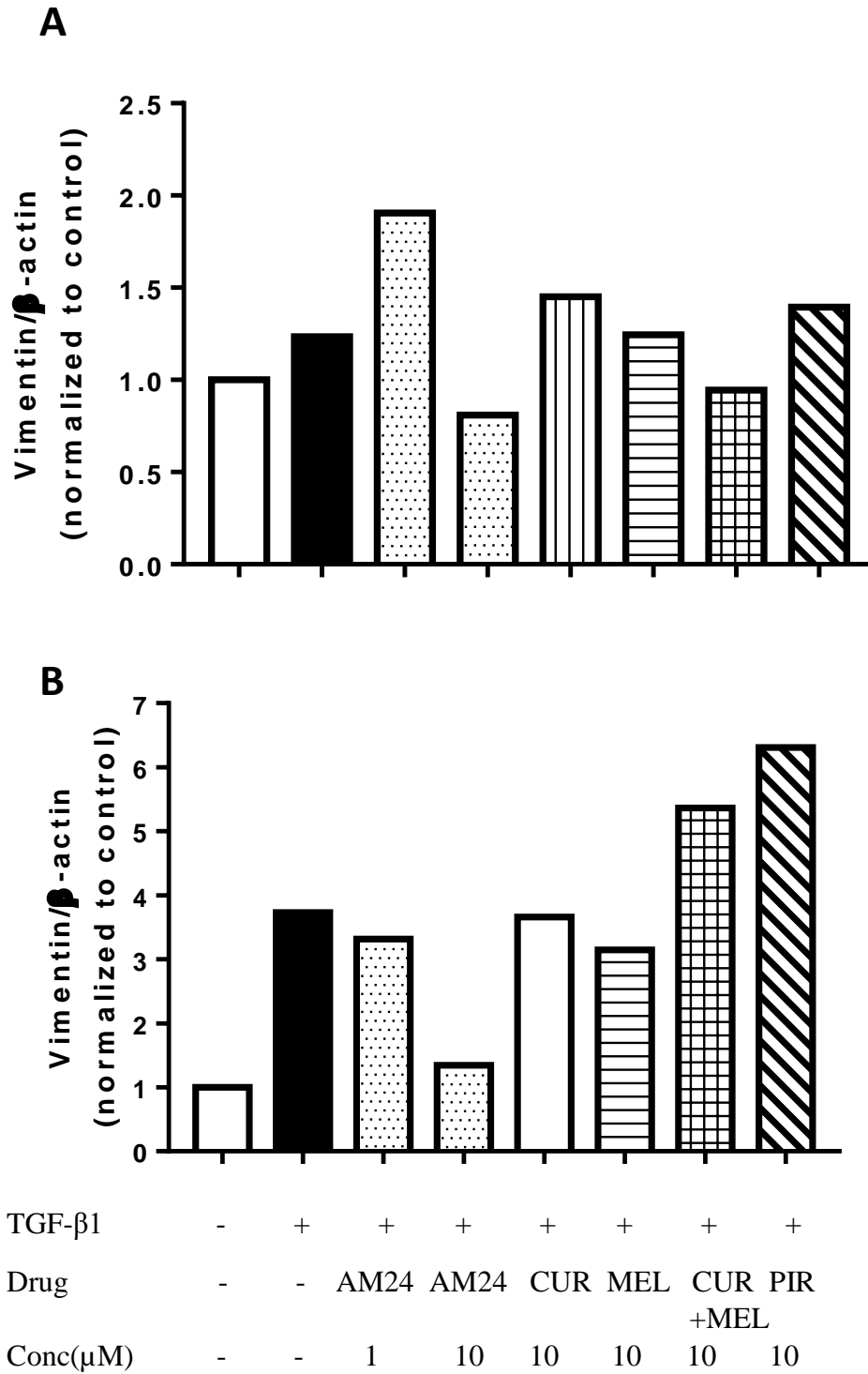


Figure 5.4: In vitro effect of test molecules AM24 (1, 10 μM), CUR, MEL, CUR+MEL and PIR at 10μM on TGF- β1 induced EMT and thus the levels of mesenchymal marker vimentin at 72 hours. A) Data are n=2 B) Data is n=1 indicating that the trend of vimentin increase/decrease remains the same despite high SD.

The TGF- β 1 exposure for 72 hours significantly reduced the E-cadherin level in the A549 cells, which was inhibited by AM24 at 10 μ M (Fig. 5.2). In addition, the vimentin level was slightly high but not significantly in the TGF- β 1 group. As a result, the vimentin expression was unaffected with the AM24 (10 μ M) treatment (Fig. 5.3). This TGF- β 1 induced reduction of E-cadherin and induction of vimentin were slightly different from the results shown by Brothwick et al (2011), where TGF- β 1 at 10 ng/ml caused ~31 % decrease in the E-cadherin level and ~57 % increase in the vimentin level in the A549 cell system. Rather, the results obtained in Figure 5.3 were identical to those obtained by Shintani et al (2007) and Hee et al (2007), where reduced E-cadherin levels were seen upon TGF- β 1 treatment in the A549 cells, but no change was for the vimentin levels. Another reason why we observed a lack of mass balance in terms of E-cadherin and vimentin levels could be due to further differentiation of mesenchymal cells to fibroblasts over this 72-hour period. Kasai et al (2005) indeed reported that TGF- β 1 exposure for 72 hours was sufficient to induce a myofibroblast marker α -SMA, in the epithelial cells, alongside morphologic features of epithelial cells altered to fibroblast-like features.

Fujiwara et al (2017) reported that PIR inhibited TGF- β 1 induced EMT in the A549 cells only at concentrations as high as 2.7 mM. Thus, AM24 was 270-times more potent than PIR. Kurimoto et al (2017) also reported that PIR and nintedanib showed no effect on the TGF- β 1 induced A549 cell EMT at 2 mM and 1 μ M, respectively. However, Nishijima et al (2016) showed that nintedanib was effective at 10 μ M for TGF- β 1 induced EMT inhibition in the A549 cells. Thus, it was at least likely that AM24 was comparable in the potency to inhibit EMT to nintedanib. MEL and CUR have also been assessed for their inhibition against TGF- β 1 induced EMT. MEL at 500 μ M was found to inhibit TGF- β 1 (10 ng/ml) induced A549 EMT but at 48 hours (Yu et al, 2016), as a less potent EMT inhibitory molecule than AM24. Li et al. (2013) studied the effect of

CUR at 1-20 μM on the TGF- β 1 (2.5 ng/ml) induced EMT in human proximal tubular cells and found that CUR at 20 μM rather upregulated E-cadherin level while reducing α -SMA levels suggesting inhibition of EMT. Thus, in comparison with these literatures, AM24 was ranked as a much more potent EMT inhibitory molecule than MEL, CUR, MEL+CUR and PIR, but perhaps equipotent to nintedanib.

The present study and many of the literatures have used A549 cells to study the effect of TGF- β 1 on EMT and to assess the ability of test molecules for inhibition. However, A549 cells are after all cancer cells, so that there may be a difference in the expression levels and their responses of E-cadherin and vimentin from those in PF lung epithelial cells. Hence, ideally, a study using primary PF lung alveolar epithelial cells should be conducted.

CHAPTER 6

***IN VIVO* INTERVENTION OF AM24 IN BLEOMYCIN-INDUCED PULMONARY FIBROSIS IN RATS**

6.1 Introduction

The *in vitro* lung fibroblast and alveolar epithelial cell studies in Chapters 4 and 5 have demonstrated that AM24 uniquely possessed more potent anti-fibrotic activities than MEL, CUR, and PIR. At 10 μ M, AM24 remarkably inhibited TGF- β 1 induced collagen synthesis, proliferation, and differentiation to myofibroblast in the MRC-5 fibroblast systems, and TGF- β 1 induced EMT in the alveolar epithelial A549 cell system. With these unique and potent *in vitro* activities, whether AM24 exerts therapeutic activities in *in vivo* models of PF was of great interest.

Since 1971, an animal model of bleomycin (BLM)-induced PF has been most widely used as a preclinical tool to investigate therapeutic potentials of drug molecules in question (Moeller et al, 2008). The model shows several histological features which resemble those seen in humans, such as obliteration of the alveolar space, increased collagen deposition, and presence of spindle shaped mesenchymal cells (Moeller et al, 2008; Schaefer, 2011). The model also has the advantage that it is easy to perform and reproducible (Moeller et al, 2008). However, the model is different from PF in humans, as it has a faster onset and is partially reversible, while PF in humans slowly progresses and is irreversible (Chua et al, 2005). Besides, pathogenic abnormalities are dependent on BLM dose, dosing route, and dosing frequency. Given these pros and cons well recognized, in this chapter, AM24 will be examined for intervention by lung delivery in the rat model of BLM-induced PF as the first *in vivo* proof-of-concept study for use of AM24 in the treatment of PF lungs.

6.2 Materials and Methods

6.2.1 Animals

All experiments were carried out, as had been approved by the VCU Institutional Animal Care and Use Committee (IACUC; AD10002000). Adult male Sprague-Dawley rats (200-250g) were received from Hilltop Lab Animals (Scottsdale, PA) and housed (2 rats per cage) in the animal facility. The facility was maintained at 20-23 °C and a relative humidity of 40-70 % with a 12-12 hours light-dark cycle. These animals were acclimatized for a week before the start of experiments.

6.2.2 A rat model of BLM-induced PF and AM24 treatment

The experimental protocol for BLM induction and AM24 treatment shown in Figure 6.1 was developed through several preliminary studies, as discussed later in Discussion. Bleomycin sulfate (BLM) was purchased from BioVision and freshly prepared in PBS (Quality Biological) for PF induction. AM24 was also freshly prepared in PBS for orotracheal solution instillation into the lungs. After the measurement of the pre-dose treadmill exercise endurance, animals received an 0.2 ml orotracheal spray instillation of BLM at 0.6 mg/kg to the lungs. At 6 hours after the BLM instillation on day 1, the first dose of AM24 (0.1 ml) was given to the lung at 0.1 mg/kg. On day 3, 5, 8, 10, 12 and 15 (i.e., ~every other day), AM24 at 0.1 mg/kg continued to be dosed to the lungs. BLM and AM24 were each administered to the lungs by orotracheal spray instillation using MicroSprayer (PennCentury, Wyndmoor, PA) under short anesthesia with 4 % isoflurane (Saluja et al, 2014). In this early study, rats were divided into the following three groups: 1) “Healthy” control (n=2): no BLM induction and no AM24 treatment; 2) “BLM” control (n=4): BLM induction and no AM24 treatment; and 3) “AM24-treated” group (n=5): BLM induction and AM24 treatment. During the study, body weight of each animal was measured. On day 12 and 15, the

post-dose treadmill exercise endurance was measured. Animals were then sacrificed on day 16 for lung removal via exsanguination under anesthesia with intraperitoneal urethane (1 g/kg; Sigma-Aldrich). The lungs were then removed from the body, and the airway lumens of the right lung lobes were tightly closed with a suture. The left lung lobe was inflated with 8-10 ml of 0.5 % agarose (Sigma-Aldrich) solution at 45 °C under a hydrostatic pressure of 20 cm, introduced through the tracheal cannula. The inflated left lung lobe was placed on ice for agarose solidification and then fixed in 10 % buffered formalin solution (Fischer chemical) at 4 °C for ≥ 24 hours. These fixed lungs were paraffin-embedded, and hematoxylin and eosin-stained airspace section slides were prepared by the VCU Pathology Services for histological and morphological assessments described below. In contrast, the right lung lobes were removed before formalin fixation and cut into small pieces for several biomarker assays, described below.

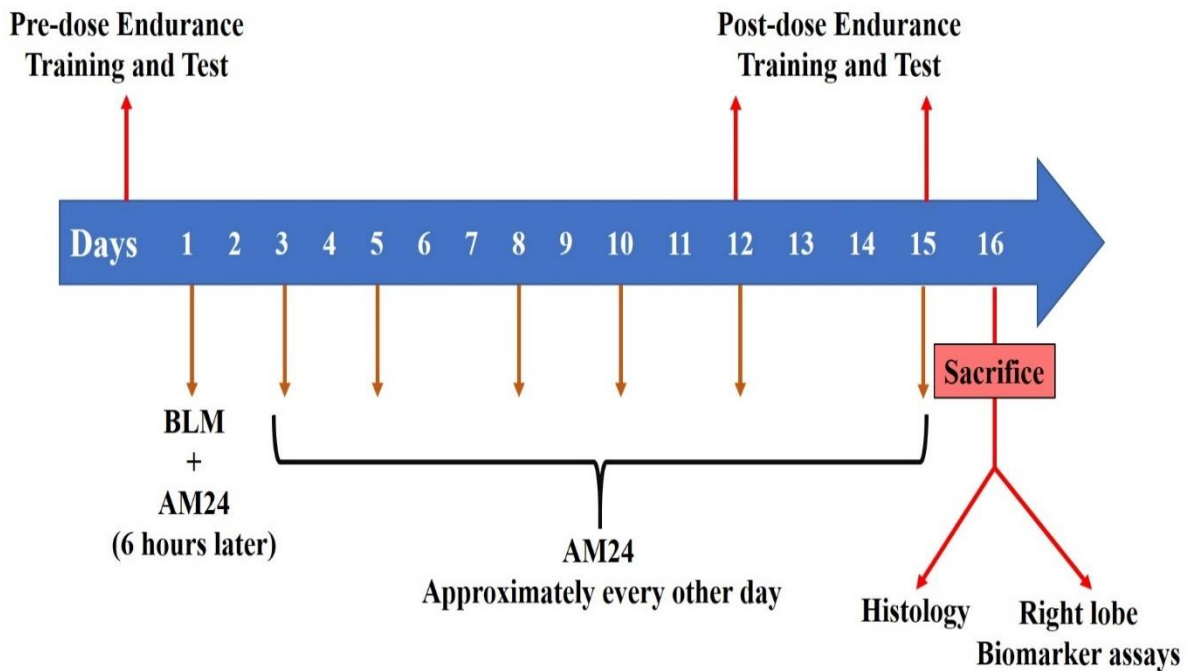


Figure 6.1: An experimental protocol for PF induction with BLM and subsequent AM24 treatment in rats, alongside several tests for assessments. While BLM was dosed to the lungs on day 1, AM24 was dosed to the lungs at 0.1 mg/kg on day 1, 3, 5, 8, 10, 12 and 15 (i.e., ~every other day).

6.2.3 Treadmill exercise endurance test

Upon receipt and acclimatization, rats were trained for a week to run on the AccuPacer rodent treadmill (Accusan Instruments, Columbus, OH) before the study. Between day 1 and 14, animals continued to be trained for the post-dose endurance test. As has been established and used in-house, exercise endurance was measured as a running time by exhaustion at a speed of 10 m/min and an inclination of 5 degrees on the treadmill. Exhaustion was judged, when animals received a 5th electrical foot shock from the bar grid or displayed an inability to return to the running belt.

The protocol for the training and endurance test is described in Appendix III. The pre-dose exercise endurance was measured on a day before day 1, whereas the post-dose exercise endurance was an average of the running times on Day 12 and 15.

6.2.4 Histological and morphological airspace examinations

Using Phenochart (PerkinElmer, Hopkinton, MA), 9 images were randomly selected from the hematoxylin and eosin-stained airspace section slides prepared above and examined for the absence or presence of fibrotic areas and alveolar structural destruction, referring to Hubner et al (2008).

6.2.5 Determination of lung tissue collagen

Lung tissue collagen was quantified by the picosirius red assay using the protocol adapted from Kliment CR. et al. (Kliment et al, 2011). The right lung lobe tissues taken above (100 mg) was homogenized in 1.5 ml of the CHAPS (3-[(3-cholamidopropyl)dimethylammonio]-1-propanesulfonate) buffer. The CHAPS buffer was composed of 50 mM TRIS, 150 mM NaCl, 10 mM CHAPS (Abcam, Cambridge, United Kingdom), 100 μ M dichloro-isocoumarin (Cayman chemical), 10 μ M E64 (trans-epoxysuccinyl-leucylamido-[4-guanidino]butane) (Cayman chemical), and 3 mM ethylenediaminetetraacetic acid *EDTA;Sigm-aldrich). After centrifugation at 10,000 rpm for 10 minutes at 4 °C, 200 μ l of the supernatant was dried in 48-well plates at 37 °C for 48 hours. As carried out in the *in vitro* cell-based studies described in Chapter 4 and Appendix I, 200 μ l of the picosirius red solution was added to each well and incubated on a shaker for 1 hour at room temperature. The wells are washed twice with PBS, followed by addition of 10 mM HCl for removal of the unbound dye. The collagen-bound dye was solubilized with 150 μ l of

100 mM NaOH, and then, the absorbance was measured at 540 nm after transfer to 96-well plates. Note that samples required 5-times dilution because the absorbance values were too high.

6.2.6 Lung tissue biomarker assessments by Western blot

Several lung tissue biomarkers were measured by Western blot analysis fully described in Appendix II. The right lung lobe tissues taken above (300 mg) were homogenized in 1 ml of the lysis buffer (1 % NP-40, 50 mM Tris, 150 mM NaCl, and protease and phosphatase inhibitor cocktails from cOmplete Mini™ and PhosSTOP™ tablets, respectively). After centrifugation at 10,000 rpm for 10 minutes at 4 °C, 40 µg protein samples of the supernatant were denatured, electrophoresed, and transferred to nitrocellulose membranes. The membranes were blocked and incubated overnight at 4 °C with each of the following primary monoclonal antibodies (mAb): a) TGF-β1 (1: 500, mouse; 13 kDa, Santa Cruz Biotechnology, Dallas, TX); b) PCNA (mouse; 29 kDa, Cell Signaling Technology, Danavers, MA); c) α-SMA (1:250; 42 kDa, Invitrogen); d) E-cadherin (1: 500, rabbit; 135 kDa, Cell Signaling Technology); e) vimentin (1: 500,rabbit; 57 kDa, Cell Signaling Technology); f) cathepsin K (1: 100, mouse; 26 kDa, Santa Cruz Biotechnology); g) β-actin (mouse; 1:5000); and h) GAPDH (1:5000). Subsequently, the membranes were incubated with HRP-conjugated goat anti-mouse or anti-rabbit IgG antibody (1: 3000; Bio-Rad) for 1 hour at room temperature. Each protein was detected using SuperSignal™ West Pico PLUS chemiluminescent substrate in the film processor. Band signals were quantified using ImageJ. Each protein signal was normalized using the corresponding β-actin or GAPDH signal obtained from the same membrane (loading control) and is expressed as mean±SD (n=3) relative to “Healthy” control (n=2).

6.2.7 Data description and statistical analysis

The majority of the data except those in Figures 6.3 and 6.4 are expressed mean \pm SD (n=3) or mean (n=2). Some data had to be eliminated due to differences in the protocol. The exercise endurance times (Figure 6.3) are shown as individual animal data measured on day 1 and day 12/15. The lung section images (Figure 6.4) are representative of each group, and visual evaluation only was made for presence or absence of fibrotic tissues and alveolar structure destruction. Where applicable, statistical analysis was carried out using GraphPad Prism[®] by ANOVA, followed by Tukey's post hoc HSD test. $p < 0.05$ was considered as significant.

6.3 Results

6.3.1 Changes of body weight and treadmill exercise endurance

Figure 6.2 shows the body weight changes of rats during 16 days of BLM instillation on day 1 with or without subsequent lung administrations of AM24 at 0.1 mg/kg (~every other day), compared to the body weight change of healthy rats. While the body weight was steadily increased in the healthy rats at an average daily rate of 4.7 g/day, the BLM instillation appeared to cause a reduction of body weight up to day 3-4, irrespective of AM24 administration. This reduction was followed by an increase at an average daily rate of 5.2 g/day in both groups of animals. All these animals were appropriately trained by day 1, evidenced by 30-55 min of the pre-dose treadmill exercise endurance, as shown in Figure 6.3. The pre-dose running times were indeed comparable across the three groups ($p>0.05$). By day 16, no change was seen in the running times of healthy rats ($p>0.05$; Fig. 6.3). However, the running times were substantially reduced (i.e., impaired) to 10.8 min ($p<0.05$), when the BLM-induced rats were left untreated. In contrast, when AM24 was dosed to the lungs at 0.1 mg/kg in the BLM-induced animals over the two weeks period, the post-dose endurance times remained only slight reduced by ~20 % (Fig. 6.3). In fact, the post-dose running times between the AM24-treated, BLM-induced rats and the healthy rats were statistically different ($p<0.05$).

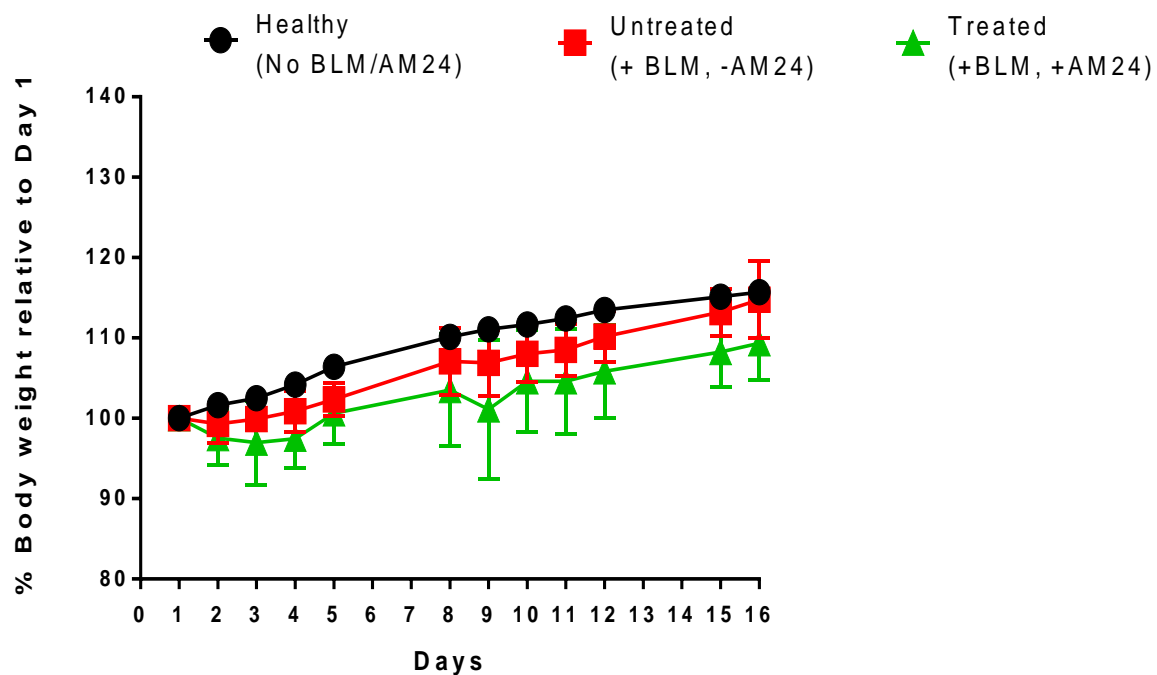


Figure 6.2: Body weight changes during 16 days in 3 groups of rats with or without BLM induction and/or AM24 treatment. Healthy: healthy rats without BLM induction and AM24 treatment; BLM + Untreated: BLM-induced rats without AM24 treatment; and BLM + Treated: BLM-induced rats treated with AM24. BLM: 0.6 mg/kg on day 1; and AM24: 0.1 mg/kg every other day over the two week period. Data: “Healthy”: mean from n=2; BLM + Untreated: mean±SD from n=4; and BLM + Treated: mean±SD from n= 5.

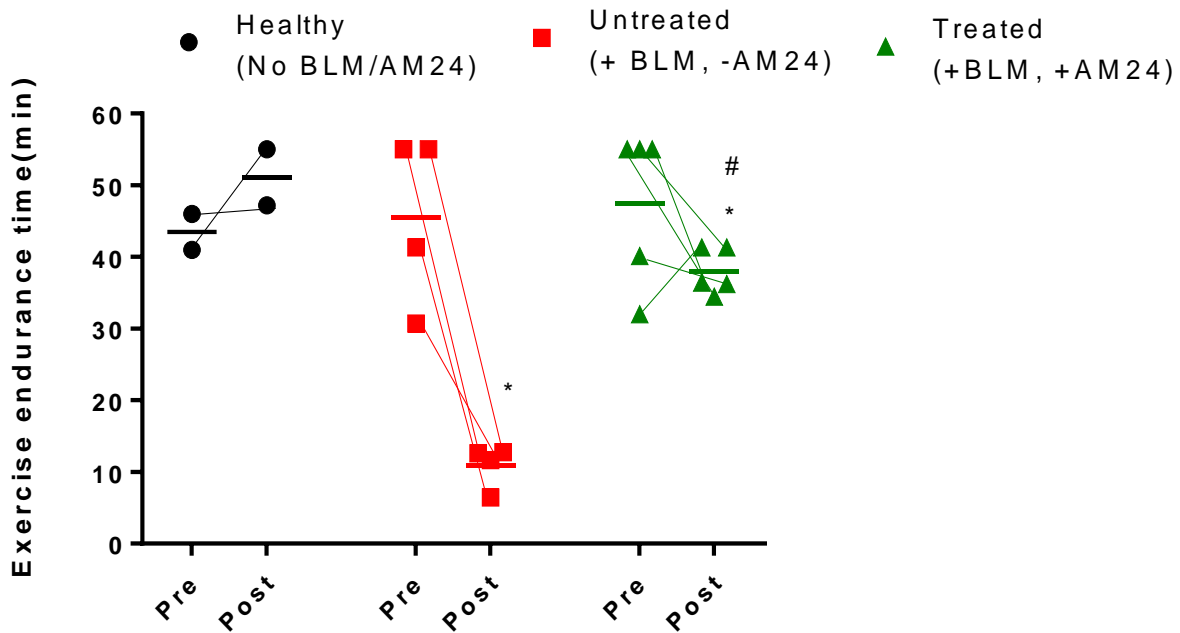


Figure 6.3: Pre- and post-dose treadmill exercise endurance in three groups of rats with or without BLM induction and/or AM24 treatment. Healthy (n=2): healthy rats without BLM induction and AM24 treatment; BLM + Untreated (n=4): BLM-induced rats without AM24 treatment; and BLM + Treated (n=5): BLM-induced rats treated with AM24. BLM: 0.6 mg/kg on day 1; and AM24: 0.1 mg/kg every other day over the two week period. Data: individual rat data. The horizontal bars represent the group mean values. *p<0.05 vs. “Healthy” group; and #p<0.05 vs. “BLM + Untreated” group, by ANOVA and Tukey’s HSD post hoc test.

6.3.2 Fibrotic tissues and alveolar structure destruction/loss

Figure 6.4 shows 9 airspace images taken from one rat as a representation of each of the three groups. Despite regional (i.e., between-image) differences, a greater degree and presence of fibrotic tissues and alveolar structure destruction/loss were seen in the “BLM + Untreated” group (Fig. 6.4.B), relative to “Healthy” rats (Fig. 6.4.A). However, the AM24 treatment appeared to enable intervention against these histological and morphological changes. In the airspace images of the “BLM + Treated” group (Fig. 6.4.C), fibrotic tissues and alveolar structure destruction/loss were much less than in the “BLM + Untreated” group (Fig. 6.4.B) and rather similar to those for the “Healthy” rats (Fig. 6.4.A).

A

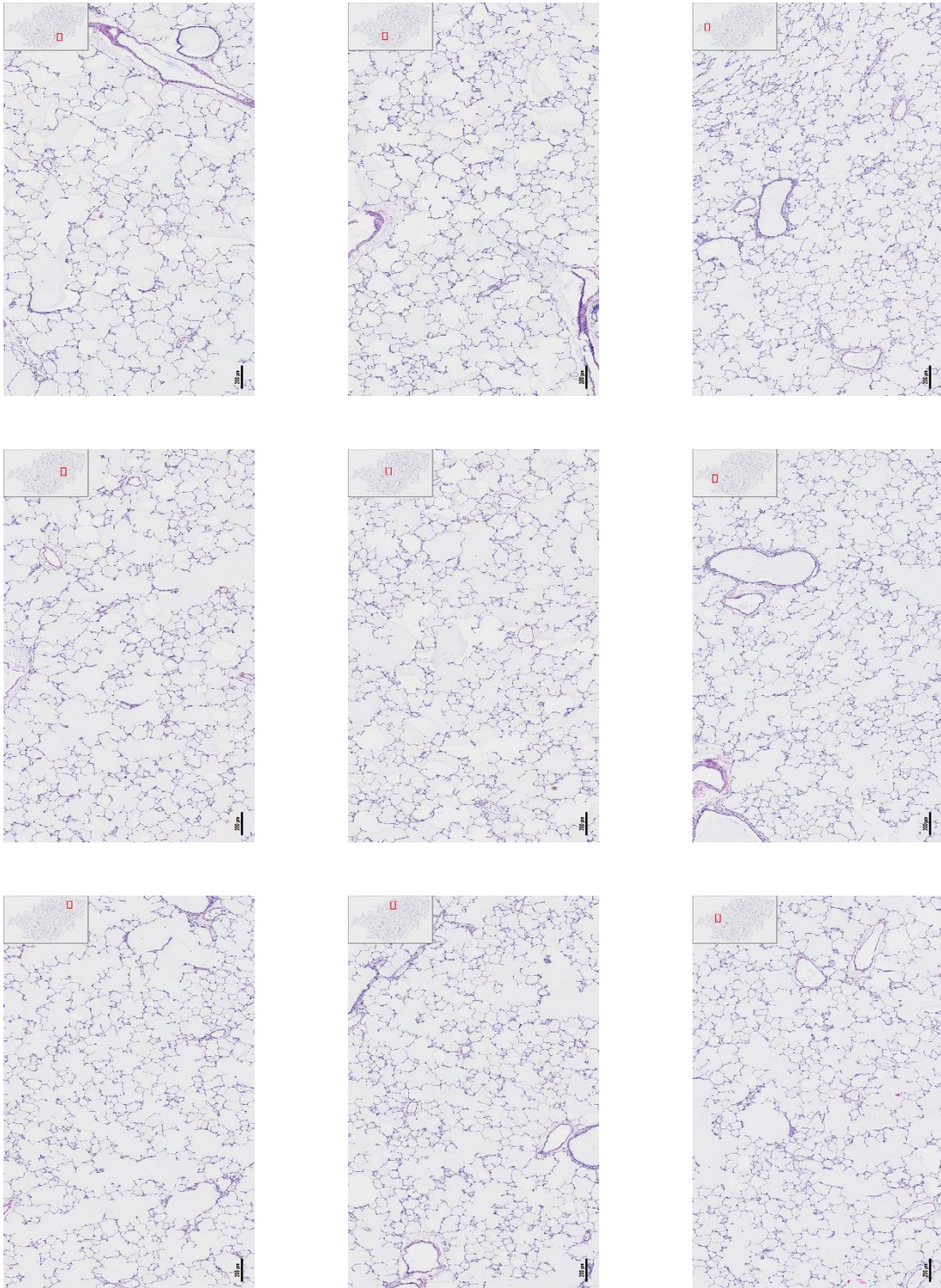


Figure 6.4: Hematoxylin-eosin stained airspace images taken from one rat as a representation of each of the 3 different induction/treatment groups - (A) “Healthy” rat. The scale bars represent 200 μm

B

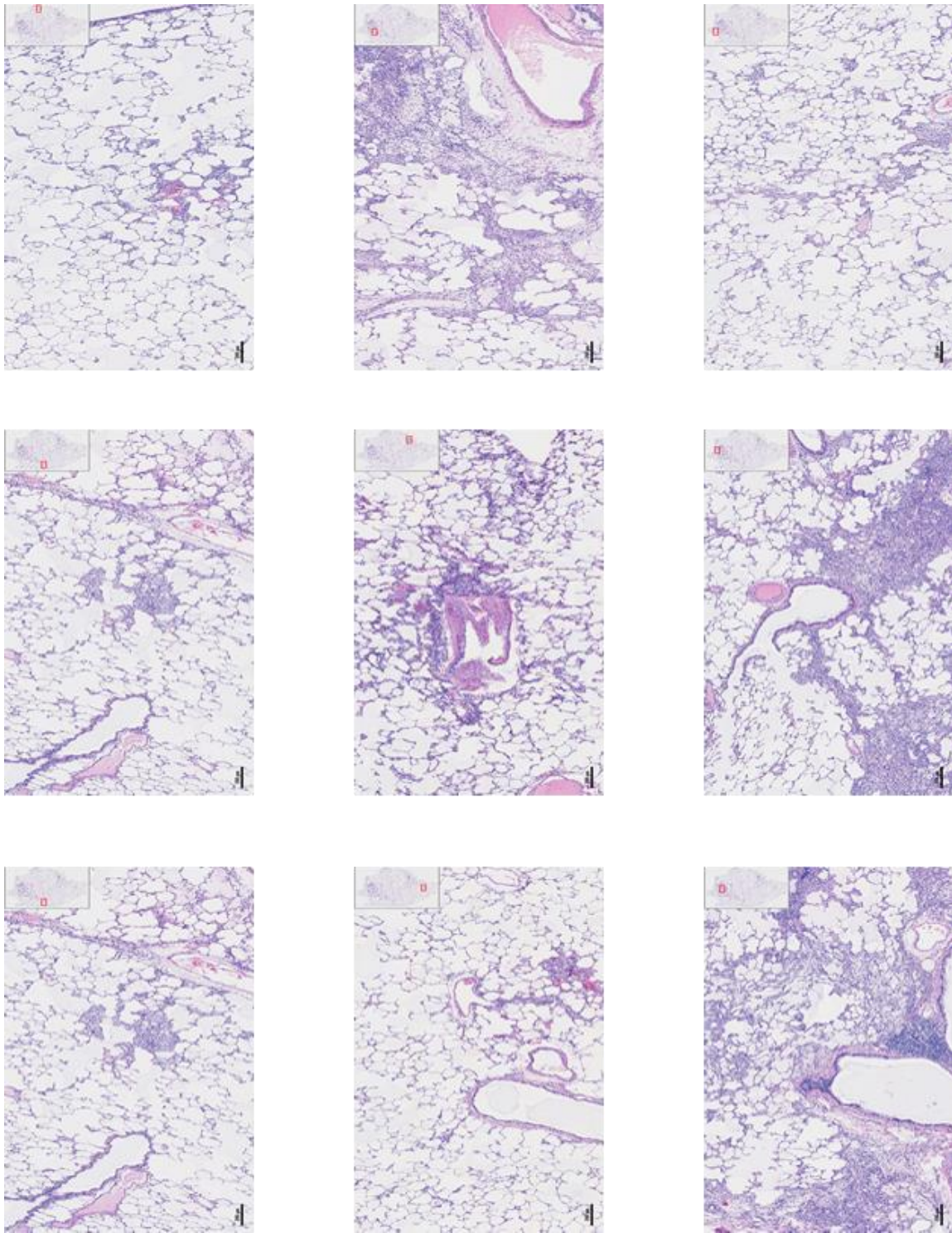


Figure 6.4: Hematoxylin-eosin stained airspace images taken from one rat as a representation of each of the 3 different induction/treatment groups - (B) “BLM + Untreated” rat. The scale bars represent 200 μm .

C

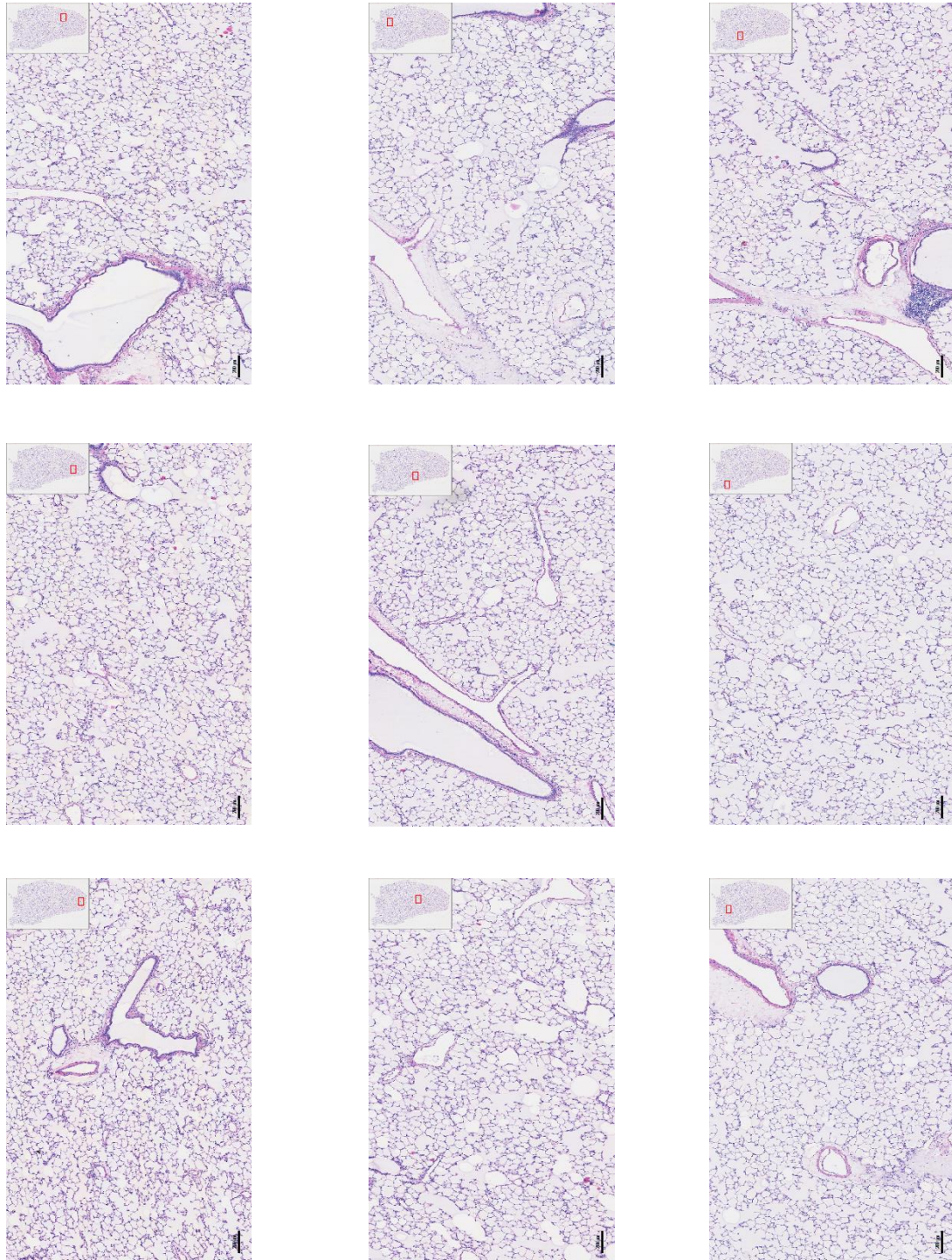


Figure 6.4: Hematoxylin-eosin stained airspace images taken from one rat as a representation of each of the 3 different induction/treatment groups - (C) “BLM + Treated” rat. The scale bars represent 200 μm .

6.3.3 Lung tissue collagen deposition

Figure 6.5 shows the lung tissue collagen in the three different induction/treatment groups, measured as the absorbance at 540 nm by the picosirius red assay. When PF was induced with BLM, but animals were left untreated, the lung tissue collagen was 3.3-fold higher than that for the “Healthy” rats ($p < 0.05$). However, when AM24 was dosed to the lungs of the BLM-induced PF rats, the induced collagen deposition was significantly inhibited by ~78 % (< 0.05).

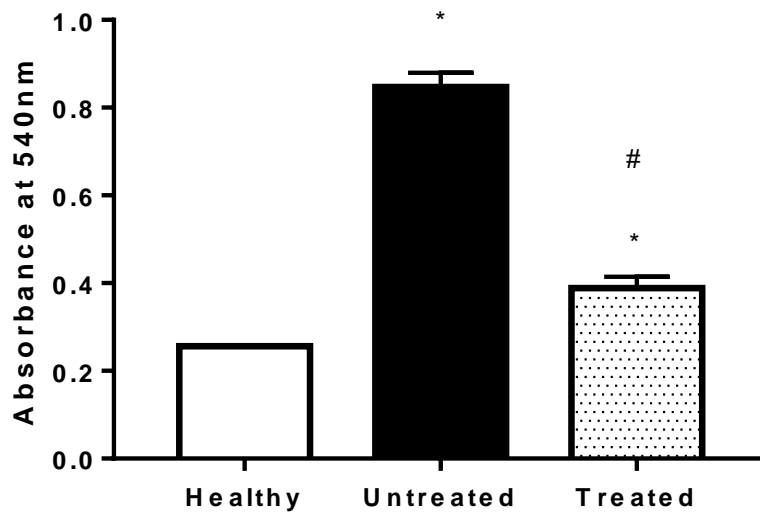


Figure 6.5: Lung tissue collagen deposition in the three different induction/treatment groups, measured as the absorbance at 540 nm by the picosirius red assay. Healthy (n=2): healthy rats without BLM induction and AM24 treatment; BLM + Untreated (n=4): BLM-induced rats without AM24 treatment; and BLM + Treated (n=5): BLM-induced rats treated with AM24. BLM: 0.6 mg/kg on day 1; and AM24: 0.1 mg/kg every other day over the two week period. Data: mean±SD. * $p < 0.05$ vs. “Healthy” group; and # $p < 0.05$ vs. “BLM + Untreated” group, by ANOVA and Tukey’s HSD post hoc test.

6.3.4 Lung expressions of TGF- β 1, PCNA, α -SMA, E-cadherin and vimentin

Since TGF- β 1 has been believed to be the “master” switch to cause PF and PF pathogenesis, the lung tissue expressions of TGF- β 1 in the three different induction/treatment groups are shown in Figure 6.6. When BLM was dosed to induce PF, but animals were left untreated, a greater level (1.8 fold) of TGF- β 1 expression was seen, compared to that in the “Healthy” rat lungs. Against this induction, the AM24 treatment seemed to cause a moderate inhibition, yet such inhibition was not significant ($p > 0.05$).

As seen in the *in vitro* studies (Chapter 4), the induced TGF- β 1 expression of the BLM-induced, untreated rat lungs shown in Figure 6.6 may have led to other pathogenic changes of induced fibroblast proliferation and differentiation to myofibroblast. Hence, Figures 6.7 and 6.8 shows the lung’s cellular proliferation marker, PCNA [proliferating cellular nuclear antigen], and differentiation marker, α -SMA, respectively. Unlike the *in vitro* studies (Chapter 4), however, in the BLM-induced model, neither the PCNA nor α -SMA level was induced, so that their inhibition was not examined and indeed shown as AM24’s efficacies.

In contrast, as shown in Figure 6.9, the lung tissue expressions of vimentin but not E-cadherin which were used as EMT markers, were significantly changed in the BLM-induced, untreated rats, compared to “healthy” rats. The mesenchymal marker, vimentin, was increased by 67 % ($p < 0.05$), which suggested induced EMT in these PF animals. However, in the AM24-treated animals, these protein expressions seemed to be normalized to the healthy animal levels, while their relatively high variabilities precluded statistical conclusions.

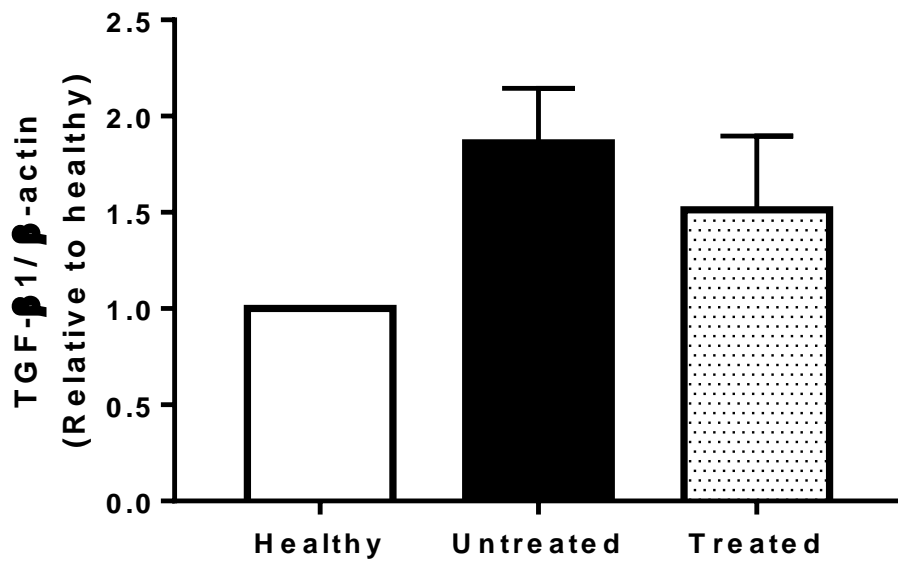
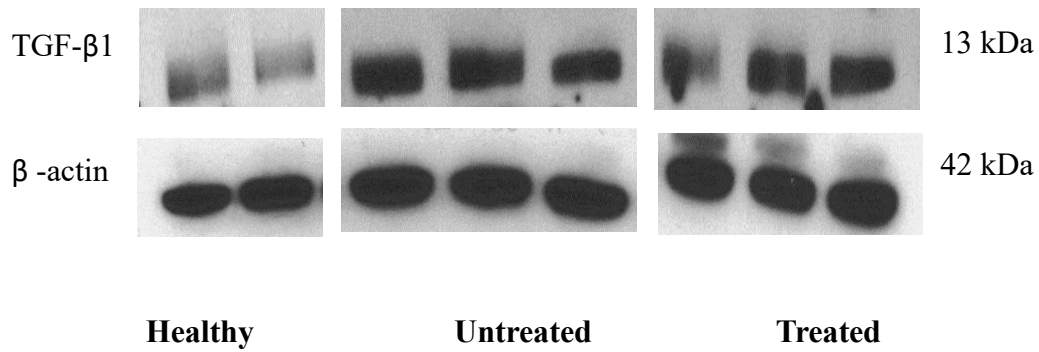


Figure 6.6: Lung tissue expressions of TGF-β1 in the three different induction/treatment groups of rats, measured by Western blot analysis: Upper panel: representative Western blot band images; and Lower panel: densitometric band signals relative to the “Healthy” rats. Data: mean for the “Healthy” rats (n=2) and mean±SD for the “BLM + Untreated “ and “BLM + Treated” rats (n=3).Data was analyzed by one-way ANOVA. No significant difference was seen amongst the 3 groups.

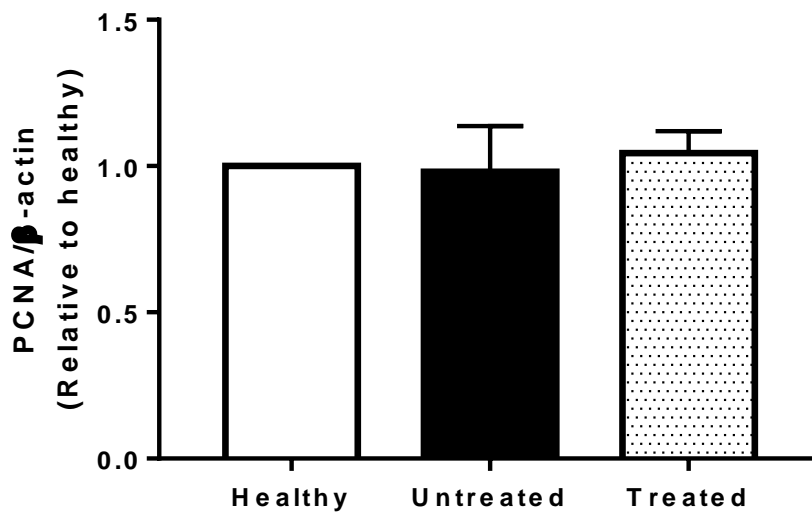
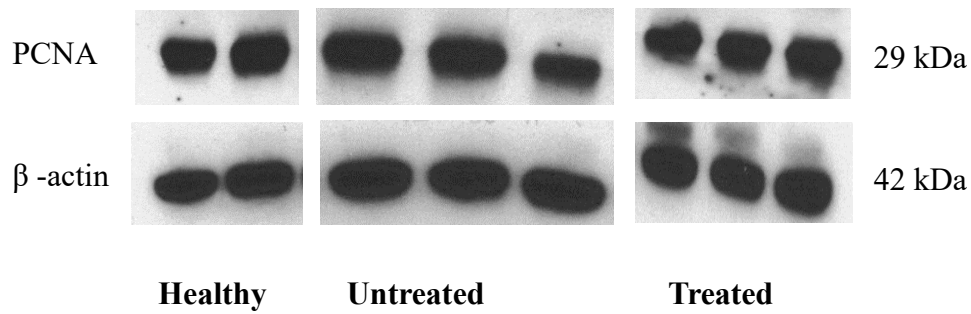


Figure 6.7: Lung tissue expressions of PCNA in the three different induction/treatment groups of rats, measured by Western blot analysis: Upper panel: representative Western blot band images; and Lower panel: densitometric band signals relative to the “Healthy” rats. Data: mean for the “Healthy” rats (n=2) and mean \pm SD for the “BLM + Untreated” and “BLM + Treated” rats (n=3). There is no statistical difference between any of the two groups, by ANOVA and Tukey’s HSD post hoc test.

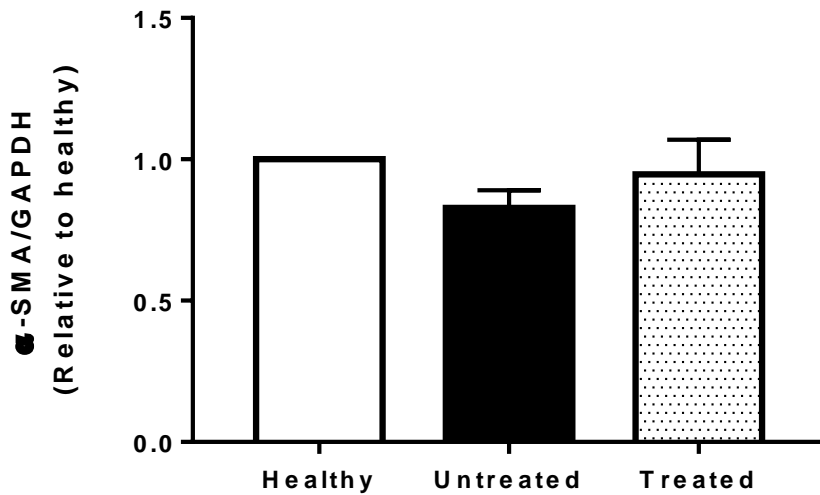
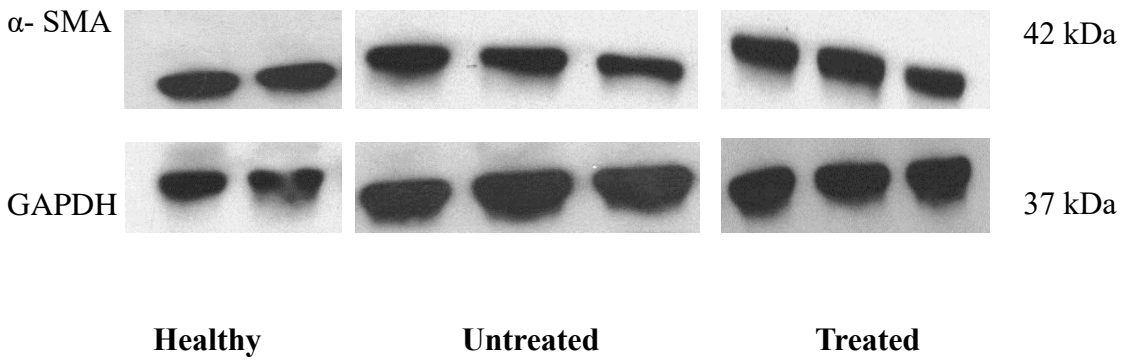
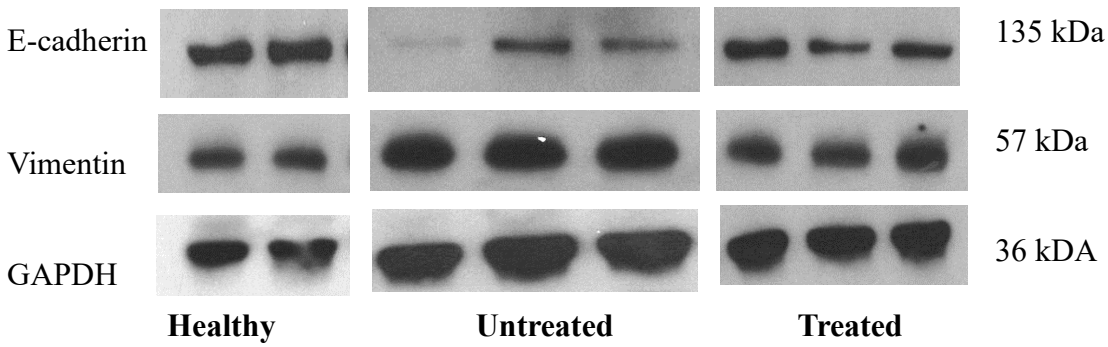
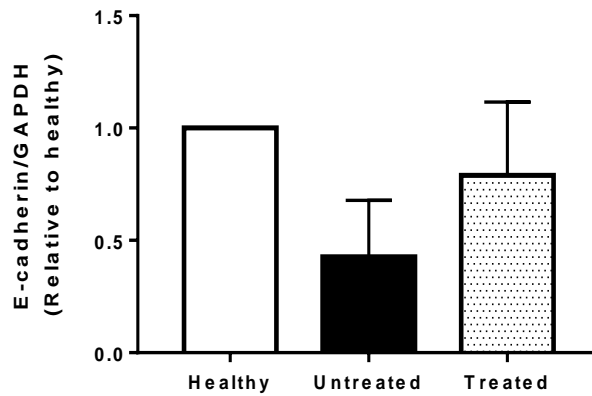


Figure 6.8: Lung tissue expressions of α -SMA in the three different induction/treatment groups of rats, measured by Western blot analysis: Upper panel: representative Western blot band images; and lower panel: Densitometric band signals relative to the “Healthy” rats. Data: mean for the “Healthy” rats (n=2) and mean \pm SD for the “BLM + Untreated” and “BLM + Treated” rats (n=3). There is no statistical difference between any of the two groups, by ANOVA and Tukey’s HSD post hoc test.



A



B

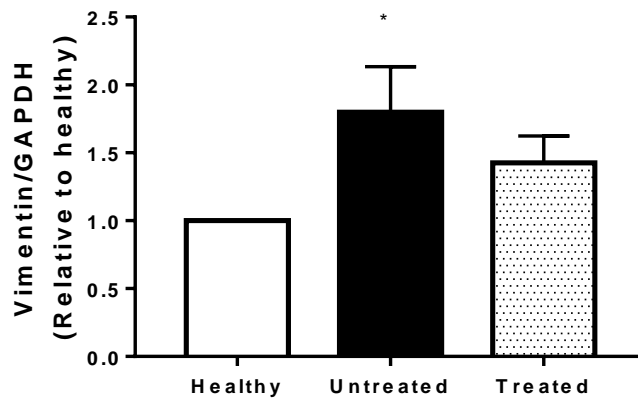


Figure 6.9: Lung tissue expressions of (A) E-cadherin and (B) vimentin in the three different induction/treatment groups of rats, measured by Western blot analysis: Upper panel: representative Western blot band images; and Lower panel: densitometric band signals relative to the “Healthy” rats. Data: mean for the “Healthy” rats (n=2) and mean±SD for the “BLM + Untreated” and “BLM + Treated” rats (n=3). *p<0.05 vs. “Healthy” group, by ANOVA and Tukey’s HSD post hoc test.

6.3.5. Lung expressions of cathepsin K

The literatures have recently suggested a pathobiologic role of cathepsin-K/L, enzymes degrading collagen, in PF lungs, and demonstrated that CUR promoted these enzymes (Srivastava M et al., 2008; Zhang D et al., 2011). Hence, as a precursor of mechanistic clarifications for the potent intervention activities of AM24, the lung tissue expression of cathepsin K was measured, yet the result became similar to the PCNA and α -SMA results described above. As shown in Figure 6.10, the lung's cathepsin K level remained unaltered in the BLM-induced rats without AM24 treatment. However, despite no statistical significance, a slightly higher level of cathepsin K was seen in the lungs of the BLM-induced animals treated with AM24.

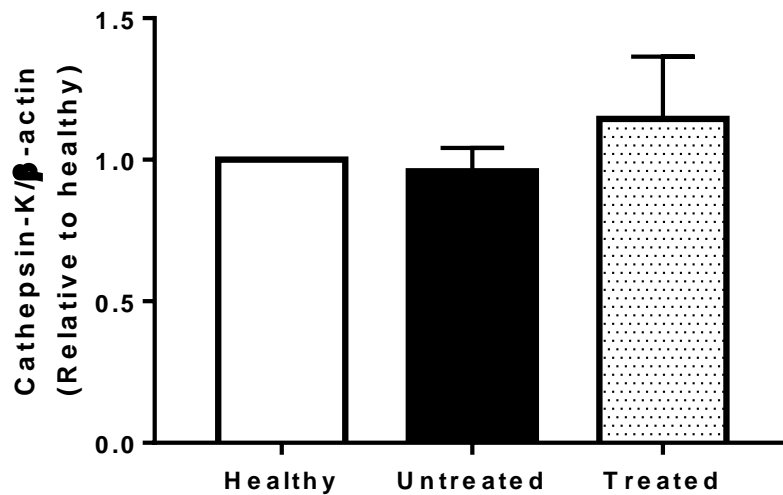
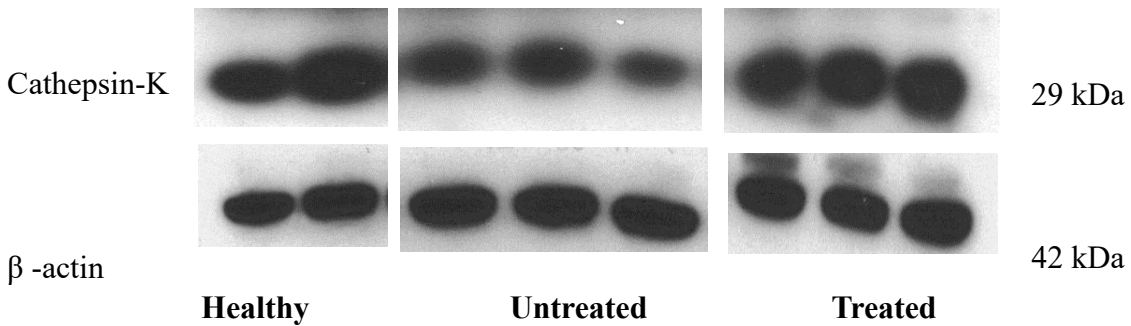


Figure 6.10: Lung tissue expressions of cathepsin K in the three different induction/treatment groups of rats, measured by Western blot analysis: Upper panel: representative Western blot band images; and lower panel: Densitometric band signals relative to the "Healthy" rats. Data: mean for the "Healthy" rats (n=2) and mean \pm SD for the "BLM + Untreated" and "BLM + Treated" rats (n=3). There is no statistical difference between any of the two groups, by ANOVA and Tukey's HSD post hoc test.

6.4 Discussion

To date, several *in vivo* rodent models for development of PF and assessment of anti-fibrotic agents are available. Silica induced rodent models are a good marker for lung injury but they are not reproducible and are difficult to deliver along with absence of characteristic fibrotic lesions. The asbestos induced model is a good model for mimicking the fibrosis caused due to exposure to asbestos, however, the inhalation treatment requires a month to cause fibrosis and the intratracheal delivery causes central fibrosis without evenly distributing the effects. Similarly, radiation induced fibrosis also takes long time for development and hence is not ideal. Fluorescent isothiocyanate induced fibrosis is a good model but lacks key fibrotic features and lesions. Specific cytokine induced models are also available, however, they can give information only about a single pathway and are generally only used for mechanistic studies of anti-fibrotic agents. From amongst the available models, BLM induced PF in male mice/rats remains the most clinically relevant model (Moore et al, 2007; Moore et al, 2013; Tashiro et al, 2017). It is said to be the ‘best characterized animal model for preclinical testing.’

Despite its widespread acceptability, there is a very high variation in the dosing as well as the dosing frequency, eg Arslan et al. suggested use of a single dose of 4 mg/kg BLM while Sewig et al. suggested using 1 mg/kg (Arslan,2002; Sewig, 2012). Given the lack of a standard protocol for BLM induced PF model, the animal study for PF was divided into two parts: 1) Establishment of appropriate lung dose of BLM to induce the disease 2) Establishment of the appropriate dose and dosing frequency of AM24 to rats. Three dose levels of BLM (0.4mg/kg, 0.6mg/kg and 0.8mg/kg) were studied while simultaneously altering AM24 doses (0.1/0.5 mg/kg daily and 0.1mg/kg every other day). A total of 22 animals were used for the establishment of the protocols.

The group allotment is given in Table 6.1. The final protocol used 0.6mg/kg of BLM to induce PF and 0.1mg/kg every other day of AM24.

Table 6.1: Experimental groups in the establishment of the dose for PF induction and treatment

| Group | n | Induction | Treatment |
|----------|----------|-----------------------|--|
| 1 | 4 | None | None |
| 2 | 3 | BLM (0.4mg/kg) | None |
| 3 | 4 | BLM (0.6mg/kg) | None |
| 4 | 1 | BLM (0.8mg/kg) | None |
| 5 | 1 | BLM (0.4mg/kg) | AM24 0.1mg/kg, daily |
| 6 | 5 | BLM (0.6mg/kg) | AM24 0.1mg/kg, Alternate days |
| 7 | 2 | BLM (0.8mg/kg) | AM24 0.1mg/kg, Alternate days |
| 8 | 2 | BLM (0.8mg/kg) | AM24 0.05mg/kg, daily |

0.6 mg/kg dose of BLM and 0.1 mg/kg of AM24 ~every other day was chosen based upon the weight variation, endurance studies (Figure 6.11) and survival. Upon selection of 0.6 mg/kg, it was seen that 0.6 mg/kg BLM when given as a single dose on day 1 did not show significant changes in fibrotic mass development. However, a former study conducted in our lab using 4 mg/kg BLM indicated the formation of very high amounts of fibrotic tissue (Figure 6.12). This observation confirms with Kim et al. who shows that the ability of BLM to induce PF is dose dependent (Kim et al.,2010). The author shows that the fibrotic features are higher at 4 mg/kg than at 2 mg/kg or 1 mg/kg indicating the concentration dependence. However, we failed to see this concentration dependent effect on development of fibrotic masses at lower doses, wherein only 0.6 mg/kg BLM showed presence of fibrotic mass, while 0.4 mg/kg and 0.8 mg/kg failed to show significant development of fibrotic mass (Figure 6.12). Also, as seen in Figure 6.4 there was regional variation

in the development of fibrotic mass within a single animal lung section. This variation in histological development of fibrotic masses may be due to the low dose of BLM, however, it could be in part attributed to handler variation, since experiments were conducted by different scientists. Thus, future studies in this project require increase in BLM doses to induce fibrosis effectively and then assess the activity of AM24.

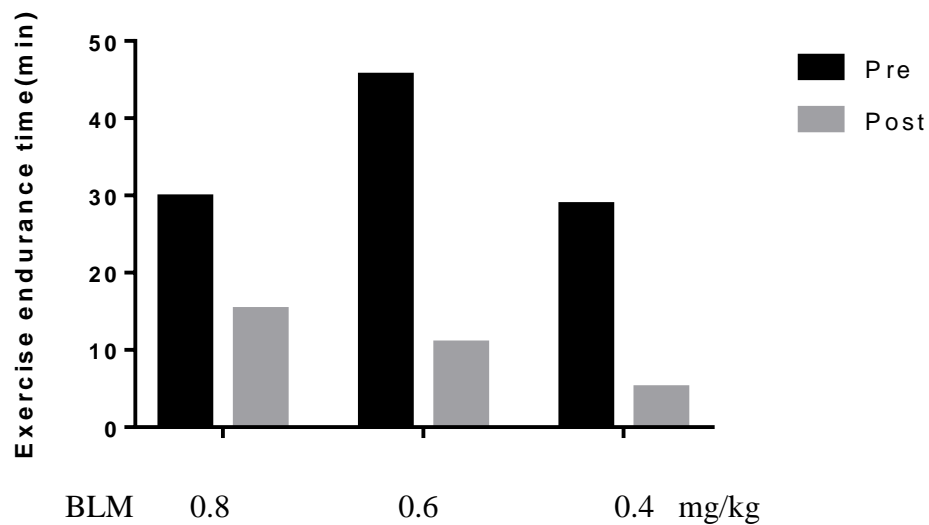
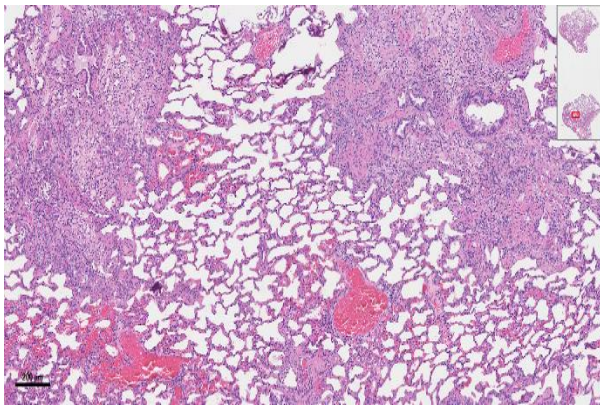
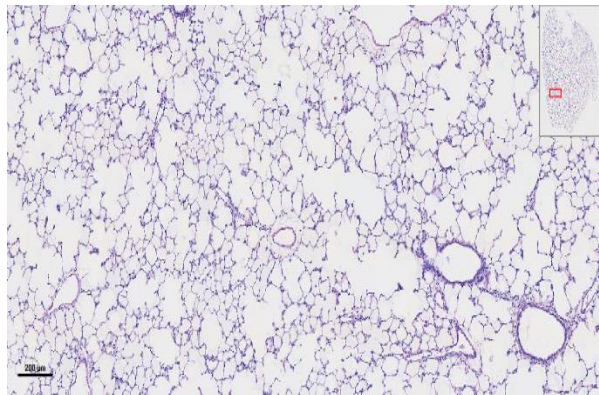


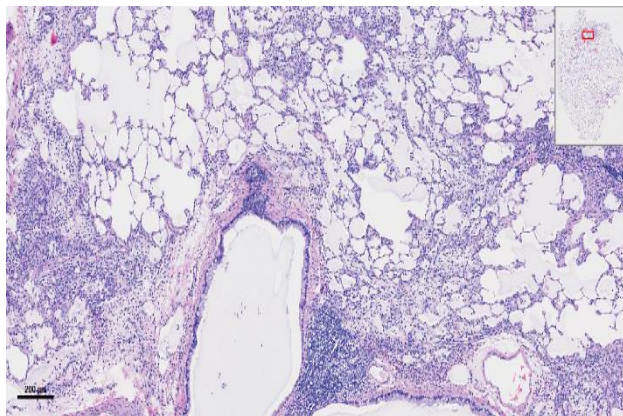
Figure 6.11: Comparison of exercise endurance time (min) across 3 doses of BLM which led to the selection of 0.6 mg/kg BLM. Data are n=1 in BLM 0.8 mg/kg group, n=1 in 0.4 mg/kg group and n=4 in 0.6 mg/kg group expressed as mean.



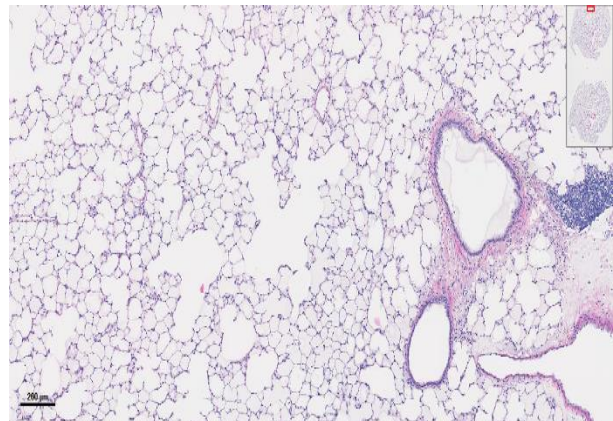
(A) BLM - 4 mg/kg



(B) BLM - 0.8 mg/kg



(C) BLM - 0.6 mg/kg



(D) BLM - 0.4 mg/kg

Figure 6.12: Representative images of 4 rats dosed with different doses of BLM for visual observation of variation in the development of fibrotic mass. (A) BLM - 4 mg/kg (B) BLM- 0.8 mg/kg (C) BLM - 0.6 mg/kg (D) BLM - 0.4 mg/kg.

The variation in the rat weights was monitored as a crude measure of the possible toxicity of both BLM and AM24. The healthy rats showed constant increase in weight (4.7 g/day) across the two-week period, while the BLM treated and BLM + AM24 treated rats showed an initial decline in the weights which was later improved showing a steady increase (5.2 g/day). This reduction in body weight seen after administration of BLM is consistent with the study conducted by Gilhodes JC. et al. where the authors saw a decrease in body weight upon treatment with BLM in a concentration dependent manner. The authors reported that at doses < 1 mg/kg, the body weight decreases upon initial dosage of BLM, but this reduction is reversed by a steady increase in weight starting from day 5/6 . However, at higher doses, the body weights continue to decrease (Gilhodes et al., 2017). Also, the possibility of AM24 causing a reduction in weight is less likely as weight reduction was not seen upon continued dosing of AM24 in the later phase of the study. Thus, it can be suggested that the initial loss of weight is due to the fibrotic effects of BLM and the subsequent increase in the weights in the BLM and BLM + AM24 group may be likely due to loss of effect of BLM (since BLM is dosed only once at a low dose) or due to the protective effect of AM24 (in the BLM + AM24 group). Weight variation could also be due to the dosing frequency and dosing time. If the dosing frequency is too high the rats may be losing weight due to the stress involved in the dosing procedure. In case of dosing times, if the rats are dosed in the evenings, it may potentially hamper their appetite leading to weight loss.

The treadmill exercise endurance test is representative of the 6-minute walk test which is used in the diagnosis of lung related disorders and is considered to be a reliable, valid, and responsive measure of disease status and thereby making it a valid endpoint for clinical trials in PF (Bois et al, 2011; Bois et al, 2014). The treadmill exercise endurance was significantly reduced

to ~10 min in the BLM treated group in the post dose measurement as compared to healthy with ~55 min. The 4.5-fold decrease in the running times was partially reversed by treatment with AM24 0.1 mg/kg every other day with only ~20% reduction in running times in comparison to healthy. This activity of AM24 was dose related, as the 0.05 mg/kg dose of AM24 could not reverse the impaired exercise endurance times, despite daily dosing which is why the 0.1 mg/kg dose was chosen (Figure 6.13). Very few literatures have studied exercise endurance as measure of deteriorating/improving lung capacity. Koch and Britton developed a method for exercise endurance testing similar to the one used in this project. However, the measurements were made in terms of distance rather than time. Using this method, Peng et al reported that there is a significant decrease in the running distances of rats induced with BLM in comparison to healthy animals (Koch and Britton, 2001; Peng et al, 2013). These results are comparable to those found in human patients where it was seen that endurance training and the 6-minute walk test is the most responsive measure for evaluating rehabilitation in PF (Arizono et al., 2014).

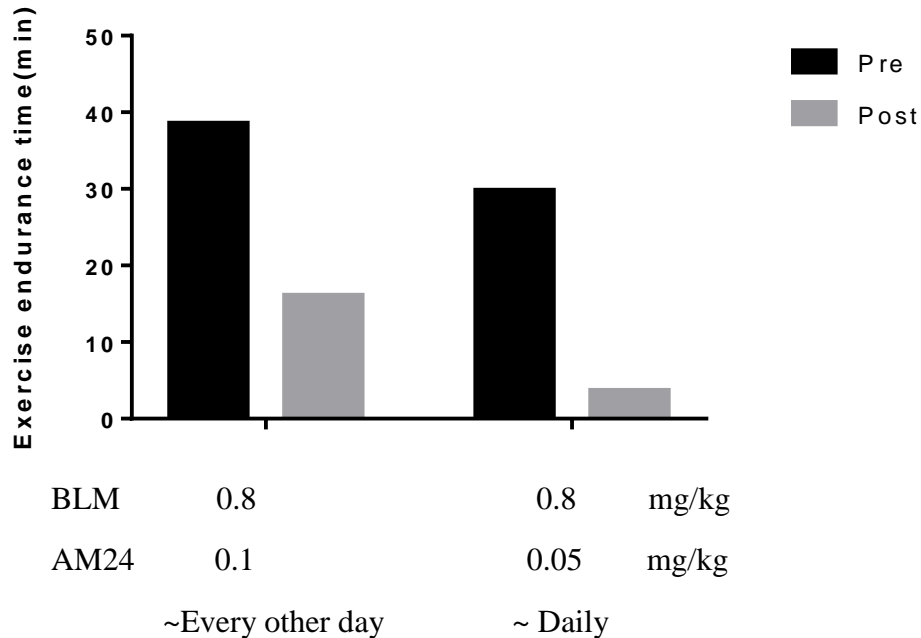


Figure 6.13: Comparison of exercise endurance time (min) across 2 doses of AM24 which led to the selection of 0.1 mg/kg of AM24. Data are n=2 in BLM + AM24 0.1 mg/kg every other day group, n=1 in BLM + AM24 0.05 mg/kg daily group.

The histological tissue sections of the group treated with 0.05 mg/kg of AM24 ~every day showed presence of some fibrotic masses as compared to the group with AM24 0.1 mg/kg dose when induced with equal doses of BLM (Figure 6.14) . This indicates that the anti-fibrotic effects of AM24 may be concentration related. Also, despite the regional variability in the histological induction of fibrotic effects when BLM was dosed at 0.6 mg/kg (Figure 6.4 (B)), AM24 at 0.1 mg/kg was able to prevent the occurrence of such fibrotic lesions (Figure 6.4 (C)).However, if this protective effect of AM24 against development of fibrotic masses will be retained in a higher dose model of BLM still needs to be studied.

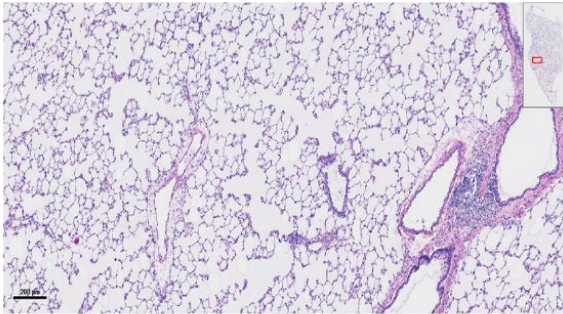
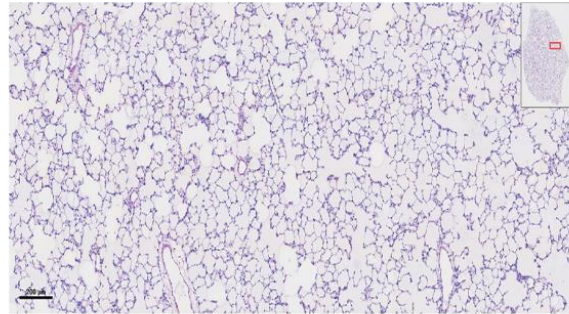
A**BLM 0.8 mg/kg + AM24 0.05 mg/kg everyday****B****BLM 0.8 mg/kg + AM24 0.1 mg/kg every other day**

Figure 6.14: Representative images of histological sections of two concentrations of AM24, (A) 0.05 mg/kg (B) 0.1 mg/kg. The scale was 200 μ M.

Although unable to successfully induce the formation of fibrotic masses in a consistent manner without regional variation, BLM at 0.6 mg/kg did cause a significant increase (3.6 fold) in collagen synthesis which was inhibited by ~78% by AM24. Upon oral administration of PIR at 50 mg/kg daily, PIR was able to significantly inhibit the induced PF. Note that, in this study the dose of BLM used was also higher (5 mg/kg) (Song et al.,2018). The bleomycin dose in this case is 8.3x higher while the drug dose is 500x higher. However, PIR was administered orally in the above case, while AM24 is given by orotracheal instillation thereby likely reducing the need for a higher dose even with an increase in the dose of BLM. Nintedanib has also been studied at an oral dose of 30/60 mg/kg in rats induced with BLM 3mg/kg where it was able to show a concentration dependent inhibitory effect in collagen level which was induced by the high dose of BLM (Wollin L.et al.,2014). However, in the above situation, the dose of BLM is 5x higher than the dose used in our study and the dose of nintedanib given was 300x/600x more. In another study, CUR

microparticles were given as an inhalation at a weekly dose of 1 mg per rat. Collagen levels which were induced by BLM (5 mg/kg) were reversed completely at this dose, while in the same study rats administered with 1 mg of CUR powders showed lower inhibition (Hu et al., 2018). This study also helps prove our belief that lung delivery helps reduce dose, since CUR is typically given at doses ~200-300 mg/kg orally (Punithavathi 2000; Zhang,2011). However, since we have proved using our *in vitro* experiments that AM24 is more potent than CUR and PIR, a dose < 1 mg per rat of AM24 could be used for orotracheal administration. Collagen levels are also known to be significantly increased in patients with PF thereby making a molecule like AM24, with potential to inhibit excessive synthesis of collagen, of great interest in the treatment of PF (Su et al., 2017)

In terms of the protein expressions , we failed to see any significant induction in the TGF- β 1, PCNA and α - SMA levels or a reduction in the E-cadherin levels in the BLM group which could be because to the low dose of BLM administered. TGF- β 1, α -SMA, PCNA levels were constant across all three groups indicating that BLM at 0.6 mg/kg failed to show any induction of TGF- β 1 and thus failed to induce differentiation of myofibroblasts to fibroblasts and proliferation. Although not statistically significant, the E-cadherin protein levels showed high levels in healthy and treated groups while the BLM group showed lower levels. However, vimentin levels were significantly lower in healthy and treated (BLM+ AM24) groups but were higher in BLM group. These trends in E-cadherin and vimentin levels indicate that EMT may have occurred but the effects are not statistically significant. In a recent study, Meng et al. demonstrated that administration of 3 mg/kg of BLM intratracheally, caused a significant increase in TGF- β 1, α -SMA and E-cadherin levels (Meng et al., 2019). These results seen by Meng et al. are consistent with those seen by Chen et al 2016, Han et al, 2018; Qiu. et al,2019; Zhuang Wu et al, 2007 and Wen et al, 2018. Wen D et al. who also showed a decrease in vimentin upon BLM induction.

However, each of these studies used a dose of BLM > 2.5 mg/kg of BLM. In another study, Mishra et al. demonstrated that BLM causes a significant increase in PCNA on day 7 upon administration of BLM while on day 14 these effects were not significant. This could in part be the reason why we did not see any difference in PCNA levels upon harvesting the lung tissue on day 16. However, note that this effect of BLM was seen at 0.4 mg in mice (Mishra et al, 1999). Thus, a higher dose of BLM could help replicate the results seen in the literature for expression of TGF- β 1, α -SMA, E-cadherin, vimentin and PCNA, thereby establishing a model that allows appropriate evaluation of AM24 as an anti-fibrotic agent.

Finally, the cathepsin-K levels were assessed to have some understanding of the mechanism of AM24. Although not statistically significant, cathepsin- K levels were found to be slightly lower in the BLM group, while it was comparatively higher in healthy and treated (BLM+AM24) groups. Cathepsin-K is a collagenolytic enzyme responsible for the breakdown of collagen and other ECM proteins (Buhling et al., 2004) It has been shown that CUR exerts its action by overexpression of this enzyme (Zhang et al., 2011). An overexpression of this enzyme would lead to increase in collagen breakdown leading to decreased collagen and thus decreased ECM deposition (Buhling et al., 2004). In a study conducted using cathepsin-K overexpressing transgenic mice lower degree of fibrosis was observed upon action by BLM, indicating the protective effect of cathepsin-K enzyme in PF (Srivastava et al., 2008). The slight increase in cathepsin-K seen in AM24 treatment group (Figure 6.10) may be indicative of the potential role of AM24 in overexpression of cathepsin-K. However, the structural component of CUR that exerts this action is unknown. Further studies are needed that include a CUR control group in order to confirm the findings of Zhang et al and understand if AM24 exerts its action due to the CUR

portion of the hybrid. This effect could also potentially help prove our hypothesis that AM24 is a hybrid having a dual acting mechanism due to each of its parent compounds.

Although significant disease induction was seen upon BLM induction in the exercise endurance testing as well as collagen assay, BLM at 0.6 mg/kg failed to show significant inductions of fibrotic lesions throughout the lung section and showed only regional fibrotic features. Also, at 0.6 mg/kg BLM failed to show a significant induction in TGF- β 1 levels and thus failed to induce proliferation (PCNA levels), differentiation (α -SMA) and EMT (E-cadherin, vimentin). Based upon the literature search of BLM induced PF model in rats over the past year (2018-2019), a dose of ~4 mg/kg given orotracheally was found to be ideal to induce significant PF effects in the rat lungs. Also, the dose response as well as the dosing frequency of AM24 could be optimized to get maximal intervention effects. It is also necessary to study MEL, CUR and MEL+CUR as controls to optimally rank the beneficial anti-fibrotic effects of AM24 in a BLM induced PF model.

Thus, this chapter provides preliminary results for the establishment of a BLM induced PF model while also showing promising results for AM24, a unique hybrid molecule of MEL and CUR, that may act as an anti-fibrotic agent by intervening in the development of BLM induced PF.

CHAPTER 7

CONCLUSIONS

This thesis project attempted identification of a novel and unique molecule to more potently treat the PF lungs with lung delivery. A MEL-CUR hybrid molecule, AM24, was examined for intervention in various *in vitro* lung cell-based systems and an *in vivo* rat model of BLM-induced experimental PF. AM24 retained the ABTS-based free radical scavenging activities of MEL and CUR, yet its activity represented with an IC₅₀ value of 25.7 μ M was equipotent to MEL, but less potent than CUR. In the *in vitro* human lung fibroblast MRC-5 cell systems, AM24 at 10 μ M inhibited PF-relevant, TGF- β 1 induced 1) collagen synthesis [measured by the picrosirius red assay] by 91 %; 2) proliferation [determined by the MTT assay] by 72 %; and 3) differentiation to myofibroblast [assessed with α -SMA level] by ~100 %. However, MEL, CUR, MEL+CUR and PIR at 10 μ M inhibited TGF- β 1 induced collagen synthesis and proliferation by 20-30%, 50-60%, while they failed to inhibit TGF- β 1 induced differentiation. In the *in vitro* human alveolar epithelial A549 cell system, AM24 at 10 μ M also significantly inhibited PF-relevant, TGF- β 1 induced EMT [assessed with E-cadherin and vimentin levels], while MEL, CUR, MEL+CUR and PIR at 10 μ M failed to inhibit induced EMT. In all these assessments, the activities of AM24 were concentration-related and shown to be more potent than its parent origin, MEL and CUR, as well as their physical admixture as indicated by the inhibition percentage. Moreover, AM24 was notably shown to be more potent (e.g., 50-times) than a FDA-approved orally-active PF drug, PIR.

AM24 was then examined for intervention with lung administration in an *in vivo* rat model of BLM-induced experimental PF. BLM was orotracheally spray-dosed to the lungs at 0.6 mg/kg

on day 1 for PF induction. AM24 was then spray-dosed to the lungs at 0.1 mg/kg 6 hours after BLM administration on day 1 and continued to be dosed on day 3, 5, 8, 10, 12 and 15 (i.e., ~every other day). Changes of body weight and treadmill exercise endurance were measured, followed by sacrifice on day 16 for the assessments of histological fibrotic tissues in the airspace and several lung tissue biomarkers. BLM dosing appeared to cause a decline of body weight up to day 3-4, followed by an increase similar to that seen in healthy animals, and this was irrespective of AM24 administration. When compared to average 47.2 min of healthy rats, the exercise endurance time was substantially reduced (i.e., impaired) to 10.86 min, when the BLM-induced animals were left untreated. However, with AM24 administrations at 0.1 mg/kg, the running time was 37.9 min despite PF induction with BLM, which was an only ~20 % reduction from that of the healthy animal level. As anticipated, a greater presence of fibrotic tissues was seen in the airspace of the BLM-induced animals without AM24 treatment. In contrast, significantly less fibrotic airspace was seen following AM24 treatment, suggesting effective intervention in the PF development in this model. Correspondingly, lung tissue collagen was elevated by 3.3-fold in the BLM-induced rats without AM24 treatment but was only by 1.5-fold with AM24 treatment, which was 78 % lower than the induced level. Although not statistically significant, the lung tissue TGF- β 1 level was slightly induced in the BLM-induced than in the healthy animals, but appeared to be induced less with AM24 treatment. However, the lung tissue levels of proliferation and differentiation markers, PCNA and α -SMA, respectively, remained not induced in the BLM-induced model, so that their inhibition was not clearly shown as AM24's efficacies. In contrast, an epithelial marker, E-cadherin, was reduced and a mesenchymal marker, vimentin, was in turn significantly increased by 1.7-fold, which suggested induced EMT in the BLM-induced rats with no AM24 treatment. However, AM24 inhibited this partial EMT induction as a part of its anti-fibrotic activities in this

animal model of PF. Finally, because recent literatures suggested a pathobiologic role of cathepsin-K/L, enzymes degrading collagen, in PF lungs, and CUR promoted these enzyme (Srivastava M et al., 2008; Zhang et al., 2011) the lung tissue cathepsin K was also measured. Similar to PCNA and α -SMA described above, the lung's cathepsin K level remained unaltered in the BLM-induced rats without AM24 treatment. However, despite no statistical significance, a slightly higher level of cathepsin K was seen in the lungs of the BLM-induced animals treated with AM24.

In overall conclusion, this thesis project has achieved an early proof-of-concept for AM24 as a novel and unique anti-pulmonary fibrotic agent for lung delivery. Through the *in vitro* studies, AM24 was identified as a highly potent anti-fibrotic molecule against TGF- β 1 induced PF-relevant pathobiologic changes in human lung fibroblast and alveolar epithelial cells, in addition to the anti-oxidative activity. As a MEL-CUR hybrid molecule, these activities were indeed more potent than those of MEL or CUR alone as well as PIR. Through the *in vivo* rat studies with BLM-induced experimental PF, AM24 was identified as a potent molecule for intervention with lung delivery just with 0.1 mg/kg doses every other day, despite a need of further improvements in this PF model for clearer pathobiologic demonstration (e.g., use of a higher BLM dose). Several questions are now of great interest for clarification, such as the mechanism(s) of remarkable actions; a real need of local lung delivery: intervention in other PF models; prevention and reversal efficacies; inhaled safety; and assessments of inhaled formulation and delivery. As a precursor of such an endeavor, the inhibitory activity of AM24 against induced collagen synthesis was shown to be opposed with a MEL receptor antagonist, LUZ. This thereby implied the involvement of the MEL receptor(s) as a potential target pathway/mechanism for anti-fibrotic activities of AM24 for the very first time.

APPENDICES

A.1 Picrosirius red assay for collagen

Picrosirius red reagent was prepared by adding 0.5g of Sirius red to 500ml of saturated picric acid.

The method was validated using calf skin collagen as a standard.

For standard curve:

1. Stock solution of 1 mg/ml was prepared using 1 mg of calf skin collagen in 0.1 M acetic acid.
2. Replicates of 0- 250 µg/ml solutions were prepared from the stock. 100 µL of this solution was aliquoted into a 1.5 ml Eppendorf tube and 500 µl of picrosirius red agent was added.
3. The centrifuge tube was vortexed and incubated at room temperature for an hour.
4. The tubes were then centrifuged at 10,000 rpm for 6 minutes.
5. 600 µl of the solution was pipetted out of the tube and 500 µL of 10 mM HCl was added.
6. The tubes were again vortexed and centrifuged at 10, 000 rpm for 6 minutes
7. The 500 µl wash buffer was then pipetted out.
8. 250 µl of 100 mM NaOH was then added and vortexed.
9. 150 µl of this solution was transferred to a 96 well plate and the absorbance was measured.

The standard curve thus obtained was linear ($R^2=0.9983$) in the range of 0-250 µg, thereby indicating that the method can detect changes in the amounts of collagen (Figure A.1).

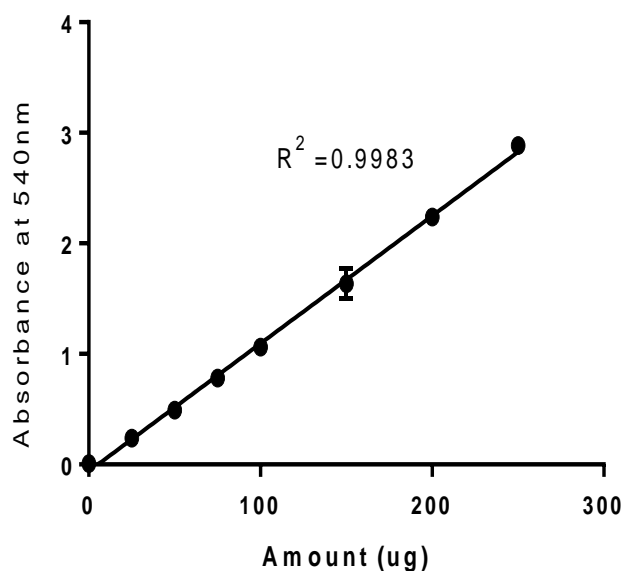


Figure A.1: A linear correlation between calf skin collagen amount added into the samples and their absorbance at 540 nm, measured by the picosirius red method for validation. Data: mean \pm SD from n=3. R²: regression coefficient.

I. Picosirius Red Collagen Assay for cells

- 1) Cells are seeded in 48 well plate at a density of 20,000
- 2) 48 hours after seeding, TGF- β 1(10ng/ml) is added
- 3) 2 hours after addition of TGF- β 1, the drug of interest is added at the concentration needed.
- 4) The cells are incubated with TGF- β 1 and drug for 48 hours at 37°C.
- 5) After 48 hours, media is aspirated, and cells are stained with Sirius red 0.1% in saturated picric acid for 1 hour (0.2ml) on a shaker at room temperature.
- 6) Unbound dye was removed using 0.2mL of 10mM HCL washes (3 washes)
- 7) Dye was solubilized with 150 μ L of 100mM NaOH.

- 8) The dye solution is then moved into a 96 well plate and the absorbance is measured at 540nm.

II. Picrosirius Red Collagen Assay for tissue

- 1) 100mg of tissue is homogenized in 1.5mL of CHAPS buffer and 200 μ L of this homogenate is added to a 48 well plate.
- 2) The 48 well plates are then kept at 37°C for drying for 48 hours.
- 3) After 48 hours, the wells are washed with PBS (thrice) followed by washing with 0.2mL of 10mM HCl(thrice) in order to remove the unbound dye.
- 4) 150 μ L of 100mM NaOH is then added to solubilize the dye. The dye solution is then shifted to a 96 well plate and absorbance is measured at 540nm.

A.2 Western Blot

Buffers:

a) Lysis buffer

- DDI water
- 1 M NaCl (Fischer BioReagents)
- Tris-HCl pH 8
- PhosphoStop tablet
- 1 protease inhibitor
- 0.1 ml NP-40

b) Wash buffer

- 6.05 g of TRIS (BioRad) + 8.76 g of NaCl
- 700 ml DDI
- pH to 7.6 with HCl
- 1 ml of tween

c) Storage buffer

- 6.05 g of TRIS + 8.76 g of NaCl
- 700 ml DDI
- pH to 7.6 with HCl

d) Running Buffer

- 10X TRIS/Glycine/SDS buffer (100 ml) + 900 ml DDI

e) Transfer Buffer

- 10X TRIS/Glycine Buffer (100 ml) + Methanol (200 ml) + 700 ml DDI

Western Blot Protocol

I. Sample preparation for cells

- 1) Western blot analysis was performed to assess protein Chapters 4,5 and 6. MRC-5, NHLF or A549 cells were plated in 10 cm dishes (1×10^6 cells/dish) and grown to confluence.

- 2) Upon confluence, TGF- β 1(10ng/ml) was added followed by addition of the drug at the required concentration. The cells were incubated with TGF- β 1 and the drug for 72 hours.
- 3) At 72 hours, the cells were kept in an ice bucket and washed with cold PBS thrice.
- 4) 0.5 mL of NP-40 lysis buffer was then added to the dishes and the cells were scrapped with cell scrapper (Corning).The cell suspension was collected in 1.5mL tubes.
- 5) The cells were then centrifuged at 10000 rpm for 10 min (Eppendorf centrifuge 5415 C). The supernatant was stored in another 1.5mL tube and the cell pellets were discarded.
- 6) 25 μ L of this supernatant is then used for the BCA assay to determine the protein content.

II. Sample preparation for tissue

- 1) 300 mg of minced right lung tissue was homogenized with 1 ml of cold NP-40 lysis buffer.
- 2) After ~1min of homogenization, the tissue extract was vortexed for 10 seconds and centrifuged at 10,000 rpm in 4°C (Aventi JE Centrifuge; Beckman Coulter).
- 3) The supernatant was collected and 2 μ l was used for the BCA assay to determine total protein content.

Western blot samples were made in Laemmli sample buffer (Bio-Rad laboratories, Hercules, CA) and β -mercaptoethanol (1:20) by denaturing the proteins at 90 °C for 5 min.

III. Gel Electrophoresis

- 1) First, the molecular weight range ladder was loaded followed by 40 μ g protein on each well of the 10 % Mini- Protean Precast Gels (Bio-Rad Laboratories) and tris/glycine/sodium dodecyl sulfate (SDS)-polyacrylamide gel electrophoresis (PAGE) was carried out at 100 V for about 1 hour.
- 2) The proteins from the gel were transferred on to a nitrocellulose at 100 V for 90 min in ice.
- 3) The nitrocellulose membranes were washed with TBST for 5 minutes and then subjected to 1 h of blocking in the blocking buffers 3% non-fat dry milk (Kroger) in TBST.
- 4) The nitrocellulose membranes were then incubated with the primary antibodies (of required protein) overnight at 4 °C.
- 5) Following day, the membranes were washed with TBST and then incubated for 80 min in appropriate secondary antibodies conjugated with HRP (Bio-Rad Laboratories) on the slow shaker at room temperature.
- 6) The membranes are washed again with TBST thrice(10 minutes each).
- 7) Membranes are then taken to the dark room and incubated in the chemiluminescent substrate (SuperSignalTM West Pico PLUS chemiluminescent, ThermoFischer) for 1 min to develop luminescence and then exposed to autoradiographic films.
- 8) The films are then developed in the dark in a film processor (X-Omat 2000A; Eastman Kodak, Rochester, NY).
- 9) The intensity and size of bands was analyzed by densitometry using Image J. Each protein was normalized with the corresponding β -actin or GAPDH signal.

A.3 Treadmill exercise endurance training and testing

Day 1: Place the rat in the treadmill and close the cover. Let rats get familiar for 5 mins. Start increasing the speed gradually in 5 min intervals starting at 2m/min, 5 m/min, 7 m/min, 10 m/min, allowing the rats to run for 5 mins at each speed. Observe if the rats are learning to avoid the shock area. After running for 5 minutes at 10m/min, place the rat back in the cage.

Day 2: Place the rat in the treadmill and close the cover. Start the treadmill for rats at 3 m/min and at 5 min intervals, increase up to 10 m/min as in Day 1, allowing the rats to run for 5 mins at each speed. Observe if the rats are learning to avoid the shock area. After running for 5 minutes at 10m/min, place the rat back in the cage.

Day 3: Place the rat in the treadmill and close the cover. Start treadmill for rats at 5 m/min and increase up to 10 m/min in 5 min intervals same as Days 1 and 2, allowing the rats to run for 5 mins at each speed. Observe if the rats are learning to avoid the shock area. After running for 5 minutes at 10m/min, place the rat back in the cage.

Day 4: Place the rat in the treadmill and close the cover. Turn on the electric shock and start the treadmill at the speed of 7.0 m/min. Start treadmill for rats at 7 m/min and after 5 mins, increase speed to 10 m/min. Let them run for 10 mins at 10 m/min. Observe if the rats are learning to avoid the shock area. If rat still cannot avoid, it may be untrainable. After running for 10 minutes at 10m/min, place the rat back in the cage.

Day 5: Place the rat in the treadmill and close the cover. Start treadmill at 10 m/min. Keep track of number of shocks and let each rat run for 30 mins (or until 5th shock if greater than 30 mins). If an extra day is needed, repeat on Day 6

A well trained, healthy rat would typically run for > 30 minutes without getting 5 shocks.

Exercise endurance test:

1. Turn on the treadmill and the electric foot shock.
2. Raise the height of the treadmill to a 5-degree angle
3. Place the rat on the treadmill and start at a speed of 10 m/min. Start the timer
4. Carefully watch the rat's running and record how many times it touches the electric foot shock up to 5 shocks
5. When the rat runs for over 30 minutes, raise the treadmill angle to 10 degrees
6. When the rat runs for over 40 minutes, raise the angle to 15 degrees

REFERENCES

- Ak, T., & Gülçin, I. (2008). Antioxidant and radical scavenging properties of curcumin. *Chemico-Biological Interactions*, 174(1), 27–37. <https://doi.org/10.1016/j.cbi.2008.05.003>
- Amorati, R., Foti, M. C., & Valgimigli, L. (2013). Antioxidant Activity of Essential Oils. *Journal of Agricultural and Food Chemistry*, 61(46), 10835–10847. <https://doi.org/10.1021/jf403496k>
- Arizono, S., Taniguchi, H., Sakamoto, K., Kondoh, Y., Kimura, T., Kataoka, K., ... Tabira, K. (2014). Endurance Time Is the Most Responsive Exercise Measurement in Idiopathic Pulmonary Fibrosis. *Respiratory Care*, 59(7), 1108–1115. <https://doi.org/10.4187/respcare.02674>
- Arslan, S. O., Zerim, M., Vural, H., & Coskun, A. (2002). The effect of melatonin on bleomycin-induced pulmonary fibrosis in rats. *Journal of Pineal Research*, 32(1), 21–25. <https://doi.org/10.1034/j.1600-079x.2002.10796.x>
- B Moore, B., Lawson, W. E., Oury, T. D., Sisson, T. H., Raghavendran, K., & Hogaboam, C. M. (2013). Animal models of fibrotic lung disease. *American Journal of Respiratory Cell and Molecular Biology*, 49(2), 167–179. <https://doi.org/10.1165/rcmb.2013-0094TR>
- Barratt, S. L., Creamer, A., Hayton, C., & Chaudhuri, N. (2018). Idiopathic Pulmonary Fibrosis (IPF): An Overview. *Journal of Clinical Medicine*, 7(8). <https://doi.org/10.3390/jcm7080201>
- Baumgartner, K. B., Samet, J. M., Stidley, C. A., Colby, T. V., & Waldron, J. A. (1997). Cigarette smoking: A risk factor for idiopathic pulmonary fibrosis. *American Journal of Respiratory and Critical Care Medicine*, 155(1), 242–248. <https://doi.org/10.1164/ajrccm.155.1.9001319>
- Beyer, C., & Distler, J. H. W. (2013). Biochimica et Biophysica Acta Tyrosine kinase signaling in fibrotic disorders Translation of basic research to human disease, 1832, 897–904. <https://doi.org/10.1016/j.bbadis.2012.06.008>
- Biernacka, A., Dobaczewski, M., & Frangogiannis, N. G. (2011). TGF- β signaling in fibrosis. *Growth Factors (Chur, Switzerland)*, 29(5), 196–202. <https://doi.org/10.3109/08977194.2011.595714>

Bois, R. M. du, Albera, C., Bradford, W. Z., Costabel, U., Leff, J. A., Noble, P. W., ... King, T. E. (2014). 6-minute walk distance is an independent predictor of mortality in patients with idiopathic pulmonary fibrosis. *European Respiratory Journal*, 43(5), 1421–1429. <https://doi.org/10.1183/09031936.00131813>

Bois, R. M. du, Weycker, D., Albera, C., Bradford, W. Z., Costabel, U., Kartashov, A., ... King, T. E. (2011). Six-Minute-Walk Test in Idiopathic Pulmonary Fibrosis. *American Journal of Respiratory and Critical Care Medicine*, 183(9), 1231–1237. <https://doi.org/10.1164/rccm.201007-1179OC>

Bonella, F., Wijsenbeek, M., Molina-Molina, M., Duck, A., Mele, R., Geissler, K., & Wuyts, W. (2016). European IPF Patient Charter: Unmet needs and a call to action for healthcare policymakers. *The European Respiratory Journal*, 47(2), 597–606. <https://doi.org/10.1183/13993003.01204-2015>

Bonner, J. C. (2004). Regulation of PDGF and its receptors in fibrotic diseases, 15, 255–273. <https://doi.org/10.1016/j.cytogfr.2004.03.006>

Borthwick, L. A., Gardner, A., De Soyza, A., Mann, D. A., & Fisher, A. J. (2011). Transforming Growth Factor- β 1 (TGF- β 1) Driven Epithelial to Mesenchymal Transition (EMT) is Accentuated by Tumour Necrosis Factor α (TNF α) via Crosstalk Between the SMAD and NF- κ B Pathways. *Cancer Microenvironment*, 5(1), 45–57. <https://doi.org/10.1007/s12307-011-0080-9>

Bühling, F., Waldburg, N., Gerber, A., Häckel, C., Krüger, S., Reinhold, D., ... Welte, T. (2000). Cathepsin K expression in human lung. *Advances in Experimental Medicine and Biology*, 477, 281–286. https://doi.org/10.1007/0-306-46826-3_30

Bühling, Frank, Röcken, C., Brasch, F., Hartig, R., Yasuda, Y., Saftig, P., ... Welte, T. (2004). Pivotal role of cathepsin K in lung fibrosis. *The American Journal of Pathology*, 164(6), 2203–2216. [https://doi.org/10.1016/S0002-9440\(10\)63777-7](https://doi.org/10.1016/S0002-9440(10)63777-7)

Clark J.G., Madtes D.K., Raghu G. Effects of platelet-derived growth-factor isoforms on human lung fibroblast proliferation and procollagen gene-expression. *Experimental lung research*. 1993; 19:327–344. [PubMed: 8319603]

Chen Y., Zhao M., Fu M., et al. The role of calcineurin in the lung fibroblasts proliferation and collagen synthesis induced by basic fibroblast growth factor. *Chin Med J (Engl)* 2003; 116: 857–862.

Chen, Xia, & Thibeault, S. L. (2012). Response of Fibroblasts to Transforming Growth Factor- β 1 on Two-Dimensional and in Three-Dimensional Hyaluronan Hydrogels. *Tissue Engineering. Part A*, 18(23–24), 2528–2538. <https://doi.org/10.1089/ten.tea.2012.0094>

Chen, Xiang, Shi, C., Meng, X., Zhang, K., Li, X., Wang, C., ... Han, X. (2016). Inhibition of Wnt/ β -catenin signaling suppresses bleomycin-induced pulmonary fibrosis by attenuating the expression of TGF- β 1 and FGF-2. *Experimental and Molecular Pathology*, 101(1), 22–30. <https://doi.org/10.1016/j.yexmp.2016.04.003>

Cheresh, P., Kim, S.-J., Tulasiram, S., & Kamp, D. W. (2013). Oxidative stress and pulmonary fibrosis. *Biochimica Et Biophysica Acta*, 1832(7), 1028–1040. <https://doi.org/10.1016/j.bbadis.2012.11.021>

Chojnacki, J. E., Liu, K., Yan, X., Toldo, S., Selden, T., Estrada, M., ... Zhang, S. (2014). Discovery of 5-(4-Hydroxyphenyl)-3-oxo-pentanoic Acid [2-(5-Methoxy-1H-indol-3-yl)-ethyl]-amide as a Neuroprotectant for Alzheimer's Disease by Hybridization of Curcumin and Melatonin. *ACS Chemical Neuroscience*, 5(8), 690–699. <https://doi.org/10.1021/cn500081s>

Chua, F., Gauldie, J., & Laurent, G. J. (2005). Pulmonary fibrosis: Searching for model answers. *American Journal of Respiratory Cell and Molecular Biology*, 33(1), 9–13. <https://doi.org/10.1165/rcmb.2005-0062TR>

Conte, E., Gili, E., Fagone, E., Fruciano, M., Iemmolo, M., & Vancheri, C. (2014). Effect of pirfenidone on proliferation, TGF- β -induced myofibroblast differentiation and fibrogenic activity of primary human lung fibroblasts. *European Journal of Pharmaceutical Sciences*, 58, 13–19. <https://doi.org/10.1016/j.ejps.2014.02.014>

Darby, I. A., & Hewitson, T. D. (2007). Fibroblast differentiation in wound healing and fibrosis. *International Review of Cytology*, 257, 143–179. [https://doi.org/10.1016/S0074-7696\(07\)57004-X](https://doi.org/10.1016/S0074-7696(07)57004-X)

Darby, I. A., Laverdet, B., Bonté, F., & Desmoulière, A. (2014). Fibroblasts and myofibroblasts in wound healing. *Clinical, Cosmetic and Investigational Dermatology*, 7, 301–311. <https://doi.org/10.2147/CCID.S50046>

Durairaj Punithavathi, Narayanan Venkatesan & Mary Babu. (n.d.). Curcumin inhibition of bleomycin-induced pulmonary fibrosis in rats. *British Journal of Pharmacology (2000)* 131, 169-172.

Eybl, V., Kotyzová, D., Č, P. & Koutenský, J. Effect of melatonin , curcumin , quercetin , and resveratrol on acute ferric nitrilotriacetate (Fe-NTA) -induced renal oxidative damage in rats. 347–353 (2008).

Fernandez, I. E., & Eickelberg, O. (2012). The Impact of TGF- β on Lung Fibrosis: From Targeting to Biomarkers. *Proceedings of the American Thoracic Society*, 9(3), 111–116. <https://doi.org/10.1513/pats.201203-023AW>

Fujimoto, H., Kobayashi, T., & Azuma, A. (2016). Idiopathic Pulmonary Fibrosis: Treatment and Prognosis. *Clinical Medicine Insights. Circulatory, Respiratory and Pulmonary Medicine*, 9(Suppl 1), 179–185. <https://doi.org/10.4137/CCRPM.S23321>

Fujiwara, A., Shintani, Y., Funaki, S., Kawamura, T., Kimura, T., Minami, M., & Okumura, M. (2017). Pirfenidone plays a biphasic role in inhibition of epithelial-mesenchymal transition in non-small cell lung cancer. *Lung Cancer*, 106, 8–16. <https://doi.org/10.1016/j.lungcan.2017.01.006>

Gilhodes, J.-C., Julé, Y., Kreuz, S., Stierstorfer, B., Stiller, D., & Wollin, L. (2017). Quantification of Pulmonary Fibrosis in a Bleomycin Mouse Model Using Automated Histological Image Analysis. *PLoS ONE*, 12(1). <https://doi.org/10.1371/journal.pone.0170561>

Grimminger, F., Günther, A., & Vancheri, C. (n.d.). The role of tyrosine kinases in the pathogenesis of idiopathic pulmonary fibrosis, 1426-1433. <https://doi.org/10.1183/09031936.00149614>

Gross, T. J., & Hunninghake, G. W. (2001). Idiopathic pulmonary fibrosis. *The New England Journal of Medicine*, 345(7), 517–525. <https://doi.org/10.1056/NEJMra003200>

Han, Q., Lin, L., Zhao, B., Wang, N., & Liu, X. (2018). Inhibition of mTOR ameliorates bleomycin-induced pulmonary fibrosis by regulating epithelial-mesenchymal transition. *Biochemical and Biophysical Research Communications*, 500(4), 839–845. <https://doi.org/10.1016/j.bbrc.2018.04.148>

Hardeland, R. (2005). Antioxidative protection by melatonin: Multiplicity of mechanisms from radical detoxification to radical avoidance. *Endocrine*, 27(2), 119–130.

- Herraiz, T., & Galisteo, J. (2004). Endogenous and dietary indoles: A class of antioxidants and radical scavengers in the ABTS assay. *Free Radical Research*, 38(3), 323–331.
- Hewlings, S. J., & Kalman, D. S. (2017). Curcumin: A Review of Its' Effects on Human Health. *Foods*, 6(10). <https://doi.org/10.3390/foods6100092>
- Hisatomi, K., Mukae, H., Sakamoto, N., Ishimatsu, Y., Kakugawa, T., Hara, S., ... Kohno, S. (2012). Pirfenidone inhibits TGF- β 1-induced over-expression of collagen type I and heat shock protein 47 in A549 cells. *BMC Pulmonary Medicine*, 12, 24. <https://doi.org/10.1186/1471-2466-12-24>
- Hosseinzadeh, A., Javad-Moosavi, S. A., Reiter, R. J., Yarahmadi, R., Ghaznavi, H., & Mehrzadi, S. (2018). Oxidative/nitrosative stress, autophagy and apoptosis as therapeutic targets of melatonin in idiopathic pulmonary fibrosis. *Expert Opinion on Therapeutic Targets*, 22(12), 1049–1061. <https://doi.org/10.1080/14728222.2018.1541318>
- Hu, Y., Li, M., Zhang, M., & Jin, Y. (2018). Inhalation treatment of idiopathic pulmonary fibrosis with curcumin large porous microparticles. *International Journal of Pharmaceutics*, 551(1–2), 212–222. <https://doi.org/10.1016/j.ijpharm.2018.09.031>
- Huang, R. Y.-J., Guilford, P., & Thiery, J. P. (2012). Early events in cell adhesion and polarity during epithelial-mesenchymal transition. *Journal of Cell Science*, 125(Pt 19), 4417–4422. <https://doi.org/10.1242/jcs.099697>
- Hübner, R.-H., Gitter, W., El Mokhtari, N. E., Mathiak, M., Both, M., Bolte, H., ... Bewig, B. (2008). Standardized quantification of pulmonary fibrosis in histological samples. *BioTechniques*, 44(4), 507–511, 514–517. <https://doi.org/10.2144/000112729>
- Inoue, Y., King, T. E., Tinkle, S. S., Dockstader, K., & Newman, L. S. (1996). Human Mast Cell Basic Fibroblast Growth Factor in Pulmonary Fibrotic Disorders, 149(6), 2037–2054
- Issa, J. P. J., Garcia-Manero, G., Giles, F. J., Mannari, R., Thomas, D., Faderl, S., ... Kantarjian, H. M. (2004). Phase 1 study of low-dose prolonged exposure schedules of the hypomethylating agent 5-aza-2'-deoxycytidine (decitabine) in hematopoietic malignancies. *Blood*, 103(5), 1635–1640. <https://doi.org/10.1182/blood-2003-03-0687>

Kalluri, R., & Weinberg, R. A. (2009). The basics of epithelial-mesenchymal transition. *The Journal of Clinical Investigation*, 119(6), 1420–1428.

<https://doi.org/10.1172/JCI39104>

Karimfar, M. H., Rostami, S., Haghani, K., Bakhtiyari, S., & Noori-Zadeh, A. (2015). Melatonin alleviates bleomycin-induced pulmonary fibrosis. *Journal of Biological Regulators and Homeostatic Agents*, 29(2), 327–334.

Kasai, H., Allen, J. T., Mason, R. M., Kamimura, T., & Zhang, Z. (2005). TGF- β 1 induces human alveolar epithelial to mesenchymal cell transition (EMT). *Respiratory Research*, 6(1), 56. <https://doi.org/10.1186/1465-9921-6-56>

Kendall, R. T., & Feghali-Bostwick, C. A. (2014). Fibroblasts in fibrosis: Novel roles and mediators. *Frontiers in Pharmacology*, 5, 123. <https://doi.org/10.3389/fphar.2014.00123>

Kim, J. H., Jang, Y. S., Eom, K.-S., Hwang, Y. I., Kang, H. R., Jang, S. H., ... Kim, D.-G. (2007). Transforming growth factor beta1 induces epithelial-to-mesenchymal transition of A549 cells. *Journal of Korean Medical Science*, 22(5), 898–904.

<https://doi.org/10.3346/jkms.2007.22.5.898>

Kim, S. N., Lee, J., Yang, H.-S., Cho, J.-W., Kwon, S., Kim, Y.-B., ... Lee, K. (2010). Dose-response Effects of Bleomycin on Inflammation and Pulmonary Fibrosis in Mice. *Toxicological Research*, 26(3), 217–222. <https://doi.org/10.5487/TR.2010.26.3.217>

King, T. E., Pardo, A., & Selman, M. (2011). Idiopathic pulmonary fibrosis. *The Lancet*, 378(9807), 1949–1961. [https://doi.org/10.1016/S0140-6736\(11\)60052-4](https://doi.org/10.1016/S0140-6736(11)60052-4)

Kinnula, V. L., Fattman, C. L., Tan, R. J., & Oury, T. D. (2005). Oxidative Stress in Pulmonary Fibrosis. *American Journal of Respiratory and Critical Care Medicine*, 172(4), 417–422. <https://doi.org/10.1164/rccm.200501-017PP>

Kliment, C. R., Englert, J. M., Crum, L. P., & Oury, T. D. (2011). A novel method for accurate collagen and biochemical assessment of pulmonary tissue utilizing one animal. *International Journal of Clinical and Experimental Pathology*, 4(4), 349–355.

Koch, L. G., & Britton, S. L. (2001). Artificial selection for intrinsic aerobic endurance running capacity in rats. *Physiological Genomics*, 5(1), 45–52.

<https://doi.org/10.1152/physiolgenomics.2001.5.1.45>

Koh, R. Y., Lim, C. L., Uhal, B. D., Abdullah, M., Vidyadaran, S., Ho, C. C., & Seow, H. F. (2015). Inhibition of transforming growth factor- β via the activin receptor-like kinase-5 inhibitor attenuates pulmonary fibrosis. *Molecular Medicine Reports*, *11*(5), 3808–3813. <https://doi.org/10.3892/mmr.2015.3193>

Kraus, R. L., Pasieczny, R., Lariosa-Willingham, K., Turner, M. S., Jiang, A., & Trauger, J. W. (2005). Antioxidant properties of minocycline: Neuroprotection in an oxidative stress assay and direct radical-scavenging activity: Antioxidant properties of minocycline. *Journal of Neurochemistry*, *94*(3), 819–827. <https://doi.org/10.1111/j.1471-4159.2005.03219.x>

Kurimoto, R., Ebata, T., Iwasawa, S., Ishiwata, T., Tada, Y., Tatsumi, K., & Takiguchi, Y. (2017). Pirfenidone may revert the epithelial-to-mesenchymal transition in human lung adenocarcinoma. *Oncology Letters*, *14*(1), 944–950. <https://doi.org/10.3892/ol.2017.6188>

Kurita, Y., Araya, J., Minagawa, S., Hara, H., Ichikawa, A., Saito, N., ... Kuwano, K. (2017). Pirfenidone inhibits myofibroblast differentiation and lung fibrosis development during insufficient mitophagy. *Respiratory Research*, *18*(1), 114. <https://doi.org/10.1186/s12931-017-0600-3>

Leask, A., & Abraham, D. J. (2004). TGF-beta signaling and the fibrotic response. *FASEB Journal: Official Publication of the Federation of American Societies for Experimental Biology*, *18*(7), 816–827. <https://doi.org/10.1096/fj.03-1273rev>

Lee, B. W., Lee, J. H., Gal, S. W., Moon, Y. H. & Hun, K. Selective ABTS Radical-Scavenging Activity of Prenylated Flavonoids from *Cudrania tricuspidata* Selective ABTS Radical-Scavenging Activity of Prenylated Flavonoids. **8451**, (2014).

Lee, J. C., Kinniry, P. A., Arguiri, E., Serota, M., Kanterakis, S., Chatterjee, S., ... Christofidou-Solomidou, M. (2010). Dietary Curcumin Increases Antioxidant Defenses in Lung, Ameliorates Radiation-Induced Pulmonary Fibrosis, and Improves Survival in Mice. *Radiation Research*, *173*(5), 590–601. <https://doi.org/10.1667/RR1522.1>

Ley, B., & Collard, H. R. (2013). Epidemiology of idiopathic pulmonary fibrosis. *Clinical Epidemiology*, *5*, 483–492. <https://doi.org/10.2147/CLEP.S54815>

Ley, B., Collard, H. R., & King, T. E. (2011). Clinical Course and Prediction of Survival in Idiopathic Pulmonary Fibrosis. *American Journal of Respiratory and Critical Care Medicine*, *183*(4), 431–440. <https://doi.org/10.1164/rccm.201006-0894CI>

Li, R., Wang, Y., Liu, Y., Chen, Q., Fu, W., Wang, H., ... Zhang, X. (2013). Curcumin inhibits transforming growth factor- β 1-induced EMT via PPAR γ pathway, not Smad pathway in renal tubular epithelial cells. *PloS One*, 8(3), e58848. <https://doi.org/10.1371/journal.pone.0058848>

Lin, X., Wen, J., Liu, R., Gao, W., Qu, B., & Yu, M. (2018). Nintedanib inhibits TGF- β -induced myofibroblast transdifferentiation in human Tenon's fibroblasts. *Molecular Vision*, 24, 789–800.

Liu, D., Gong, L., Zhu, H., Pu, S., Wu, Y., Zhang, W., & Huang, G. (2016). Curcumin Inhibits Transforming Growth Factor β Induced Differentiation of Mouse Lung Fibroblasts to Myofibroblasts. *Frontiers in Pharmacology*, 7. <https://doi.org/10.3389/fphar.2016.00419>

Liu, R.-M., & Gaston Pravia, K. A. (2010). Oxidative stress and glutathione in TGF- β -mediated fibrogenesis. *Free Radical Biology & Medicine*, 48(1), 1. <https://doi.org/10.1016/j.freeradbiomed.2009.09.026>

Lota, H. K., & Wells, A. U. (2013). The evolving pharmacotherapy of pulmonary fibrosis. *Expert Opinion on Pharmacotherapy*, 14(1), 79–89. <https://doi.org/10.1517/14656566.2013.758250>

Loveman, E., Copley, V. R., Scott, D. A., Colquitt, J. L., Clegg, A. J., & O'Reilly, K. M. A. (2015). Comparing new treatments for idiopathic pulmonary fibrosis--a network meta-analysis. *BMC Pulmonary Medicine*, 15, 37. <https://doi.org/10.1186/s12890-015-0034-y>

Lynch, D. A., Sverzellati, N., Travis, W. D., Brown, K. K., Colby, T. V., Galvin, J. R., ... Wells, A. U. (2018). Diagnostic criteria for idiopathic pulmonary fibrosis: A Fleischner Society White Paper. *The Lancet. Respiratory Medicine*, 6(2), 138–153. [https://doi.org/10.1016/S2213-2600\(17\)30433-2](https://doi.org/10.1016/S2213-2600(17)30433-2)

Melloni, B. (1996). Original articles Effect of exposure to silica on human alveolar macrophages in supporting growth activity in type, 28(3), 781–786

Mendez, M. G., Kojima, S.-I., & Goldman, R. D. (2010). Vimentin induces changes in cell shape, motility, and adhesion during the epithelial to mesenchymal transition. *FASEB Journal: Official Publication of the Federation of American Societies for Experimental Biology*, 24(6), 1838–1851. <https://doi.org/10.1096/fj.09-151639>

Meng, L., Zhang, X., Wang, H., Dong, H., Gu, X., Yu, X., & Liu, Y. (2019). Yangyin Yiqi Mixture Ameliorates Bleomycin-Induced Pulmonary Fibrosis in Rats through Inhibiting TGF- β 1/Smad Pathway and Epithelial to Mesenchymal Transition. *Evidence-Based Complementary and Alternative Medicine : ECAM*, 2019.

<https://doi.org/10.1155/2019/2710509>

Meyer, K. C. (2017). Pulmonary fibrosis, part I: Epidemiology, pathogenesis, and diagnosis. *Expert Review of Respiratory Medicine*, 11(5), 343–359.

<https://doi.org/10.1080/17476348.2017.1312346>

Mishra, A., Doyle, N. A., & Martin, W. J. (2000). Bleomycin-Mediated Pulmonary Toxicity. *American Journal of Respiratory Cell and Molecular Biology*, 22(5), 543–549.

<https://doi.org/10.1165/ajrcmb.22.5.3851>

Moeller, A., Ask, K., Warburton, D., Gauldie, J., & Kolb, M. (2008). The bleomycin animal model: A useful tool to investigate treatment options for idiopathic pulmonary fibrosis? *The International Journal of Biochemistry & Cell Biology*, 40(3), 362–382.

<https://doi.org/10.1016/j.biocel.2007.08.011>

Moore, B. B., & Hogaboam, C. M. (2008). Murine models of pulmonary fibrosis. *American Journal of Physiology-Lung Cellular and Molecular Physiology*, 294(2), L152–L160.

<https://doi.org/10.1152/ajplung.00313.2007>

Nishijima, N., Seike, M., Soeno, C., Chiba, M., Miyanaga, A., Noro, R., ... Gemma, A. (2016). miR-200/ZEB axis regulates sensitivity to nintedanib in non-small cell lung cancer cells. *International Journal of Oncology*, 48(3), 937–944.

<https://doi.org/10.3892/ijo.2016.3331>

Nishijima, K., Ng, Y. S., Zhong, L., Bradley, J., Schubert, W., Jo, N., ... Shima, D. T. (2007). Vascular endothelial growth factor-A is a survival factor for retinal neurons and a critical neuroprotectant during the adaptive response to ischemic injury. *American Journal of Pathology*, 171(1), 53–67.

<https://doi.org/10.2353/ajpath.2007.061237>

Olegário, J. G. P., Silva, M. V., Machado, J. R., Rocha, L. P., Reis, M. A., Guimarães, C. S. de O., & Corrêa, R. R. M. (2013). Pulmonary Innate Immune Response and Melatonin Receptors in the Perinatal Stress [Research article]. <https://doi.org/10.1155/2013/340959>

Peng, R., Sridhar, S., Tyagi, G., Phillips, J. E., Garrido, R., Harris, P., ... Stevenson, C. S. (2013). Bleomycin Induces Molecular Changes Directly Relevant to Idiopathic Pulmonary Fibrosis: A Model for “Active” Disease. *PLOS ONE*, 8(4), e59348.

<https://doi.org/10.1371/journal.pone.0059348>

Phan, S. H. (2008). Biology of Fibroblasts and Myofibroblasts. *Proceedings of the American Thoracic Society*, 5(3), 334–337. <https://doi.org/10.1513/pats.200708-146DR>

Priyadarsini, K. Indira. (2009). Photophysics, photochemistry and photobiology of curcumin: Studies from organic solutions, bio-mimetics and living cells. *Journal of Photochemistry and Photobiology C: Photochemistry Reviews*, 10(2), 81–95. <https://doi.org/10.1016/j.jphotochemrev.2009.05.001>

Priyadarsini, K. Indira, Maity, D. K., Naik, G. H., Kumar, M. S., Unnikrishnan, M. K., Satav, J. G., & Mohan, H. (2003). Role of phenolic O-H and methylene hydrogen on the free radical reactions and antioxidant activity of curcumin. *Free Radical Biology & Medicine*, 35(5), 475–484.

Priyadarsini, Kavirayani Indira. (2014). The chemistry of curcumin: From extraction to therapeutic agent. *Molecules (Basel, Switzerland)*, 19(12), 20091–20112. <https://doi.org/10.3390/molecules191220091>

Pulmonary Fibrosis Medications | American Lung Association. (n.d.). Retrieved February 23, 2019, from <https://www.lung.org/lung-health-and-diseases/lung-disease-lookup/pulmonary-fibrosis/patients/how-is-pulmonary-fibrosis-treated/medications.html>

Qiu, Y., Pan, X., & Hu, Y. (2019). Polydatin ameliorates pulmonary fibrosis by suppressing inflammation and the epithelial mesenchymal transition via inhibiting the TGF- β /Smad signaling pathway. *RSC Advances*, 9(14), 8104–8112. <https://doi.org/10.1039/C8RA08659A>

Raghu, G., Collard, H. R., Egan, J. J., Martinez, F. J., Behr, J., Brown, K. K., ... Schönemann, H. J. (2011). An Official ATS/ERS/JRS/ALAT Statement: Idiopathic Pulmonary Fibrosis: Evidence-based Guidelines for Diagnosis and Management. *American Journal of Respiratory and Critical Care Medicine*, 183(6), 788–824. <https://doi.org/10.1164/rccm.2009-040GL>

Raghu, G., Remy-Jardin, M., Myers, J. L., Richeldi, L., Ryerson, C. J., Lederer, D. J., ... Wilson, K. C. (2018). Diagnosis of Idiopathic Pulmonary Fibrosis. An Official ATS/ERS/JRS/ALAT Clinical Practice Guideline. *American Journal of Respiratory and Critical Care Medicine*, 198(5), e44–e68. <https://doi.org/10.1164/rccm.201807-1255ST>

Saidi, A., Kasabova, M., Vanderlynden, L., Wartenberg, M., Kara-Ali, G. H., Marc, D., ... Lalmanach, G. (2019). Curcumin inhibits the TGF- β 1-dependent differentiation of

lung fibroblasts via PPAR γ -driven upregulation of cathepsins B and L. *Scientific Reports*, 9. <https://doi.org/10.1038/s41598-018-36858-3>

Saluja, B., Li, H., Desai, U. R., Voelkel, N. F., & Sakagami, M. (2014). Sulfated caffeic acid dehydropolymer attenuates elastase and cigarette smoke extract-induced emphysema in rats: Sustained activity and a need of pulmonary delivery. *Lung*, 192(4), 481–492. <https://doi.org/10.1007/s00408-014-9597-2>

Saluja, B., Thakkar, J. N., Li, H., Desai, U. R., & Sakagami, M. (2013). Novel low molecular weight lignins as potential anti-emphysema agents: In vitro triple inhibitory activity against elastase, oxidation and inflammation. *Pulmonary Pharmacology & Therapeutics*, 26(2), 296–304. <https://doi.org/10.1016/j.pupt.2012.12.009>

Schaefer, C. J., Ruhrmund, D. W., Pan, L., Seiwert, S. D., & Kossen, K. (2011). Antifibrotic activities of pirfenidone in animal models. *European Respiratory Review*, 20(120), 85–97. <https://doi.org/10.1183/09059180.00001111>

Schünemann, H. J., Jaeschke, R., Cook, D. J., Bria, W. F., El-Solh, A. A., Ernst, A., ... ATS Documents Development and Implementation Committee. (2006). An official ATS statement: Grading the quality of evidence and strength of recommendations in ATS guidelines and recommendations. *American Journal of Respiratory and Critical Care Medicine*, 174(5), 605–614. <https://doi.org/10.1164/rccm.200602-197ST>

Sewing, A. C. P., Kantores, C., Ivanovska, J., Lee, A. H., Masood, A., Jain, A., ... Jankov, R. P. (2012). Therapeutic hypercapnia prevents bleomycin-induced pulmonary hypertension in neonatal rats by limiting macrophage-derived tumor necrosis factor- α . *American Journal of Physiology. Lung Cellular and Molecular Physiology*, 303(1), L75-87. <https://doi.org/10.1152/ajplung.00072.2012>

Sgalla, G., Iovene, B., Calvello, M., Ori, M., Varone, F., & Richeldi, L. (2018). Idiopathic pulmonary fibrosis: Pathogenesis and management. *Respiratory Research*, 19. <https://doi.org/10.1186/s12931-018-0730-2>

Shintani, Y., Maeda, M., Chaika, N., Johnson, K. R., & Wheelock, M. J. (2008). Collagen I Promotes Epithelial-to-Mesenchymal Transition in Lung Cancer Cells via Transforming Growth Factor- β Signaling. *American Journal of Respiratory Cell and Molecular Biology*, 38(1), 95–104. <https://doi.org/10.1165/rcmb.2007-0071OC>

Smith, M. R., Gangireddy, S. R., Narala, V. R., Hogaboam, C. M., Standiford, T. J., Christensen, P. J., ... Reddy, R. C. (2010). Curcumin inhibits fibrosis-related effects in IPF fibroblasts and in mice following bleomycin-induced lung injury. *American Journal*

of Physiology. *Lung Cellular and Molecular Physiology*, 298(5), L616-625.
<https://doi.org/10.1152/ajplung.00002.2009>

Song, X., Yu, W., & Guo, F. (2018). Pirfenidone suppresses bleomycin-induced pulmonary fibrosis and periostin expression in rats. *Experimental and Therapeutic Medicine*, 16(3), 1800–1806. <https://doi.org/10.3892/etm.2018.6378>

Spagnolo, P., Tzouvelekis, A., & Bonella, F. (2018). The Management of Patients With Idiopathic Pulmonary Fibrosis. *Frontiers in Medicine*, 5.
<https://doi.org/10.3389/fmed.2018.00148>

Srivastava, M., Steinwede, K., Kiviranta, R., Morko, J., Hoymann, H.-G., Länger, F., ... Maus, U. A. (2008). Overexpression of cathepsin K in mice decreases collagen deposition and lung resistance in response to bleomycin-induced pulmonary fibrosis. *Respiratory Research*, 9, 54. <https://doi.org/10.1186/1465-9921-9-54>

Stahnke, T., Kowtharapu, B. S., Stachs, O., Schmitz, K.-P., Wurm, J., Wree, A., ... Hovakimyan, M. (2017). Suppression of TGF- β pathway by pirfenidone decreases extracellular matrix deposition in ocular fibroblasts in vitro. *PLoS ONE*, 12(2).
<https://doi.org/10.1371/journal.pone.0172592>

Stone, R. C., Pastar, I., Ojeh, N., Chen, V., Liu, S., Garzon, K. I., & Tomic-Canic, M. (2016). Epithelial-Mesenchymal Transition in Tissue Repair and Fibrosis. *Cell and Tissue Research*, 365(3), 495–506. <https://doi.org/10.1007/s00441-016-2464-0>

Su, Y., Gu, H., Weng, D., Zhou, Y., Li, Q., Zhang, F., ... Li, H. (2017). Association of serum levels of laminin, type IV collagen, procollagen III N-terminal peptide, and hyaluronic acid with the progression of interstitial lung disease. *Medicine*, 96(18).
<https://doi.org/10.1097/MD.00000000000006617>

Sun, Y., Zhang, Y., & Chi, P. (2018). Pirfenidone suppresses TGF- β 1-induced human intestinal fibroblasts activities by regulating proliferation and apoptosis via the inhibition of the Smad and PI3K/AKT signaling pathway. *Molecular Medicine Reports*, 18(4), 3907–3913. <https://doi.org/10.3892/mmr.2018.9423>

Symptoms of Pulmonary Fibrosis | American Lung Association. (n.d.). Retrieved April 17, 2019, from <https://www.lung.org/lung-health-and-diseases/lung-disease-lookup/pulmonary-fibrosis/introduction/symptoms.html>

Tan, D., Reiter, R. J., Manchester, L. C., Yan, M., El-Sawi, M., Sainz, R. M., ... Hardelan, M. C. A. and R. (2002, January 31). Chemical and Physical Properties and Potential

Mechanisms: Melatonin as a Broad Spectrum Antioxidant and Free Radical Scavenger. Retrieved June 22, 2019, from Current Topics in Medicinal Chemistry website: <http://www.eurekaselect.com/81329/article>

Tashiro, J., Rubio, G. A., Limper, A. H., Williams, K., Elliot, S. J., Ninou, I., ... Glassberg, M. K. (2017). Exploring Animal Models That Resemble Idiopathic Pulmonary Fibrosis. *Frontiers in Medicine*, 4. <https://doi.org/10.3389/fmed.2017.00118>

Tatler, A. L., & Jenkins, G. (2012). TGF- β activation and lung fibrosis. *Proceedings of the American Thoracic Society*, 9(3), 130–136. <https://doi.org/10.1513/pats.201201-003AW>

Verrecchia, F., & Mauviel, A. (2007). Transforming growth factor- β and fibrosis. *World Journal of Gastroenterology : WJG*, 13(22), 3056–3062. <https://doi.org/10.3748/wjg.v13.i22.3056>

Volk, S. W., Iqbal, S. A., & Bayat, A. (2013). Interactions of the Extracellular Matrix and Progenitor Cells in Cutaneous Wound Healing. *Advances in Wound Care*, 2(6), 261–272. <https://doi.org/10.1089/wound.2012.0417>

Wells, A. U. (2013). Managing diagnostic procedures in idiopathic pulmonary fibrosis. *European Respiratory Review*, 22(128), 158–162. <https://doi.org/10.1183/09059180.00001213>

Weng, D., Chen, J., Li, H., Liu, F., Zhou, L., Liu, H., ... Ge, B. (2018). 2-aminopurine suppresses the TGF- β 1-induced epithelial–mesenchymal transition and attenuates bleomycin-induced pulmonary fibrosis. *Cell Death Discovery*, 4(1), 17. <https://doi.org/10.1038/s41420-017-0016-3>

Wilson, M., & Wynn, T. (2009). Pulmonary fibrosis: Pathogenesis, etiology and regulation. *Mucosal Immunology*, 2(2), 103–121. <https://doi.org/10.1038/mi.2008.85>

Wollin, L., Maillet, I., Quesniaux, V., Holweg, A., & Ryffel, B. (2014). Antifibrotic and Anti-inflammatory Activity of the Tyrosine Kinase Inhibitor Nintedanib in Experimental Models of Lung Fibrosis. *Journal of Pharmacology and Experimental Therapeutics*, 349(2), 209–220. <https://doi.org/10.1124/jpet.113.208223>

Wolters, P. J., Collard, H. R., & Jones, K. D. (2014). Pathogenesis of idiopathic pulmonary fibrosis. *Annual Review of Pathology*, 9, 157–179. <https://doi.org/10.1146/annurev-pathol-012513-104706>

Wollin, L., Wex, E., Pautsch, A., Schnapp, G., Hostettler, K. E., Stowasser, S., & Kolb, M. (n.d.). Mode of action of nintedanib in the treatment of idiopathic pulmonary fibrosis, 1434–1445. <https://doi.org/10.1183/09031936.00174914>

Wu, Z., Yang, L., Cai, L., Zhang, M., Cheng, X., Yang, X., & Xu, J. (2007). Detection of epithelial to mesenchymal transition in airways of a bleomycin induced pulmonary fibrosis model derived from an alpha-smooth muscle actin-Cre transgenic mouse. *Respiratory Research*, 8, 1. <https://doi.org/10.1186/1465-9921-8-1>

Wynn, T. A. (2011). Integrating mechanisms of pulmonary fibrosis. *The Journal of Experimental Medicine*, 208(7), 1339–1350. <https://doi.org/10.1084/jem.20110551>

Xu, J., Lamouille, S., & Derynck, R. (2009). TGF- β -induced epithelial to mesenchymal transition. *Cell Research*, 19(2), 156–172. <https://doi.org/10.1038/cr.2009.5>

Xu, Q., Norman, J. T., Shrivastav, S., Lucio-Cazana, J., & Kopp, J. B. (2007). In vitro models of TGF- β -induced fibrosis suitable for high-throughput screening of antifibrotic agents. *American Journal of Physiology-Renal Physiology*, 293(2), F631–F640. <https://doi.org/10.1152/ajprenal.00379.2006>

Yu, N., Sun, Y.-T., Su, X.-M., He, M., Dai, B., & Kang, J. (2016). Melatonin attenuates TGF β 1-induced epithelial-mesenchymal transition in lung alveolar epithelial cells. *Molecular Medicine Reports*, 14(6), 5567–5572. <https://doi.org/10.3892/mmr.2016.5950>

Yue, X., Shan, B., & Lasky, J. A. (2010). TGF- β : Titan of Lung Fibrogenesis. *Current Enzyme Inhibition*, 6(2). <https://doi.org/10.2174/10067>

Zeki Yildirim, Mahir Kotuk, Hasan Erdogan, Mustafa Iraz, Murat Yagmurca, Irfan Kuku, & Ersin Fadillioglu. (n.d.). Preventive effect of melatonin on bleomycin-induced lung fibrosis in rats. *J. Pineal Res.* (2006); 40:27–33.

Zent, J., & Guo, L.-W. (2018). Signaling Mechanisms of Myofibroblastic Activation: Outside-in and Inside-Out. *Cellular Physiology and Biochemistry*, 49(3), 848–868. <https://doi.org/10.1159/000493217>

Zhang, D., Huang, C., Yang, C., Liu, R. J., Wang, J., Niu, J., & Brömme, D. (2011). Antifibrotic effects of curcumin are associated with overexpression of cathepsins K and L in bleomycin treated mice and human fibroblasts. *Respiratory Research*, 12(1), 154. <https://doi.org/10.1186/1465-9921-12-154>

Zhang, M., Cao, S.-R., Zhang, R., Jin, J.-L., & Zhu, Y.-F. (2014). The inhibitory effect of salvianolic acid B on TGF- β 1-induced proliferation and differentiation in lung fibroblasts. *Experimental Lung Research*, 40(4), 172–185.
<https://doi.org/10.3109/01902148.2014.895070>

Zhao, H., Wu, Q.-Q., Cao, L.-F., Qing, H.-Y., Zhang, C., Chen, Y.-H., ... Xu, D.-X. (2014). Melatonin Inhibits Endoplasmic Reticulum Stress and Epithelial-Mesenchymal Transition during Bleomycin-Induced Pulmonary Fibrosis in Mice. *PLoS ONE*, 9(5).
<https://doi.org/10.1371/journal.pone.0097266>

Zhao, X., Sun, J., Su, W., Shan, H., Zhang, B., Wang, Y., ... Liang, H. (2018). Melatonin Protects against Lung Fibrosis by Regulating the Hippo/YAP Pathway. *International Journal of Molecular Sciences*, 19(4). <https://doi.org/10.3390/ijms19041118>

Zisman DA, Keane MP, Belperio JA, Strieter RM, Lynch JP. (n.d.). Pulmonary fibrosis. *Methods Mol Med*. 2005;117:3-44.

DATA SHEETS

Results for ABTS radical scavenging activity

1) Melatonin

| Mel (uM) | 1 | 2 | 3 | 4 | 5 | 6 | 7 | Mean | SD |
|----------|-------|-------|-------|-------|-------|-------|-------|-------|-------|
| 0.0 | 1.000 | 0.992 | 1.021 | 0.987 | 0.982 | 1.004 | 1.014 | 1.000 | 0.014 |
| 0.1 | 1.046 | 1.146 | 1.088 | | | | | 1.093 | 0.050 |
| 1.0 | 0.893 | 0.972 | 0.932 | 1.030 | 1.151 | 1.072 | | 1.008 | 0.095 |
| 5.0 | 0.784 | 0.774 | 0.893 | 0.935 | 0.898 | 0.893 | | 0.863 | 0.067 |
| 10.0 | | | | 0.829 | 0.835 | 0.813 | | 0.826 | 0.011 |
| 20.0 | 0.540 | 0.610 | 0.518 | 0.518 | 0.518 | | | 0.541 | 0.040 |
| 50.0 | 0.347 | 0.431 | 0.380 | 0.386 | 0.391 | | | 0.387 | 0.030 |
| 100.0 | | | | 0.285 | 0.290 | 0.290 | | 0.289 | 0.003 |
| 250.0 | | | | 0.106 | 0.111 | 0.063 | | 0.093 | 0.026 |

2) Curcumin

| CUR (uM) | 1 | 2 | 3 | 4 | 5 | 6 | 7 | Mean | SD |
|----------|-------|-------|-------|-------|-------|-------|-------|-------|-------|
| 0.0 | 1.000 | 1.044 | 0.956 | 1.000 | 1.028 | 0.960 | 1.013 | 1.000 | 0.033 |
| 0.1 | 1.151 | 0.908 | 1.269 | 1.020 | | | | 1.087 | 0.157 |
| 1.0 | 1.024 | 0.828 | 0.828 | 1.168 | 0.983 | 1.227 | 0.945 | 1.000 | 0.154 |
| 2.5 | 0.806 | 0.656 | 1.020 | | | | | 0.827 | 0.183 |
| 5.0 | 0.700 | 0.706 | 0.741 | | | | | 0.715 | 0.022 |
| 10.0 | 0.623 | 0.506 | 0.500 | 0.529 | | | | 0.539 | 0.057 |
| 25.0 | 0.267 | 0.267 | 0.287 | | | | | 0.273 | 0.012 |
| 50.0 | 0.185 | 0.178 | 0.122 | 0.181 | | | | 0.167 | 0.030 |
| 100.0 | 0.113 | 0.121 | | | | | | 0.117 | 0.005 |
| 250.0 | 0.000 | 0.000 | 0.000 | | | | | 0.000 | 0.000 |

3) AM24

| AM24(uM) | 1.000 | 2.000 | 3 | 4 | 5 | 6 | 7 | Mean | SD |
|----------|-------|-------|-------|-------|-------|-------|-------|-------|-------|
| 0.0 | 1.000 | 1.044 | 0.956 | 1.000 | 1.028 | 0.960 | 1.013 | 1.000 | 0.033 |
| 0.1 | 1.067 | 0.798 | 0.958 | | | | | 0.941 | 0.135 |
| 1.0 | 1.143 | 0.824 | 1.109 | | | | | 1.025 | 0.175 |
| 5.0 | 0.878 | 0.833 | 0.911 | | | | | 0.874 | 0.039 |
| 10.0 | 0.502 | 0.617 | 0.689 | | | | | 0.602 | 0.095 |
| 25.0 | 0.500 | 0.544 | 0.617 | | | | | 0.554 | 0.059 |
| 36.0 | 0.461 | 0.439 | 0.506 | | | | | 0.469 | 0.034 |
| 50.0 | 0.258 | 0.283 | 0.356 | 0.389 | | | | 0.322 | 0.061 |
| 100.0 | 0.167 | 0.250 | 0.189 | | | | | 0.202 | 0.043 |
| 192.0 | 0.056 | 0.094 | 0.133 | | | | | 0.094 | 0.039 |

Results for in vitro collagen assay with MRC-5 cells

| | TGF-B | Drug | Concentration(uM) | 1 | 2 | 3 | 4 | 5 | 6 | 7 | 8 | Mean | SD |
|------------------|-------|--------------|-------------------|-------|-------|-------|-------|-------|-------|-------|-------|-------|-------|
| Control | - | - | - | 0.205 | 0.207 | 0.223 | 0.212 | 0.252 | 0.230 | 0.230 | 0.248 | 0.226 | 0.019 |
| Positive control | + | - | - | 0.686 | 0.686 | 0.776 | 0.787 | 0.859 | 0.689 | 0.845 | 0.707 | 0.754 | 0.072 |
| Treatment | + | AM 24 | 10 | 0.281 | 0.325 | 0.247 | 0.298 | 0.273 | | | | 0.285 | 0.029 |
| Treatment | + | AM 24 | 7.5 | 0.826 | 0.806 | 0.778 | | | | | | 0.803 | 0.024 |
| Treatment | + | AM 24 | 5 | 0.665 | 0.680 | 0.728 | 0.741 | 0.587 | 0.594 | 0.572 | | 0.662 | 0.068 |
| Treatment | + | AM 24 | 1 | 0.740 | 0.800 | 0.840 | 0.573 | 0.750 | 0.744 | 0.725 | | 0.739 | 0.075 |
| Treatment | + | AM 24 | 0.1 | 0.739 | 0.691 | 0.704 | 0.636 | | | | | 0.693 | 0.043 |
| Drug Only | - | AM 24 | 10 | 0.297 | 0.278 | 0.279 | 0.275 | | | | | 0.281 | 0.010 |
| Treatment | + | CUR | 10 | 0.595 | 0.577 | 0.646 | 0.589 | 0.642 | 0.658 | | | 0.684 | 0.005 |
| Drug Only | - | CUR | 10 | 0.168 | 0.196 | 0.185 | | | | | | 0.183 | 0.014 |
| Treatment | + | MEL | 10 | 0.618 | 0.579 | 0.625 | 0.638 | 0.623 | 0.634 | | | 0.620 | 0.007 |
| Treatment | + | MEL | 1 | 0.690 | 0.788 | 0.683 | | | | | | 0.610 | 0.034 |
| Drug only | - | MEL | 10 | 0.241 | 0.196 | 0.206 | | | | | | 0.762 | 0.006 |
| Treatment | + | PIR | 10 | 0.748 | 0.771 | 0.745 | 0.686 | | | | | 0.738 | 0.036 |
| Treatment | + | PIR | 500 | 0.352 | 0.373 | 0.328 | 0.349 | | | | | 0.351 | 0.018 |
| Drug only | - | PIR | 10 | 0.185 | 0.188 | 0.199 | | | | | | 0.528 | 0.012 |
| Treatment | + | CUR+MEL | 10 | 0.753 | 0.816 | 0.801 | | | | | | 0.790 | 0.033 |
| Treatment | + | Luz+ AM24 | 100nM+ 10uM | 0.743 | 0.763 | 0.663 | | | | | | 0.723 | 0.053 |
| Inhibitor only | - | Luz | 100nM | 0.339 | 0.286 | 0.316 | | | | | | 0.314 | 0.027 |
| PC+ Inhibitor | + | Luz | 100nM | 0.740 | 0.731 | 0.738 | | | | | | 0.736 | 0.005 |

Results for in vitro collagen assay with NHLF cells

| TGF-B1 | Drug | Concentration(μ M) | 1.000 | 2.000 | 3.000 | 4.000 | 5.000 | 6.000 | Mean | SD |
|--------|------|-------------------------|-------|-------|-------|-------|-------|-------|-------|-------|
| - | - | - | 0.329 | 0.375 | 0.399 | 0.429 | 0.248 | 0.227 | 0.335 | 0.082 |
| + | - | - | 0.607 | 0.456 | 0.640 | 0.654 | 0.716 | 0.736 | 0.635 | 0.100 |
| + | AM24 | 10 | 0.365 | 0.492 | 0.528 | | | | 0.462 | 0.086 |
| + | MEL | 10 | 0.389 | 0.676 | 0.621 | 0.637 | 0.634 | | 0.580 | 0.129 |
| + | CUR | 10 | 0.426 | 0.377 | 0.437 | 0.567 | 0.560 | | | |

Results for in vitro proliferation (MTT) assay at 48 hours in MRC-5 cells

| TGF | Drug (10 μ M) | 1 | 2 | 3 | 4 | 5 | 6 | 7 | Mean | SD |
|--------|-------------------|-------|-------|-------|-------|-------|-------|-------|-------|-------|
| 0 hour | - | 0.230 | | 0.230 | | 0.230 | 0.234 | | 0.231 | 0.002 |
| - | - | 0.184 | 0.157 | 0.143 | 0.158 | 0.315 | 0.320 | 0.259 | 0.219 | 0.077 |
| + | - | 0.224 | 0.166 | 0.160 | 0.150 | 0.268 | 0.273 | 0.254 | 0.214 | 0.054 |
| + | AM24 | 0.164 | 0.145 | | | 0.214 | 0.216 | 0.219 | 0.192 | 0.035 |
| + | CUR | 0.125 | 0.135 | 0.161 | 0.167 | 0.290 | 0.198 | 0.185 | 0.180 | 0.055 |
| + | MEL | 0.148 | 0.170 | 0.179 | 0.171 | 0.297 | 0.155 | 0.215 | 0.191 | 0.052 |
| + | PIR | 0.175 | 0.142 | | | 0.330 | 0.156 | 0.201 | 0.201 | 0.076 |

Results for in vitro proliferation (MTT) assay at 72 hours in MRC-5 cells

| TGF-B1 | Drug | Concentration (uM) | 1 | 2 | 3 | Mean | SD |
|--------|---------|--------------------|-------|-------|-------|-------|-------|
| 0 hour | - | - | 0.230 | 0.230 | 0.234 | 0.231 | 0.002 |
| - | - | - | 0.282 | 0.245 | 0.262 | 0.263 | 0.019 |
| + | - | - | 0.566 | 0.773 | 0.673 | 0.671 | 0.104 |
| + | AM24 | 1 | 0.438 | 0.426 | 0.453 | 0.439 | 0.014 |
| + | AM24 | 5 | 0.401 | 0.501 | 0.402 | 0.435 | 0.057 |
| + | AM24 | 7.5 | 0.440 | 0.431 | 0.385 | 0.419 | 0.030 |
| + | AM24 | 10 | 0.337 | 0.389 | 0.397 | 0.374 | 0.033 |
| + | CUR | 10 | 0.448 | 0.487 | 0.461 | 0.465 | 0.020 |
| + | MEL | 10 | 0.440 | 0.482 | 0.435 | 0.452 | 0.026 |
| + | CUR+MEL | 10 | 0.424 | 0.455 | 0.445 | 0.441 | 0.016 |
| + | PIR | 10 | 0.444 | 0.485 | 0.416 | 0.448 | 0.035 |
| + | PIR | 500 | 0.311 | 0.254 | 0.395 | 0.320 | 0.071 |
| - | AM24 | 10 | 0.319 | 0.429 | 0.342 | 0.363 | 0.058 |
| - | CUR | 10 | 0.331 | 0.198 | 0.357 | 0.295 | 0.085 |
| - | MEL | 10 | 0.323 | 0.361 | 0.343 | 0.342 | 0.019 |

In vitro differentiation (α - SMA expression)

Protein levels of α - SMA in MRC-5 cells

| α -SMA/GAPDH | | | | | | | |
|---------------------|---------|-----------|-------|-------|-------|-------|-------|
| TGF-B1 | Drug | Concentra | 1 | 2 | 3 | Mean | SD |
| - | - | - | 1.000 | 1.000 | 1.000 | 1.000 | 0.000 |
| + | - | - | 1.754 | 1.745 | 1.818 | 1.772 | 0.040 |
| + | AM24 | 1 | 2.558 | 2.544 | 2.590 | 2.564 | 0.024 |
| + | AM24 | 10 | 0.334 | 0.338 | 0.338 | 0.337 | 0.003 |
| + | CUR | 10 | 2.545 | 2.484 | 2.554 | 2.528 | 0.038 |
| + | MEL | 10 | 3.392 | 3.144 | 3.358 | 3.298 | 0.134 |
| + | CUR+MEL | 10 | 2.934 | 2.966 | 3.042 | 2.981 | 0.055 |
| + | PIR | 10 | 3.076 | 2.965 | 2.878 | 2.973 | 0.099 |

In vitro EMT (protein levels of E-cadherin and Vimentin)

1) Protein levels of E-cadherin in A549 cells

| TGF-B1 | Drug | Concentration (uM) | | | | Mean | SD |
|--------|---------|--------------------|-------|-------|-------|-------|-------|
| - | - | - | 1.000 | 1.000 | 1.000 | 1.000 | 0.000 |
| + | - | - | 0.299 | 0.155 | 0.357 | 0.270 | 0.104 |
| + | AM24 | 1 | 0.248 | 0.357 | 0.486 | 0.364 | 0.119 |
| + | AM24 | 10 | 0.900 | 0.898 | 1.179 | 0.992 | 0.161 |
| + | CUR | 10 | 0.330 | 0.446 | 0.438 | 0.405 | 0.065 |
| + | MEL | 10 | 0.340 | 0.358 | 0.345 | 0.348 | 0.009 |
| + | CUR+MEL | 10 | 0.200 | 0.254 | 0.450 | 0.301 | 0.131 |
| + | PIR | 10 | 0.161 | 0.311 | 0.535 | 0.336 | 0.188 |

2) Protein levels of Vimentin in A549 cells

| TGF-B1 | Drug | Concentration (uM) | 1 | 2 | 3 | Mean | SD |
|--------|---------|--------------------|-------|-------|-------|-------|-------|
| - | - | - | 1.000 | 1.000 | 1.000 | 1.000 | 0.000 |
| + | - | - | 1.219 | 1.247 | 3.730 | 2.065 | 1.442 |
| + | AM24 | 1 | 1.350 | 2.462 | 3.319 | 2.377 | 0.987 |
| + | AM24 | 10 | 0.698 | 0.924 | 1.344 | 0.989 | 0.328 |
| + | CUR | 10 | 1.191 | 1.709 | 3.662 | 2.187 | 1.303 |
| + | MEL | 10 | 1.562 | 0.927 | 3.149 | 1.879 | 1.145 |
| + | CUR+MEL | 10 | 1.207 | 0.681 | 5.364 | 2.417 | 2.566 |
| + | PIR | 10 | 1.721 | 1.067 | 6.309 | 3.032 | 2.857 |

In vivo weight variation in rats

| Groups | | Weight on Day 1 | | | % Body weight relative to Day 1 | | | | | | | | | |
|-----------|-----|-----------------|-----|-----|---------------------------------|-----|-----|-----|-----|-----|-----|-----|-----|-----|
| Healthy | H38 | 324 | 100 | 103 | 105 | 105 | 109 | 115 | 115 | 116 | 117 | 118 | 120 | 122 |
| | H39 | 339 | 100 | 100 | 100 | 103 | 104 | 105 | 107 | 108 | 108 | 109 | 110 | 109 |
| Untreated | F9 | 347 | 100 | 99 | 100 | 101 | 103 | 110 | 110 | 111 | 111 | 114 | 116 | 120 |
| | F10 | 360 | 100 | 99 | 100 | 100 | 102 | 110 | 110 | 111 | 111 | 111 | 115 | 117 |
| | F15 | 345 | 100 | 102 | 101 | 104 | 104 | 107 | 106 | 107 | 108 | 110 | 112 | 112 |
| | F16 | 332 | 100 | 97 | 99 | 98 | 99 | 101 | 101 | 103 | 104 | 106 | 109 | 109 |
| Treated | F11 | 363 | 100 | 102 | 102 | 102 | 107 | 113 | 110 | 114 | 114 | 114 | 115 | 116 |
| | F12 | 335 | 100 | 98 | 100 | 97 | 100 | 106 | 106 | 105 | 107 | 108 | 111 | 112 |
| | F14 | 324 | 100 | 100 | 100 | 100 | 102 | 106 | 105 | 106 | 105 | 106 | 108 | 109 |
| | F17 | 321 | 100 | 94 | 90 | 90 | 94 | 97 | 96 | 99 | 99 | 101 | 105 | 106 |
| | F18 | 327 | 100 | 95 | 94 | 93 | 94 | 98 | 97 | 99 | 99 | 100 | 104 | 105 |

Pre and Post Endurance times for rats

| Groups | | Pre | Post |
|-----------|-----|------|------|
| Healthy | H38 | 41.0 | 55.0 |
| | H39 | 46.0 | 47.2 |
| Untreated | F9 | 30.7 | 11.6 |
| | F10 | 41.3 | 6.5 |
| | F15 | 55.0 | 12.8 |
| | F16 | 55.0 | 12.6 |
| Treated | F11 | 32.0 | 41.3 |
| | F12 | 40.1 | 36.2 |
| | F14 | 55.0 | 34.5 |
| | F17 | 55.0 | 41.3 |
| | F18 | 55.0 | 36.4 |

In vivo collagen levels in rat lungs by picrosirius red assay

| Groups | | | Mean | SD |
|-----------|-----|-------|-------|-------|
| Healthy | H38 | 0.259 | | |
| | H39 | 0.253 | 0.256 | |
| Untreated | F9 | 0.856 | | |
| | F10 | 0.834 | | |
| | F15 | 0.887 | | |
| | F16 | 0.810 | 0.844 | 0.033 |
| Treated | F11 | 0.372 | | |
| | F12 | 0.413 | | |
| | F14 | 0.418 | | |
| | F17 | 0.357 | | |
| | F18 | 0.383 | 0.389 | 0.026 |

Protein levels in rat lung homogenates

1) TGF-B1 protein expression levels

| TGF-B1/Bactin | 1 | 2 | 3 | Mean | SD |
|---------------|-------|-------|-------|-------|-------|
| Healthy | 1.111 | 0.888 | | 1.000 | 0.158 |
| Untreated | 2.059 | 1.536 | 1.989 | 1.861 | 0.284 |
| Treated | 1.194 | 1.939 | 1.411 | 1.515 | 0.383 |

2) PCNA protein expression levels

| PCNA/B-actin | 1 | 2 | 3 | Mean | SD |
|--------------|-------|-------|-------|-------|-------|
| Healthy | 1.010 | 0.989 | | 1.000 | |
| Untreated | 1.093 | 0.801 | 1.046 | 0.980 | 0.157 |
| Treated | 1.071 | 1.102 | 0.961 | 1.045 | 0.074 |

3) Protein level expression of α -SMA

| α -SMA/GAPDH | 1 | 2 | 3 | Mean | SD |
|---------------------|------|------|------|------|------|
| Healthy | 1.03 | 0.97 | | 1.00 | 0.04 |
| Untreated | 0.86 | 0.87 | 0.76 | 0.83 | 0.06 |
| Treated | 0.97 | 1.05 | 0.81 | 0.95 | 0.12 |

4) Protein level expression of E-cadherin

| E-cadherin/GAPDH | 1 | 2 | 3 | Mean | SD |
|------------------|-------|-------|-------|-------|-------|
| Healthy | 1.118 | 0.882 | | 1.000 | 0.167 |
| Untreated | 0.202 | 0.698 | 0.382 | 0.427 | 0.251 |
| Treated | 1.15 | 0.686 | 0.528 | 0.788 | 0.323 |

5) Protein level expressions of Vimentin

| Vimentin/GAPDH | 1 | 2 | 3 | Mean | SD |
|----------------|-------|-------|-------|-------|-------|
| Healthy | 1.064 | 0.935 | | 1.000 | 0.091 |
| Untreated | 1.467 | 1.794 | 2.137 | 1.799 | 0.335 |
| Treated | 1.535 | 1.548 | 1.199 | 1.427 | 0.198 |

6) Protein level expressions of Cathepsin-K

| Cathepsin-K/B-actin | 1 | 2 | 3 | Mean | SD |
|---------------------|-------|-------|-------|-------|-------|
| Healthy | 1.007 | 0.992 | | 1.000 | 0.011 |
| Untreated | 1.046 | 0.883 | 0.949 | 0.959 | 0.082 |
| Treated | 0.935 | 1.372 | 1.126 | 1.144 | 0.219 |

Exercise endurance testing of various doses of BLM and AM24

| | Pre | Post |
|---------------------------------|-------|-------|
| BLM 0.8 mg/kg | 29.78 | 15.19 |
| BLM 0.8 mg/kg + AM24 0.05 mg/kg | 29.79 | 3.63 |
| BLM 0.8 mg/kg +AM24 0.1 mg/kg | 38.79 | 14.55 |
| BLM 0.8 mg/kg +AM24 0.1 mg/kg | 38.27 | 17.58 |
| BLM 0.4 mg/kg + AM24 0.1 mg/kg | 32.53 | 34.22 |
| BLM 0.4 mg/kg | 28.79 | 5.06 |